Higgs physics at the LHC

Nan Lu

March 14, 2026

Large Hadron Collider - the energy frontier

Proton-proton collision in 2018:

- Beam energy: 6.5 TeV
- Peak luminosity: up to $2.1 \times 10^{34} cm^{-2} s^{-1}$
- Proton/bunch: 10^{11}
- Bunch crossing: 25 ns

https://videos.cern.ch/record/2020780

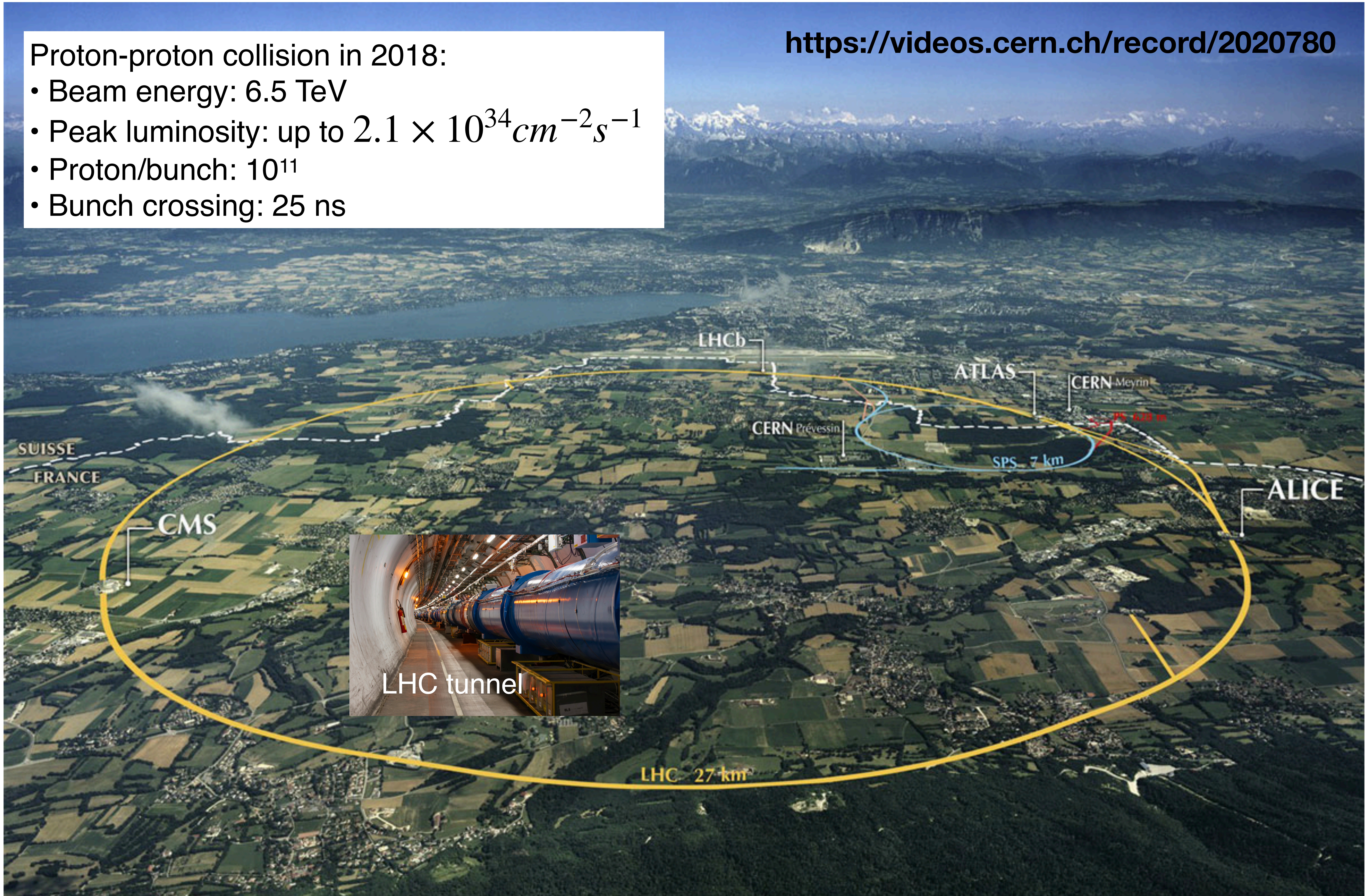

Two general purpose detector: ATLAS and CMS

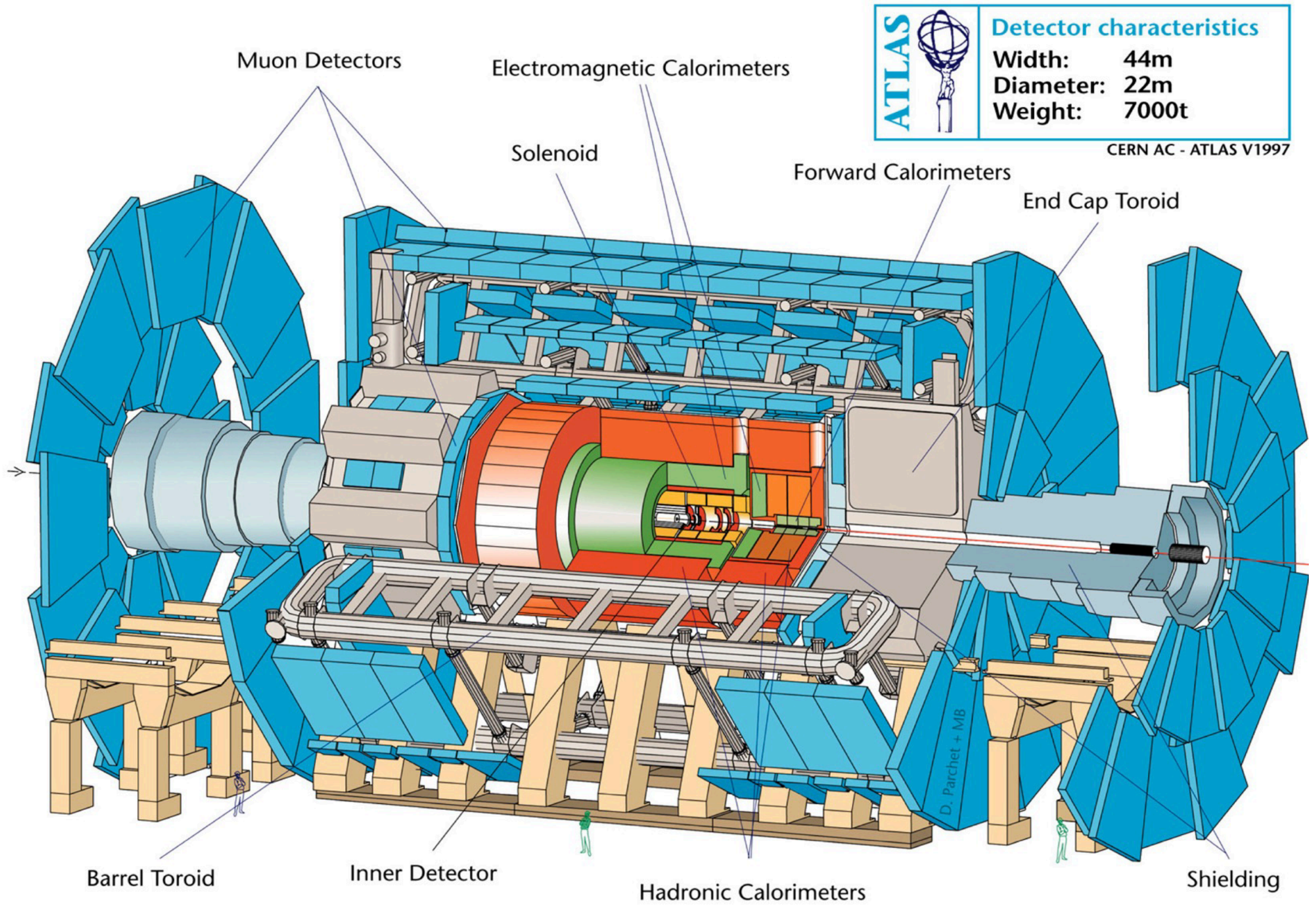

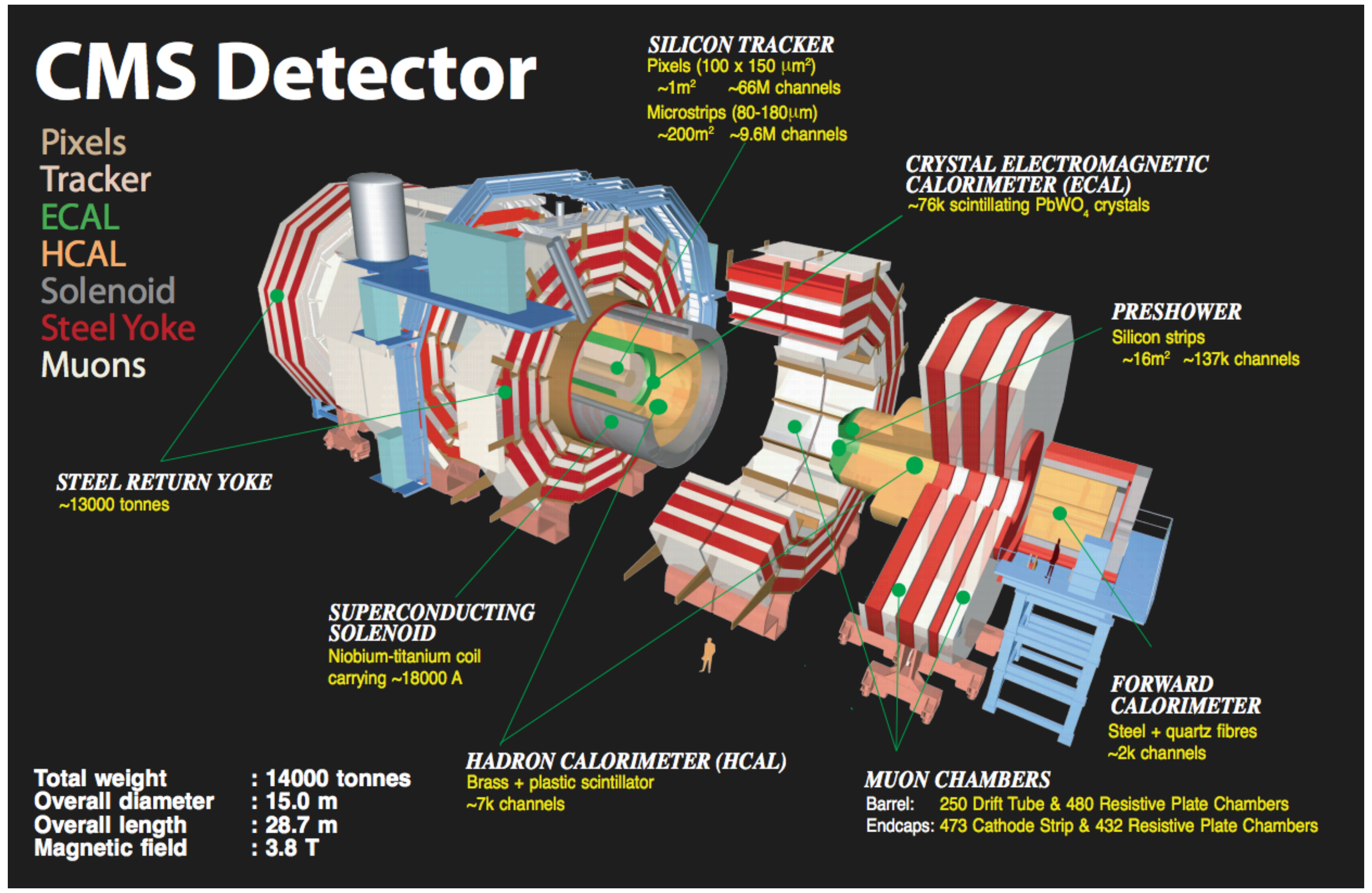

Total weight	: 14000 tonnes
Overall diameter	: 15.0 m
Overall length	: 28.7 m
Magnetic field	: 3.8 T

Powerful microscope sensitive to a wide range of physics:

1. Search and study the Higgs boson
2. Measurement of the Standard Model (SM)
3. New physics beyond the Standard Model (BSM)

Particle detection

CMS detector and Particle Flow

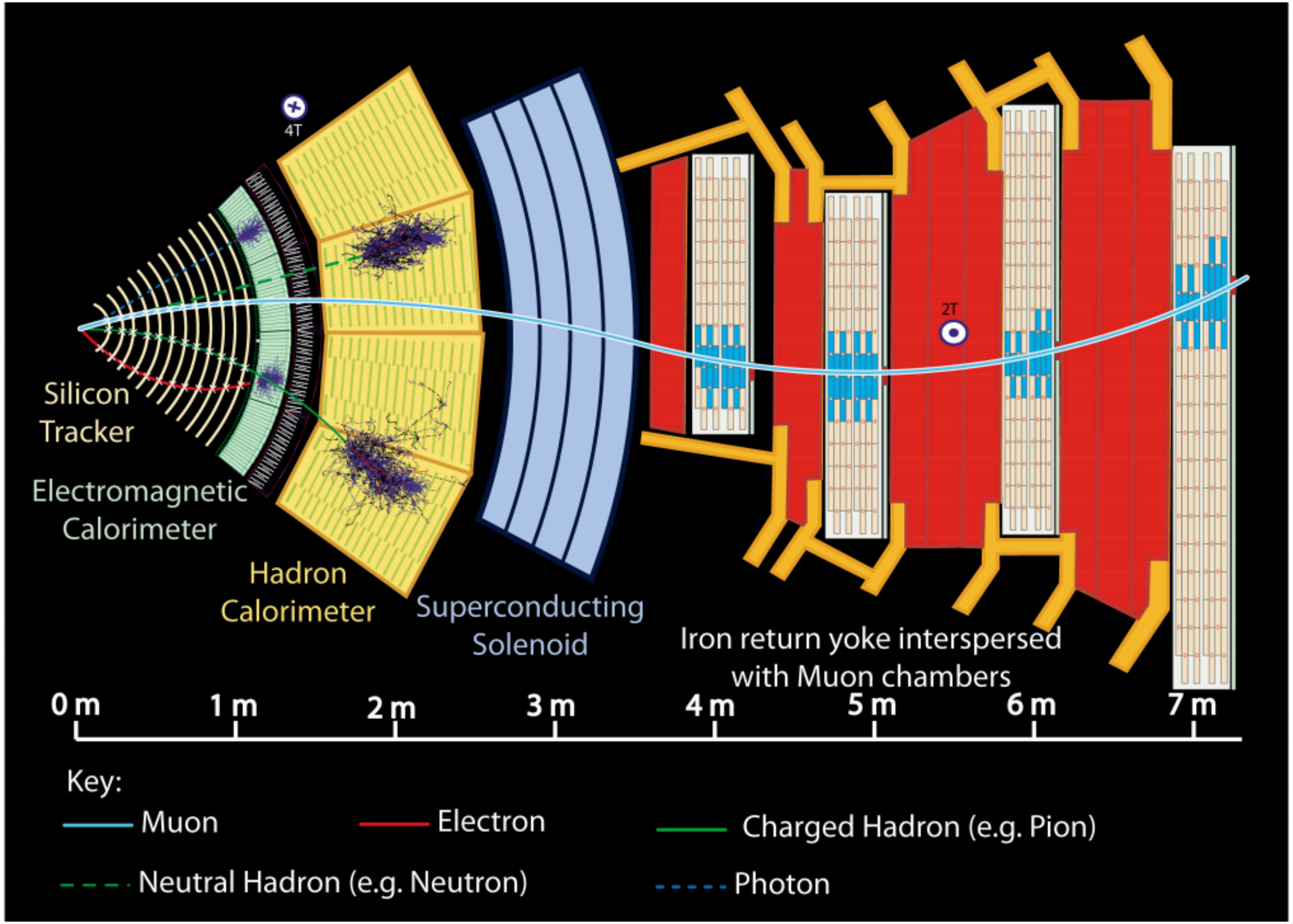

LHC and HL-LHC roadmap

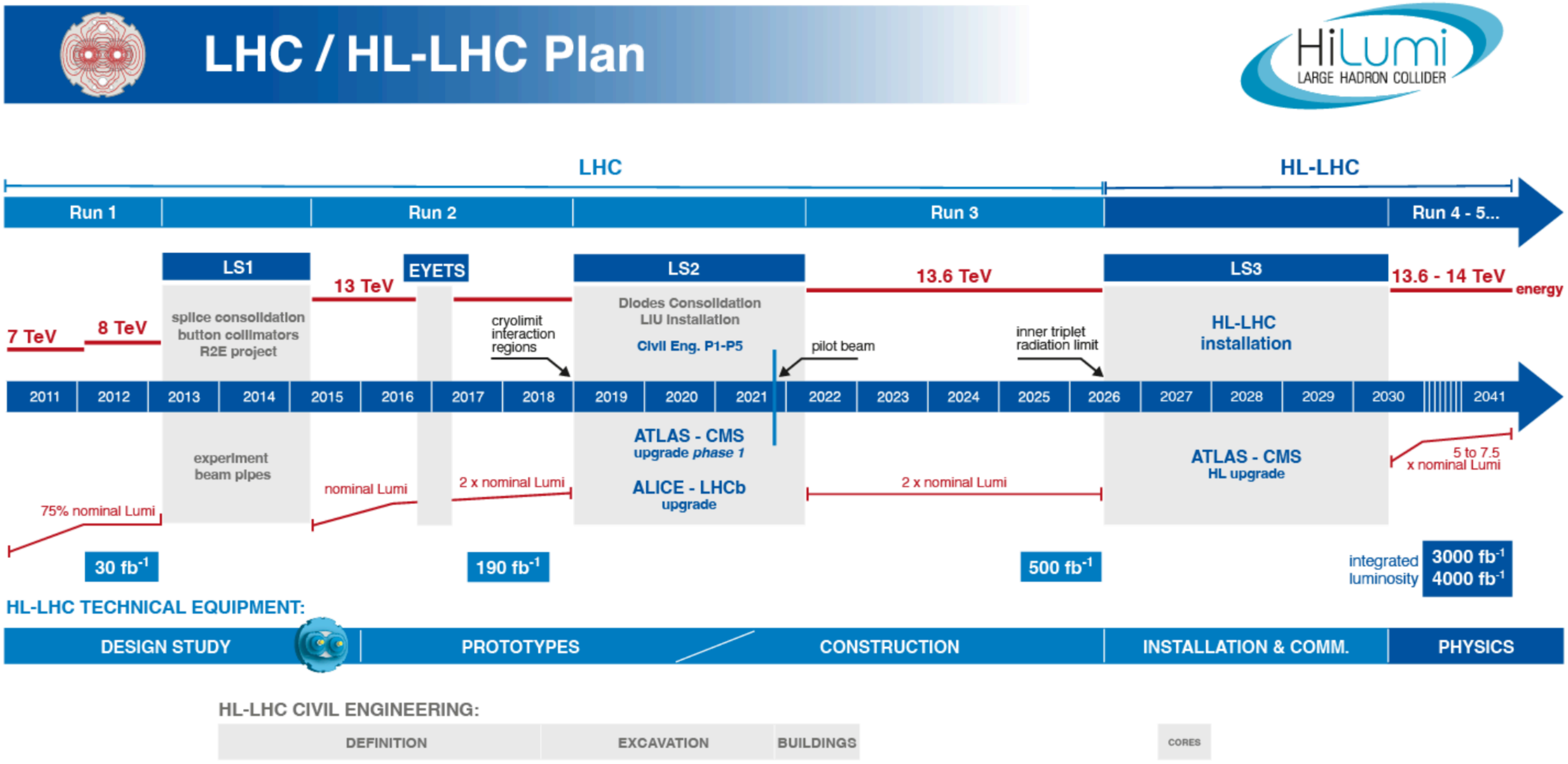

https://project-hl-lhc-industry.web.cern.ch/content/project-schedule

The Standard Model Higgs Boson

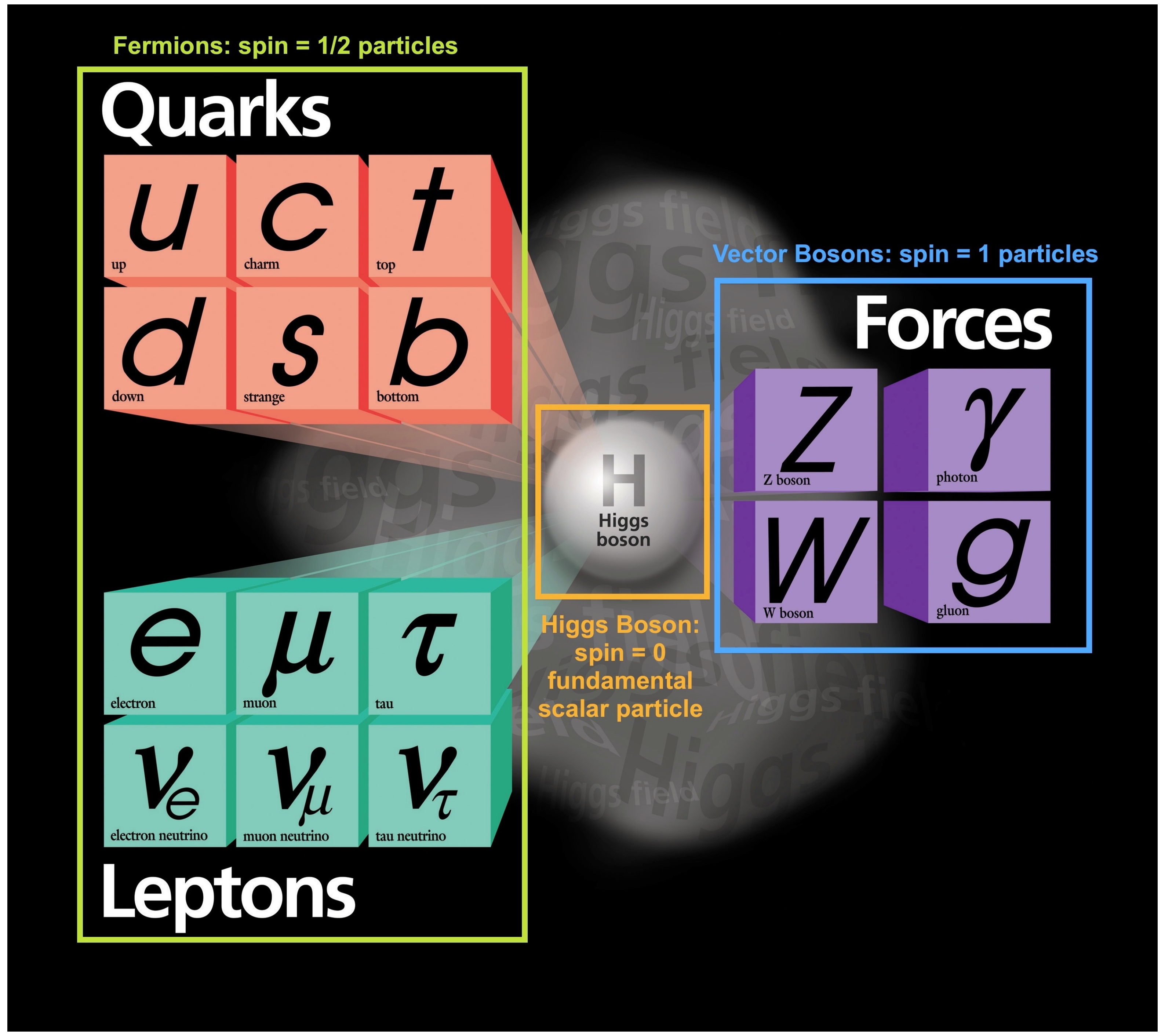

- Quarks, charged leptons, W/Z bosons acquire mass through the Brout-Englert-Higgs (BEH) mechanism in the Standard Model

- Higgs boson physics is one of the most important goals of LHC physics program

Higgs boson main production mechanism at the LHC

125 GeV Higgs boson production cross section @13 TeV

Gluon-fusion (ggH)
48.5 pb ~87%

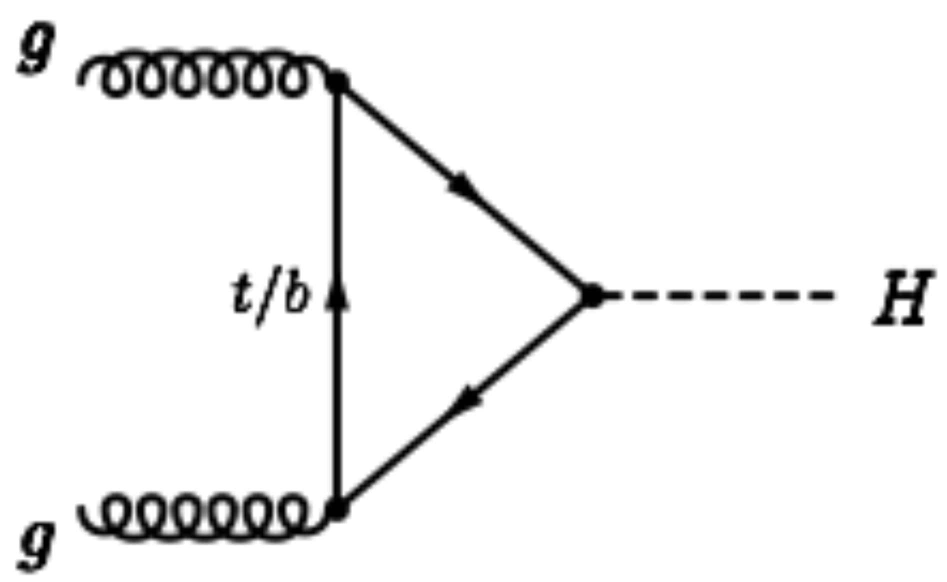

Vector boson fusion (VBF)
3.8 pb ~7%

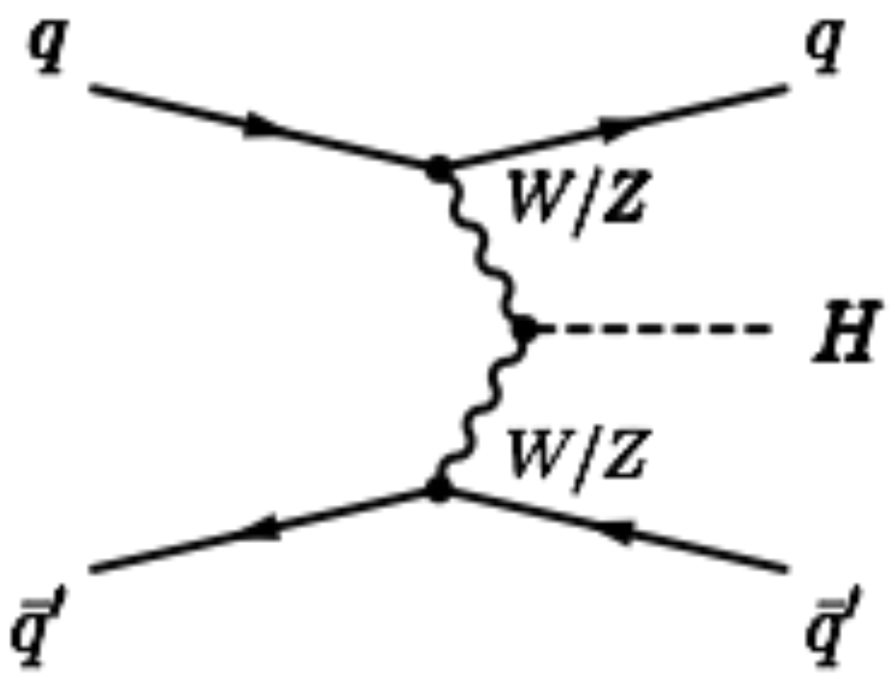

Associated Higgs production with a W or Z boson (VH):
2.3 pb ~ 4%

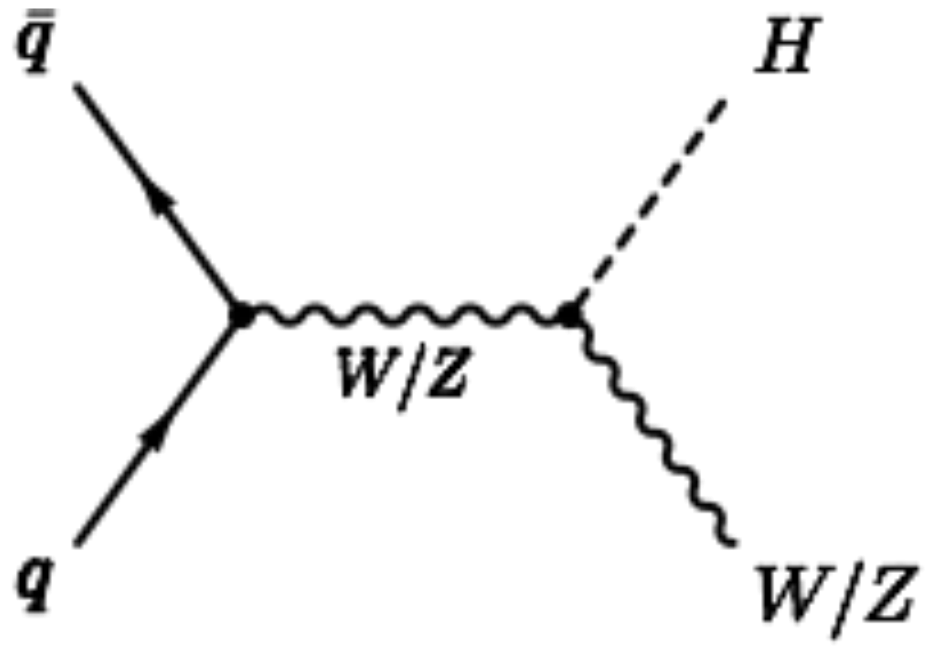

Associated Higgs production with a top quark pair (ttH): 0.5 pb ~1%

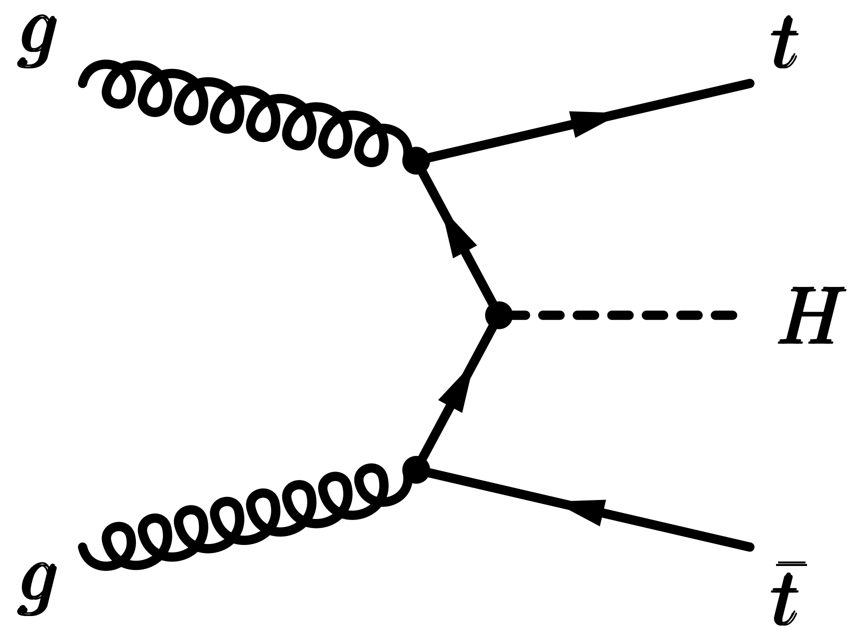

Higgs boson main decay channels

- *bosonic decays in precision measurement stage: γγ, ZZ*→4l, WW**
- *fermionic decays: bb, ττ observed*
- *channels not yet observed: cc, μμ, Zγ, …*

ZZ, WW

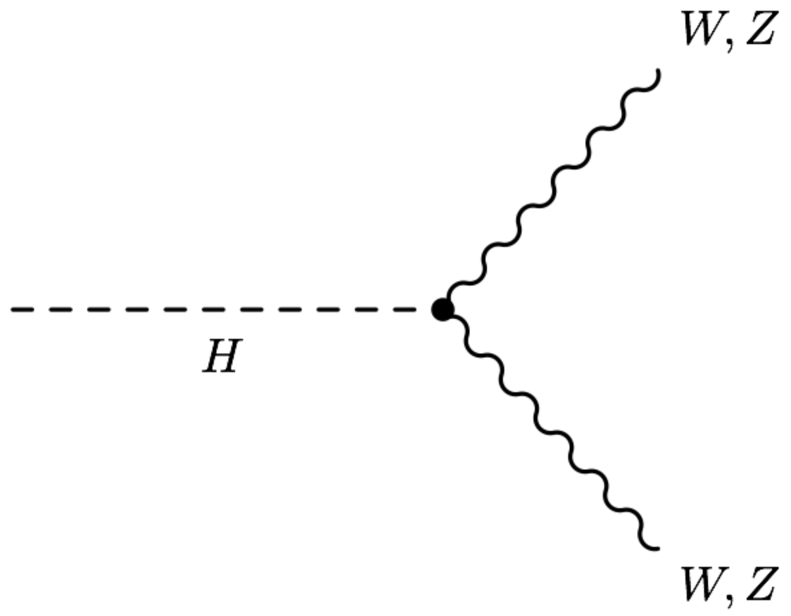

bb, ττ, μμ

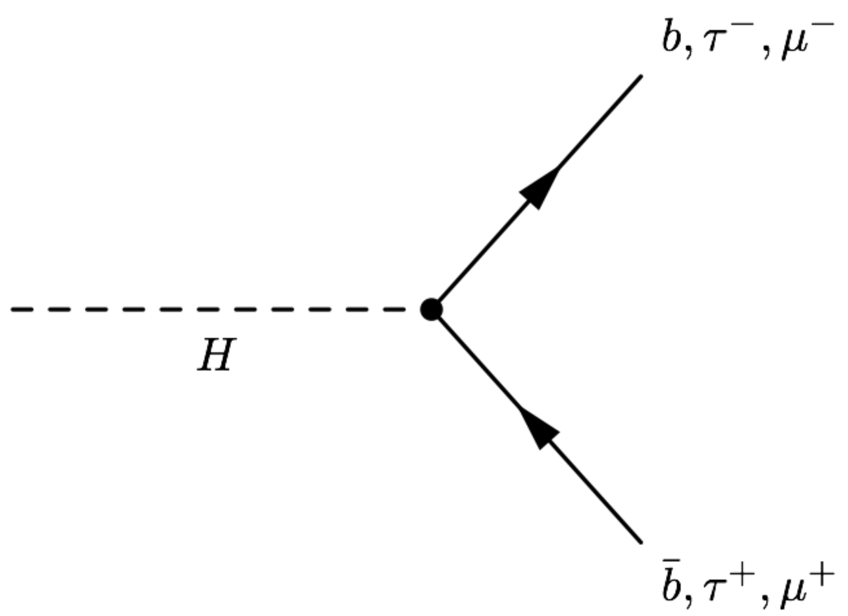

γγ, Zγ

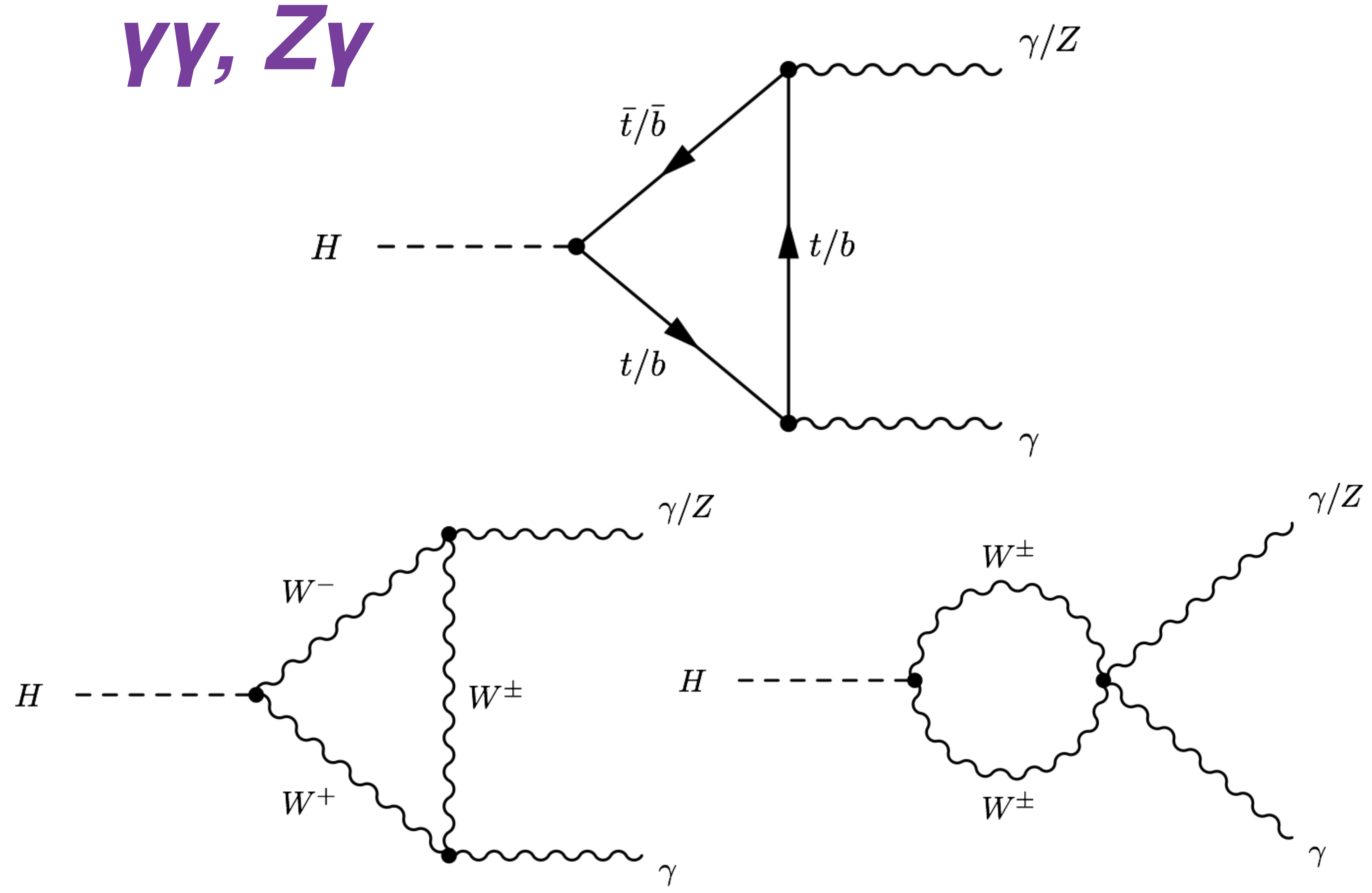

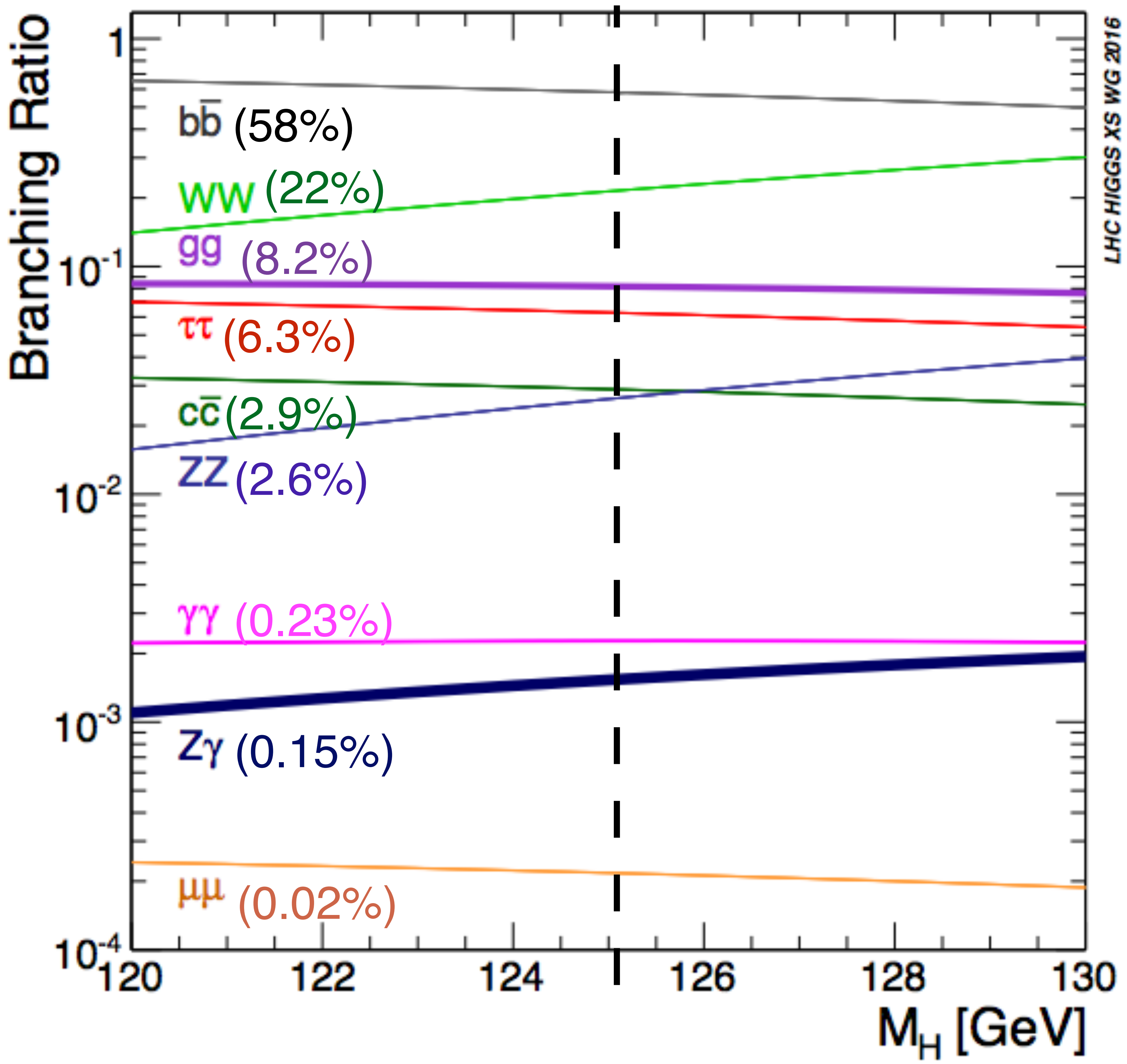

Higgs as tool for new physics

Precision measurements of Higgs boson properties as tool to search for new physics.

- Measurements of production and decay rates
    - Loop-induced ggF and H→γγ processes are particularly interesting because they are sensitive to new particle in the loops
- Exploit differential distributions
    - Very low/high $p_T(H)$ regime sensitive BSM
    - Modified Higgs boson CP lead to altered kinematic distributions

ggF:

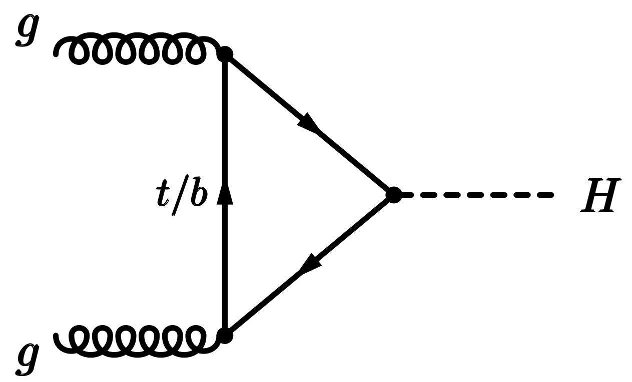

H→γγ:

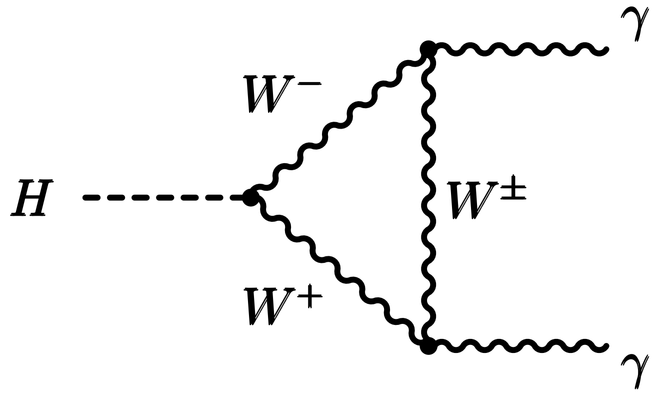

Higgs plus jet production at 14 TeV

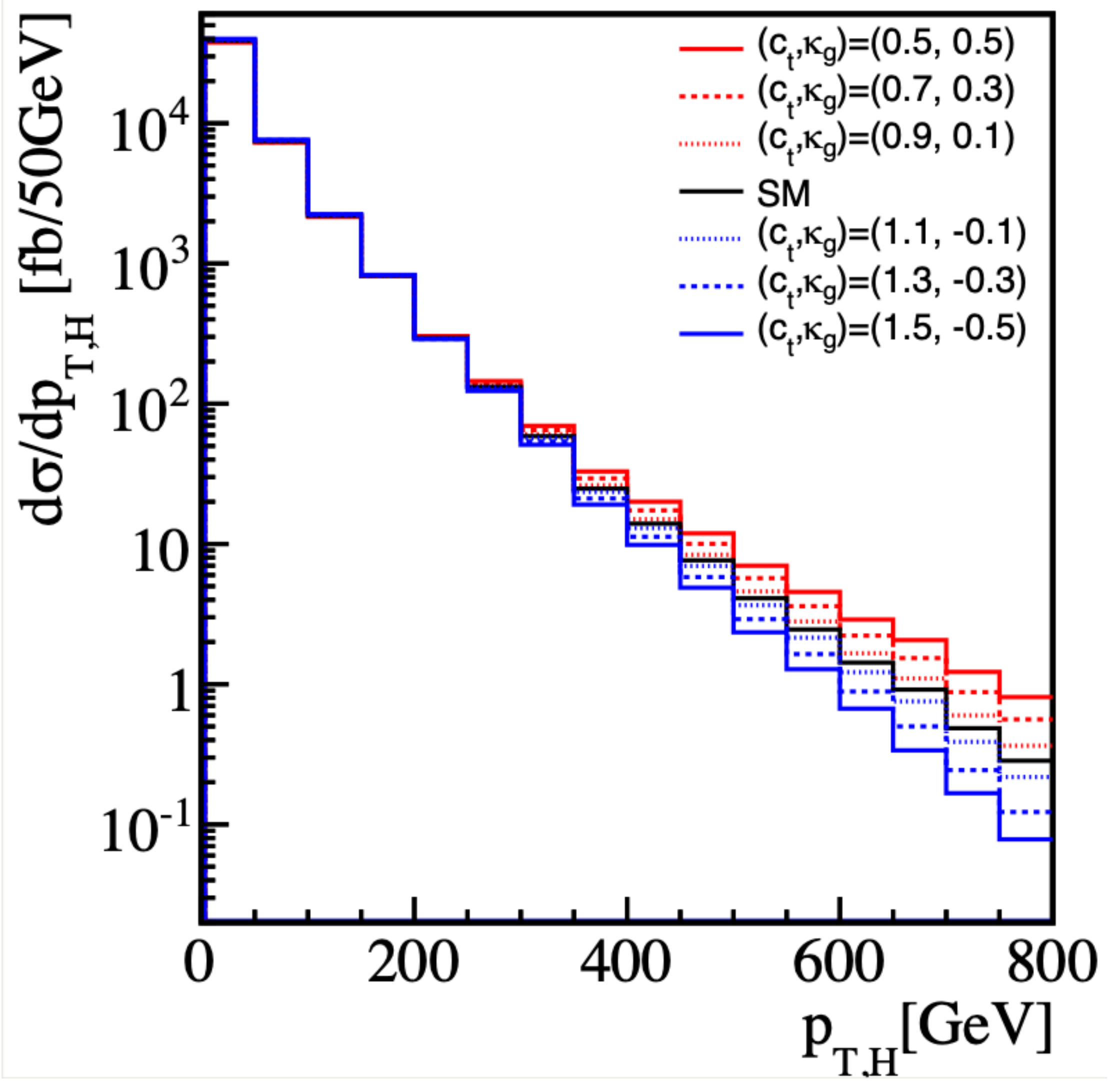

arxiv:1405.4295

Run 1 Higgs physics highlight

EPJC 75 (2015) 476

Spin-0 nature established, data strongly favors CP event compared to CP odd, agrees with SM.

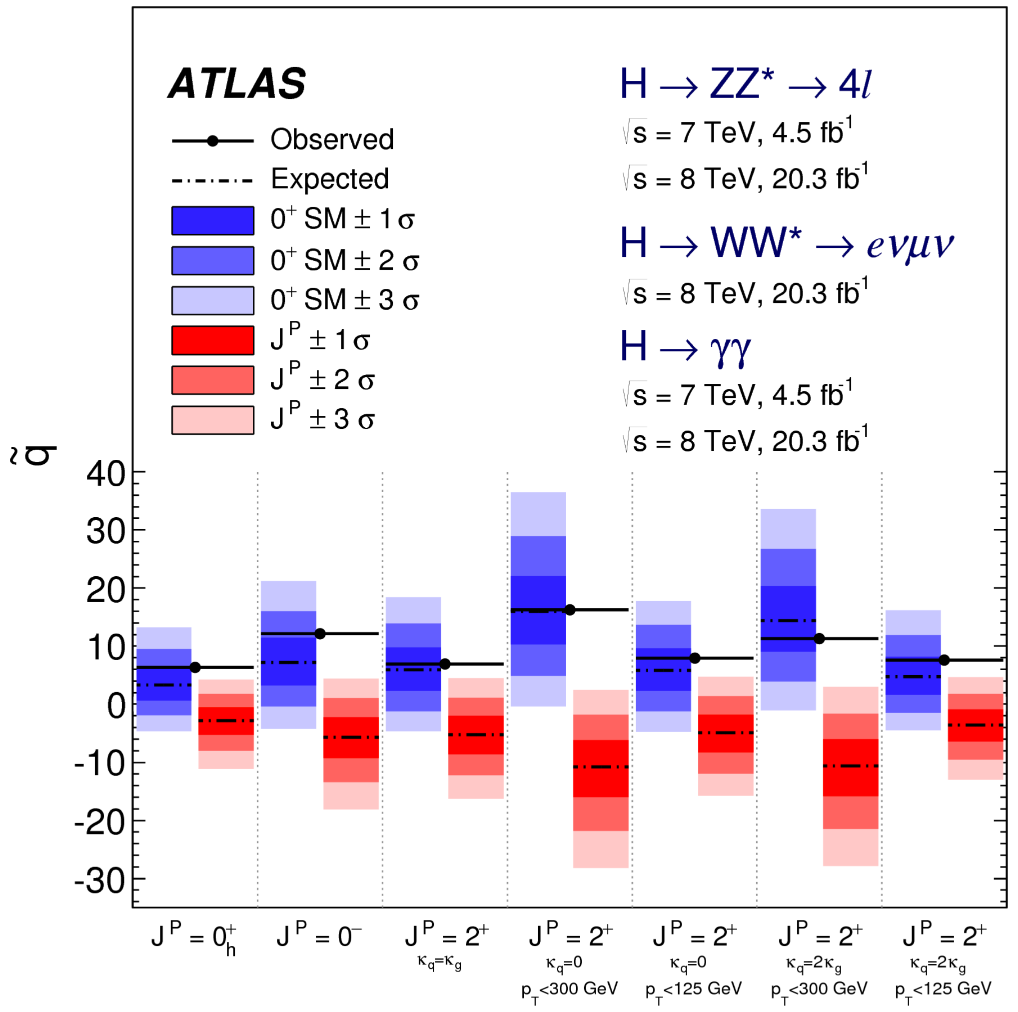

PRL 114 (2015) 191803

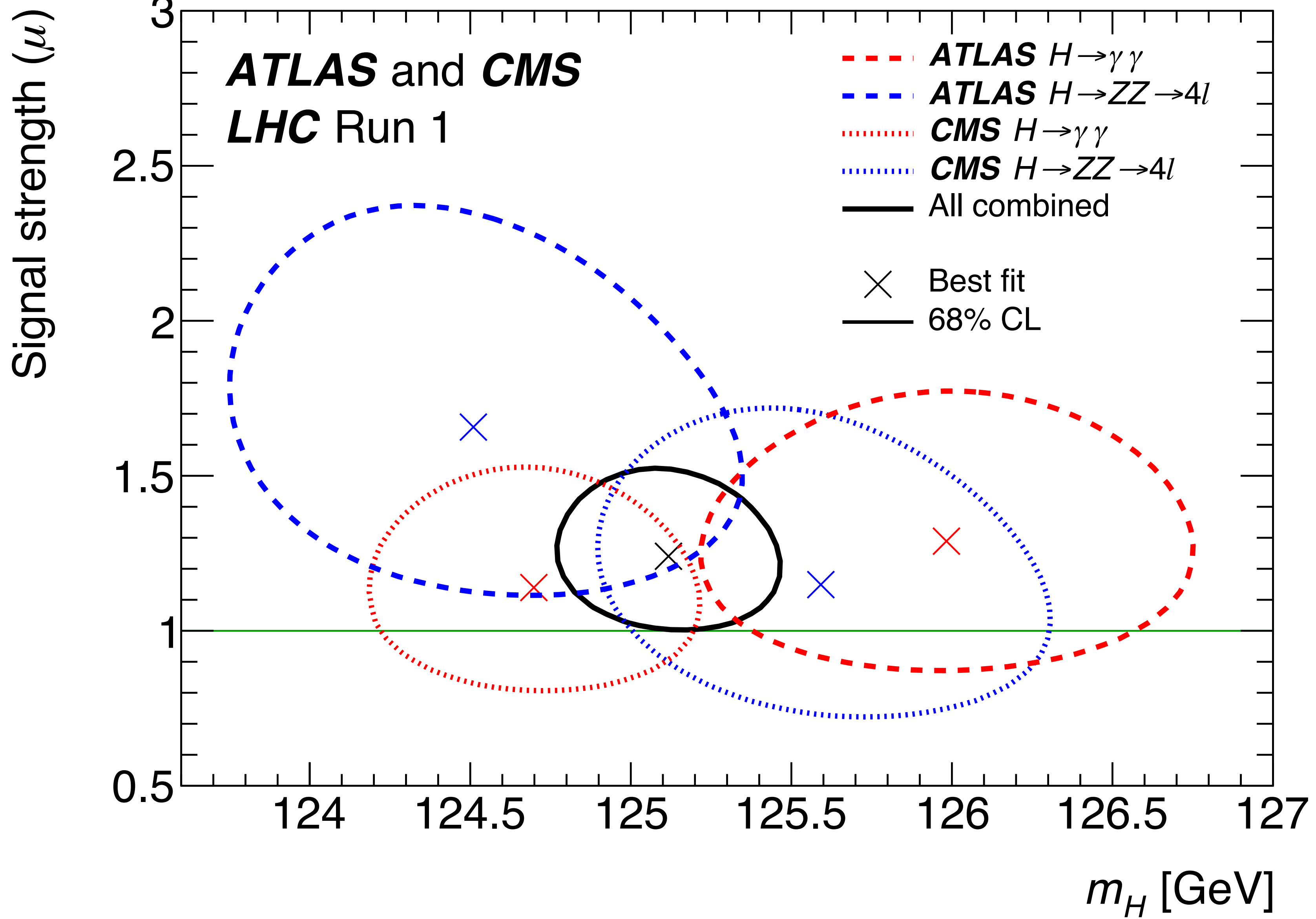

Mass measured at 0.2% precision

No significant deviations from SM in Higgs boson production and decay rate

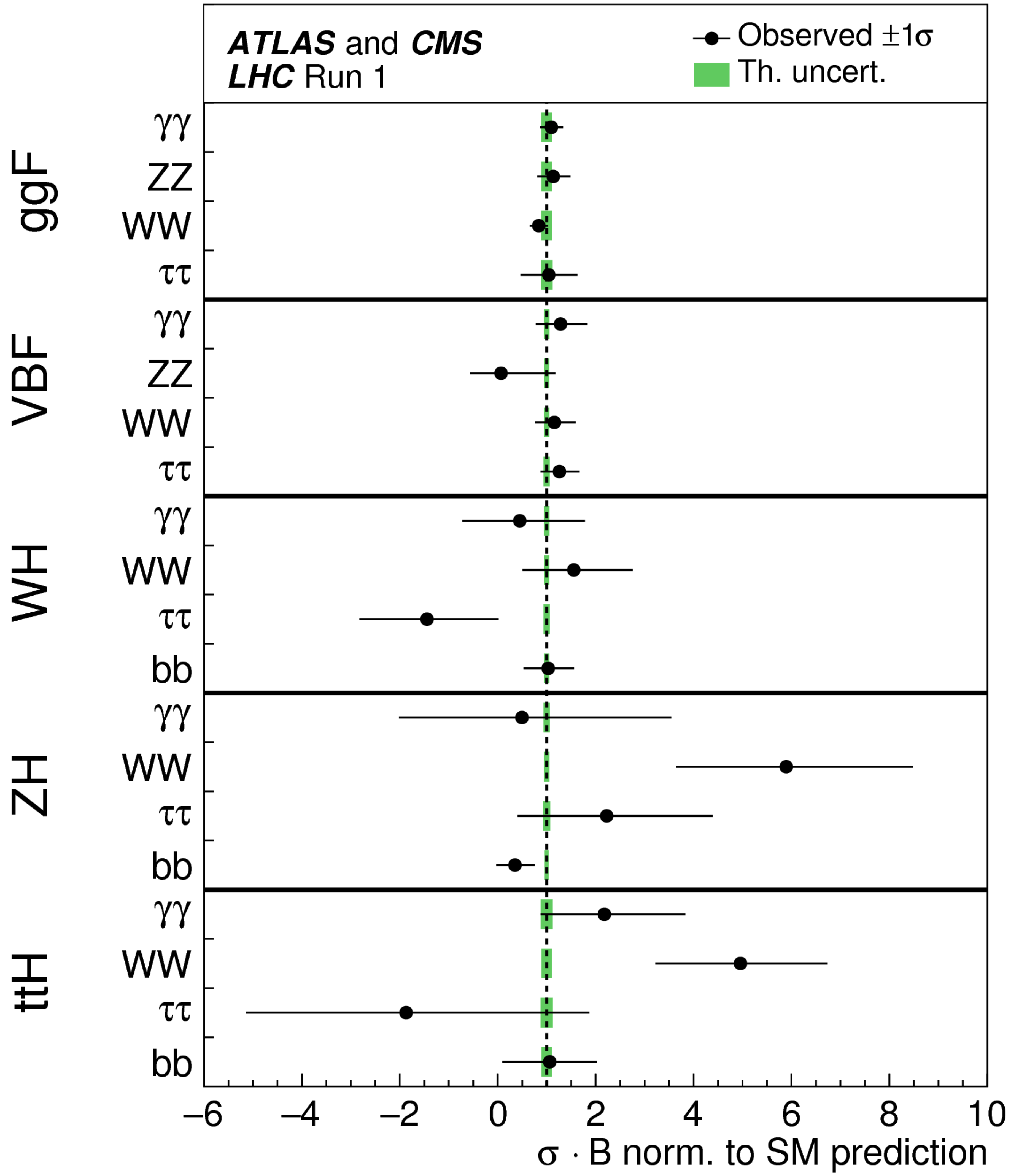

JHEP 08 (2016) 045

Measurement of Higgs boson mass

Phys. Lett. B 847 (2023) 138315

- $H\to ZZ^*\to 4l$ and $H\to\gamma\gamma$ are used to measure Higgs boson mass: fully reconstructed with high resolution

H→ZZ*→4l mass distribution

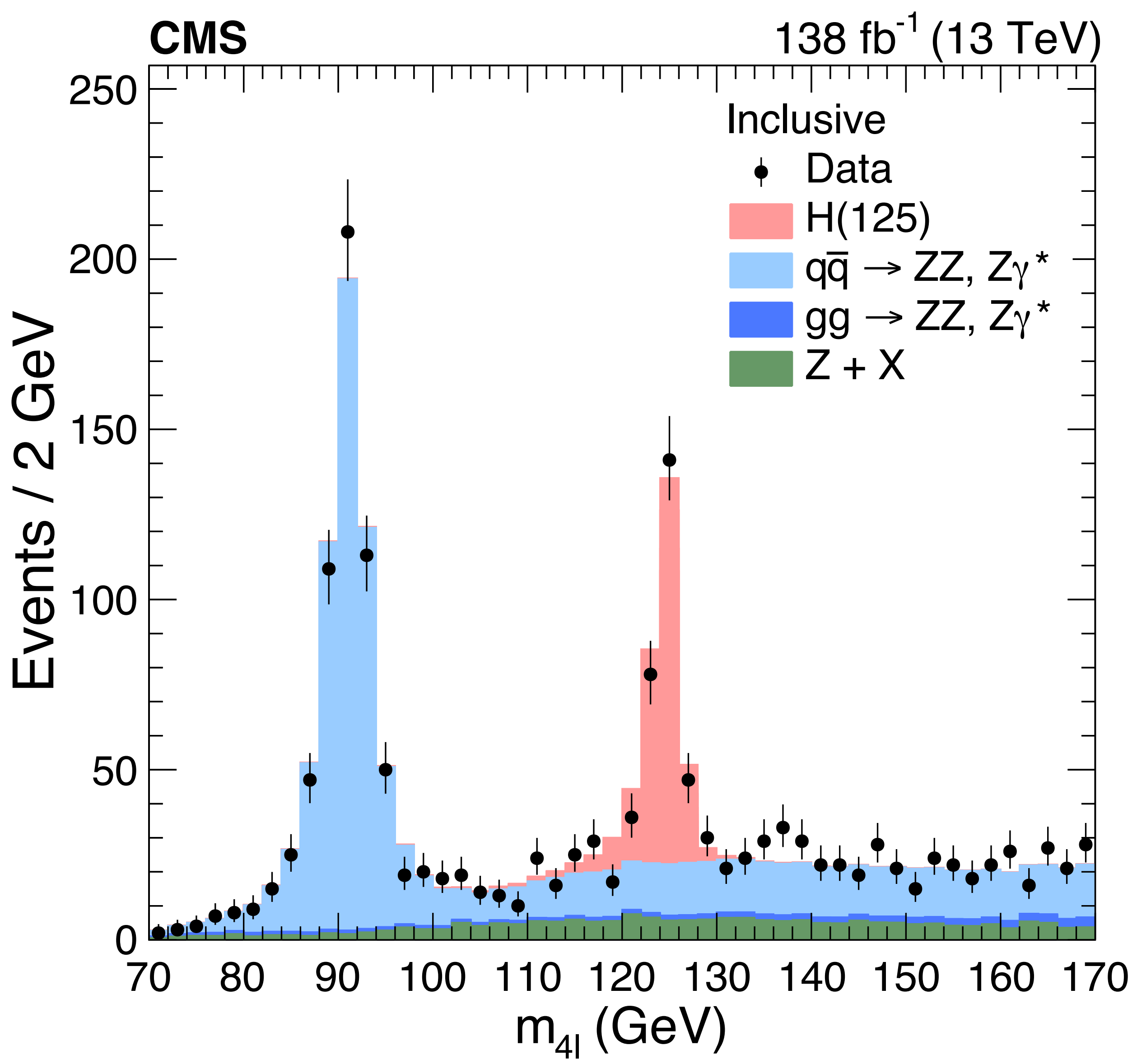

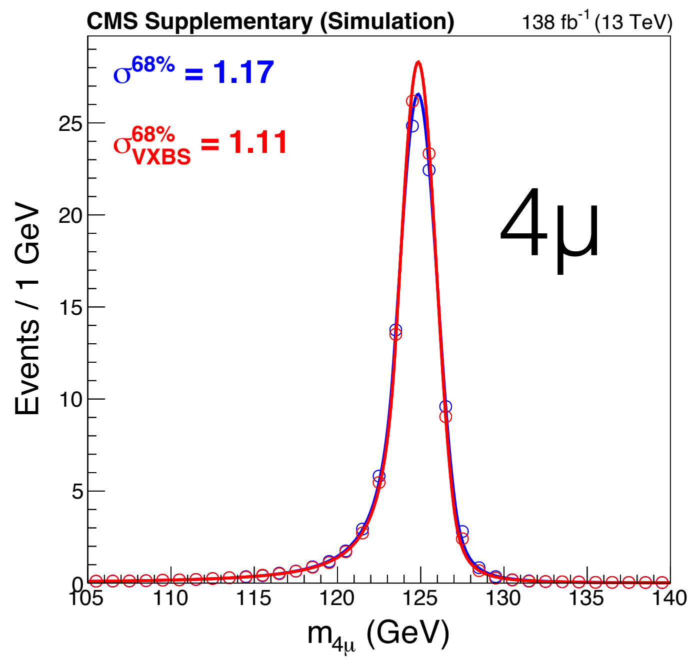

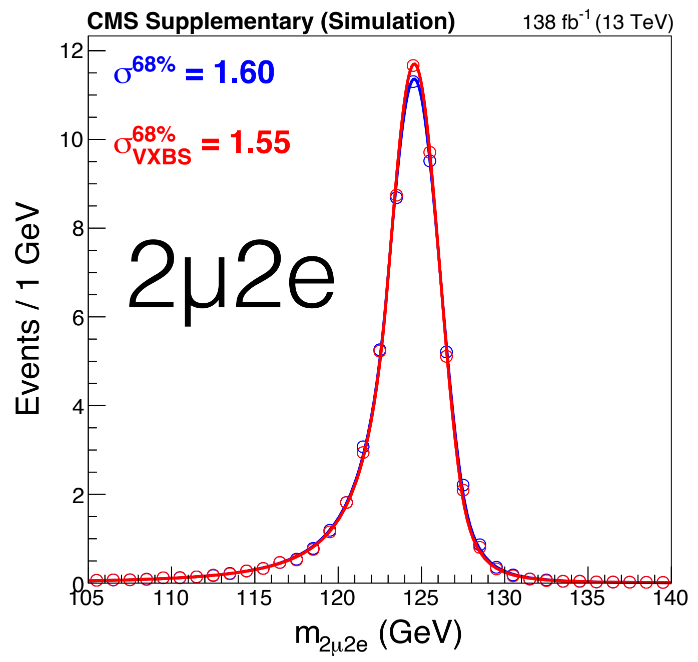

H→γγ mass distribution

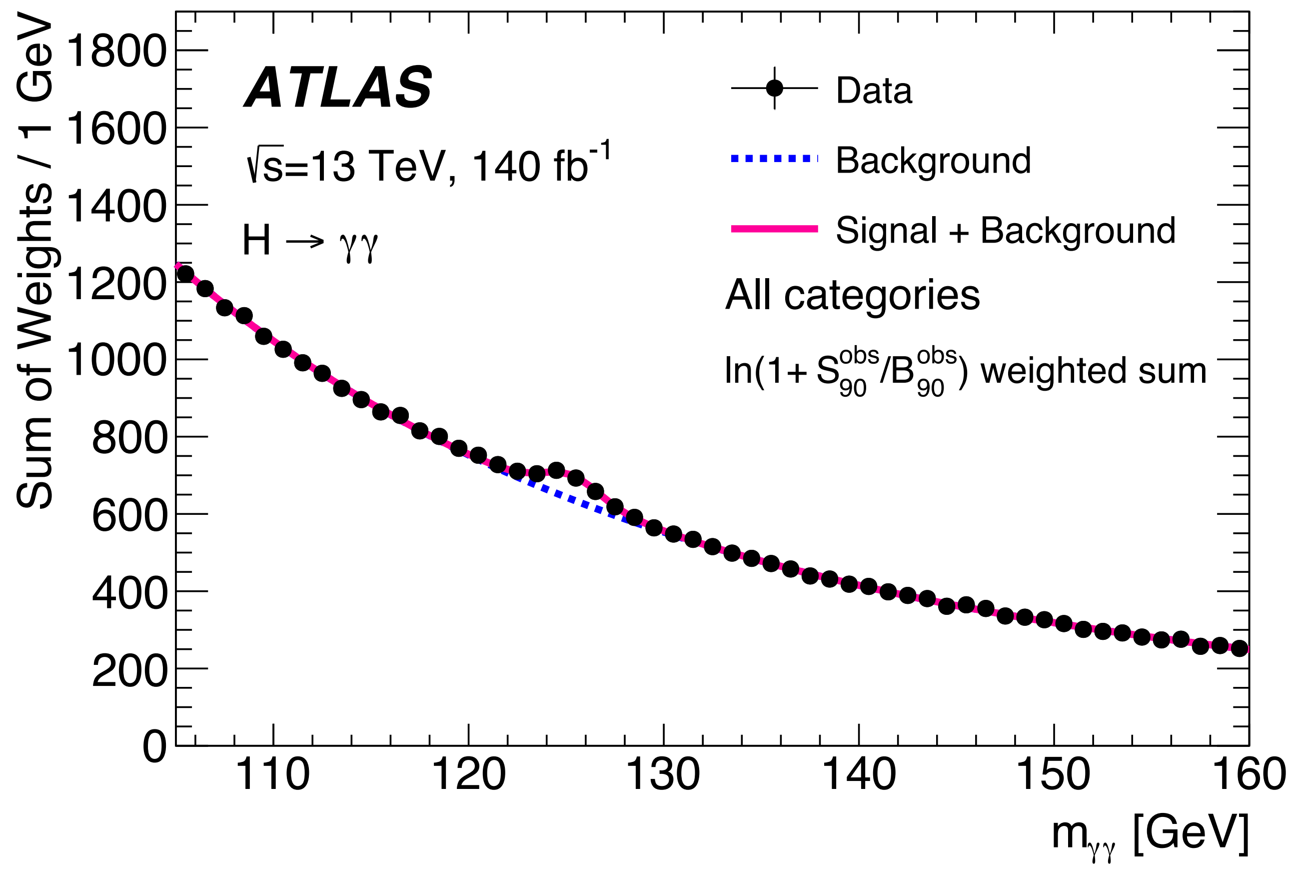

$m_{\gamma\gamma}$ in categories with the best and worst experimental resolutions categories

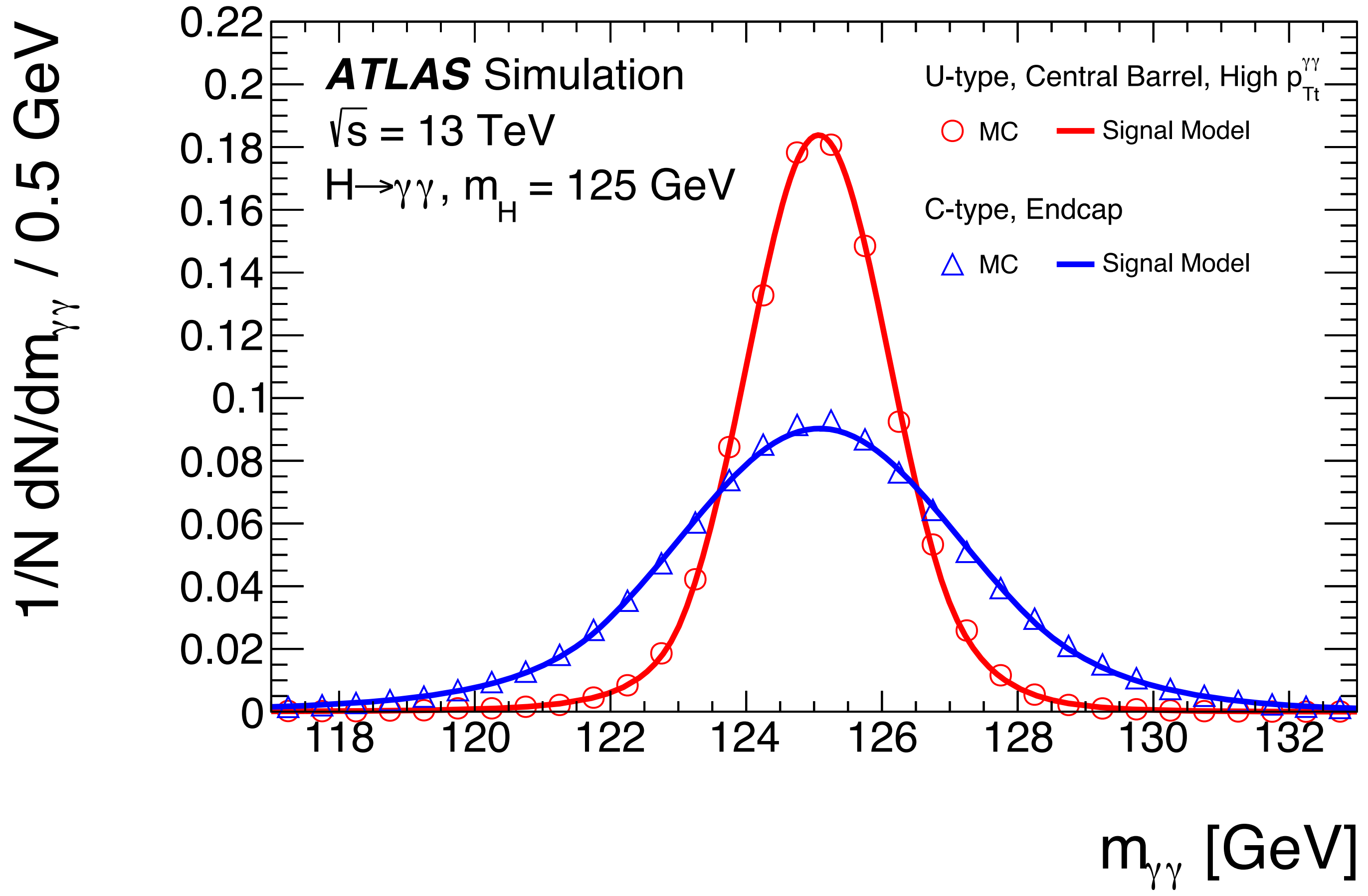

Measurement of Higgs boson mass

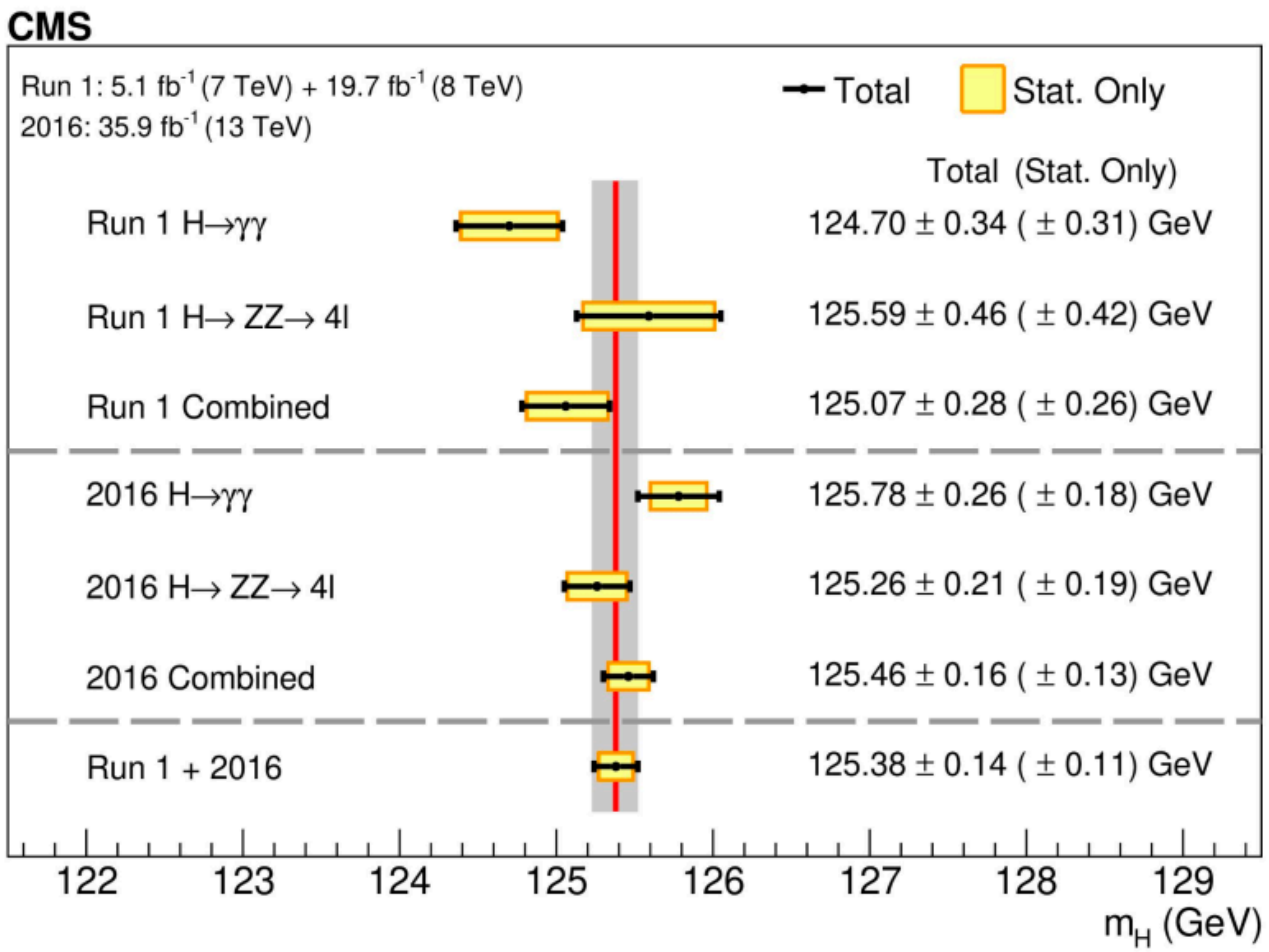

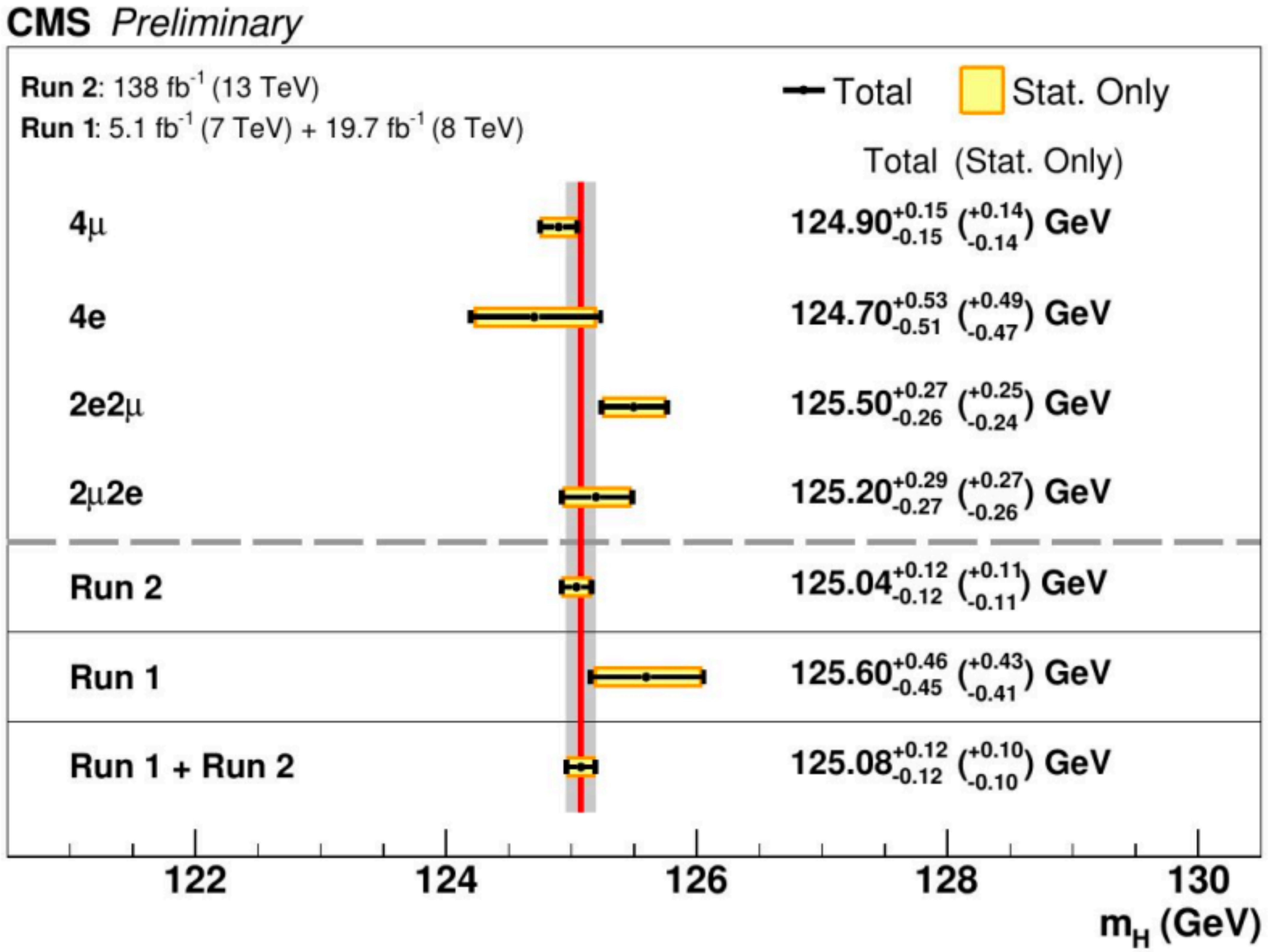

- Using two high resolution channels: H→γγ & H→ZZ*→4l
  - CMS+ATLAS Run1 combination: **m_H = 125.09 ± 0.24 GeV**
  - CMS: H→γγ & H→ZZ*→4l Run1 + 2016 data: **m_H = 125.38 ± 0.12 (±0.10 Stat. only) GeV**
  - CMS: H→ZZ*→4l Run 1+ Run 2 data: **m_H = 125.08 ± 0.14 (±0.11 Stat. only) GeV**
- Combined measurement still dominated by statistical uncertainty

Phys. Lett. B 805 (2020) 135425
Phys. Rev. Letters 131 (2023) 251802
Phys. Lett. B 843 (2023) 137880
HIG-21-019, submitted to PRD

Measurement of Higgs boson mass

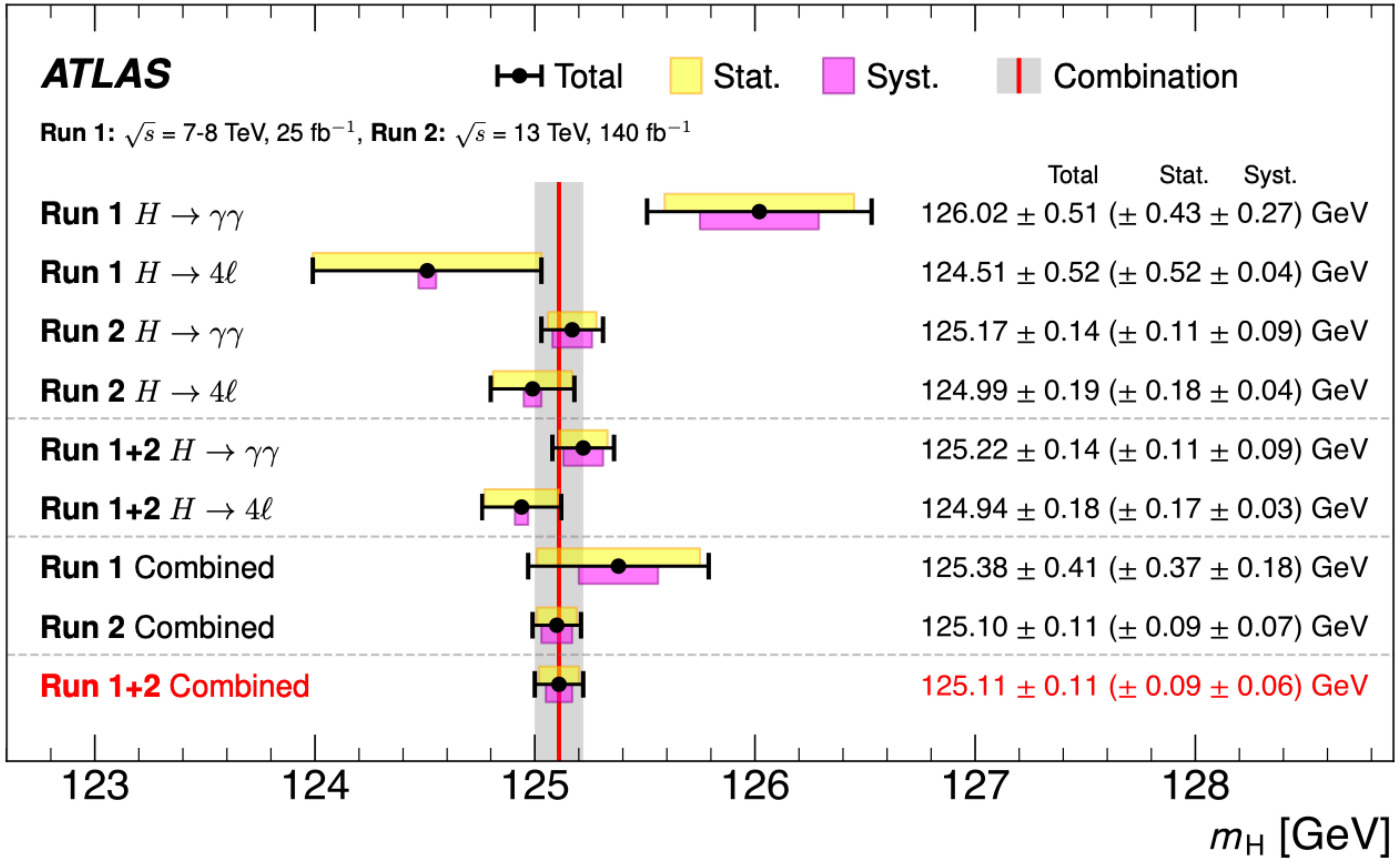

Phys. Lett. B 805 (2020) 135425
Phys. Rev. Letters 131 (2023) 251802
Phys. Lett. B 843 (2023) 137880
HIG-21-019, submitted to PRD

- Using two high resolution channels: H→γγ & H→ZZ*→4l
  - CMS+ATLAS Run1 combination: **m_H = 125.09 ± 0.24 GeV**
  - ATLAS Run 1 + Run 2 data: $m_H = 125.11 \pm 0.09(Stats.) \pm 0.06(Sys.)$ **GeV**
- Combined measurement still dominated by statistical uncertainty

Input channels to ATLAS and CMS combined measurements of Higgs boson couplings in Run 2

ATLAS: Nature 607, 52–59 (2022)

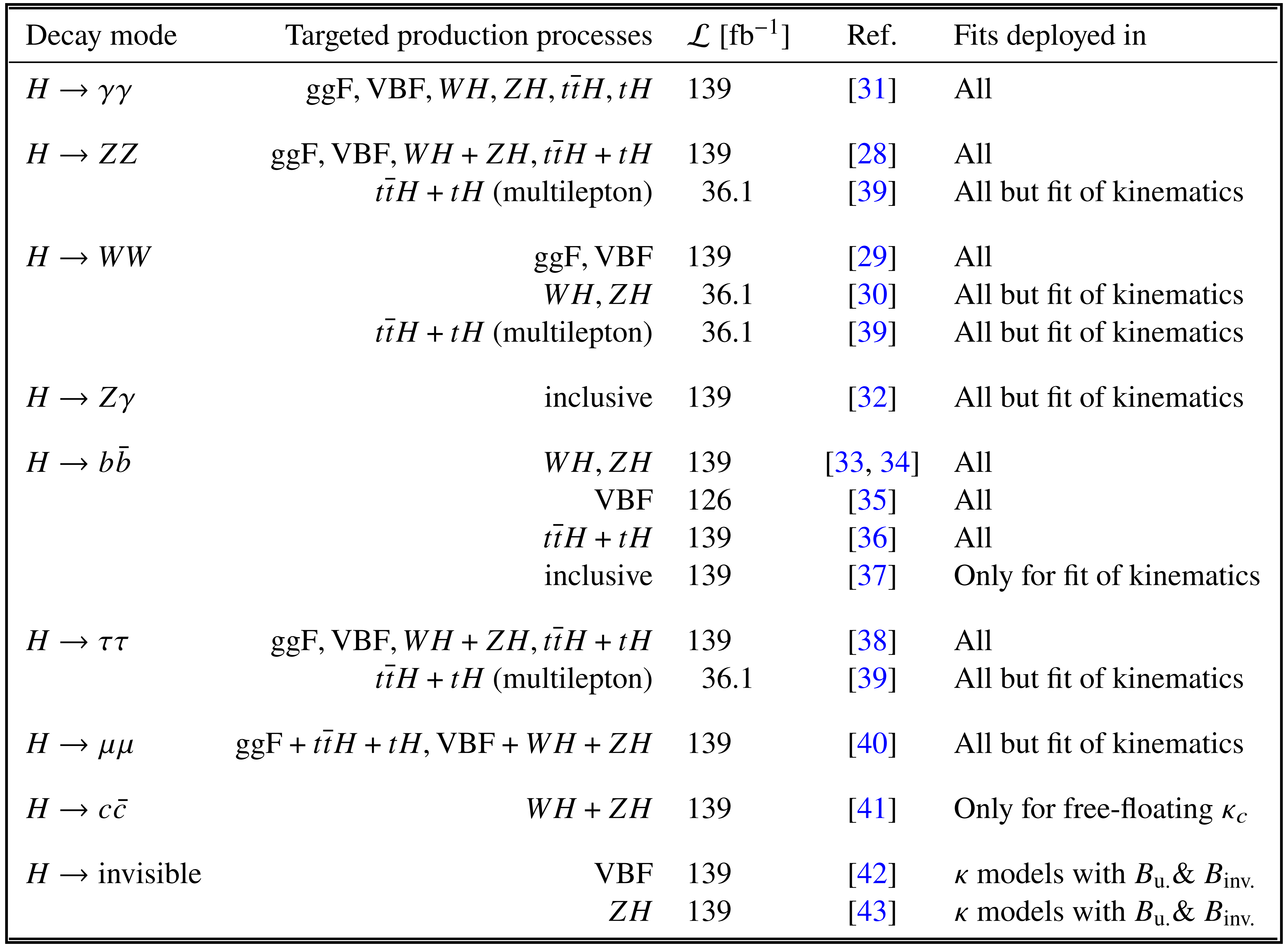

Decay mode	Targeted production processes	$\mathcal{L}$ [fb^{-1}]	Ref.	Fits deployed in
$H \to \gamma\gamma$	ggF, VBF, $WH, ZH, t\bar{t}H, tH$	139	[31]	All
$H \to ZZ$	ggF, VBF, $WH + ZH, t\bar{t}H + tH$	139	[28]	All
	$t\bar{t}H + tH$ (multilepton)	36.1	[39]	All but fit of kinematics
$H \to WW$	ggF, VBF	139	[29]	All
	WH, ZH	36.1	[30]	All but fit of kinematics
	$t\bar{t}H + tH$ (multilepton)	36.1	[39]	All but fit of kinematics
$H \to Z\gamma$	inclusive	139	[32]	All but fit of kinematics
$H \to b\bar{b}$	WH, ZH	139	[33, 34]	All
	VBF	126	[35]	All
	$t\bar{t}H + tH$	139	[36]	All
	inclusive	139	[37]	Only for fit of kinematics
$H \to \tau\tau$	ggF, VBF, $WH + ZH, t\bar{t}H + tH$	139	[38]	All
	$t\bar{t}H + tH$ (multilepton)	36.1	[39]	All but fit of kinematics
$H \to \mu\mu$	ggF + $t\bar{t}H + tH$, VBF + $WH + ZH$	139	[40]	All but fit of kinematics
$H \to c\bar{c}$	$WH + ZH$	139	[41]	Only for free-floating κ_c
$H \to$ invisible	VBF	139	[42]	κ models with $B_{\text{u.}}$& $B_{\text{inv.}}$
	ZH	139	[43]	κ models with $B_{\text{u.}}$& $B_{\text{inv.}}$

CMS: Nature 607, 60–68 (2022)

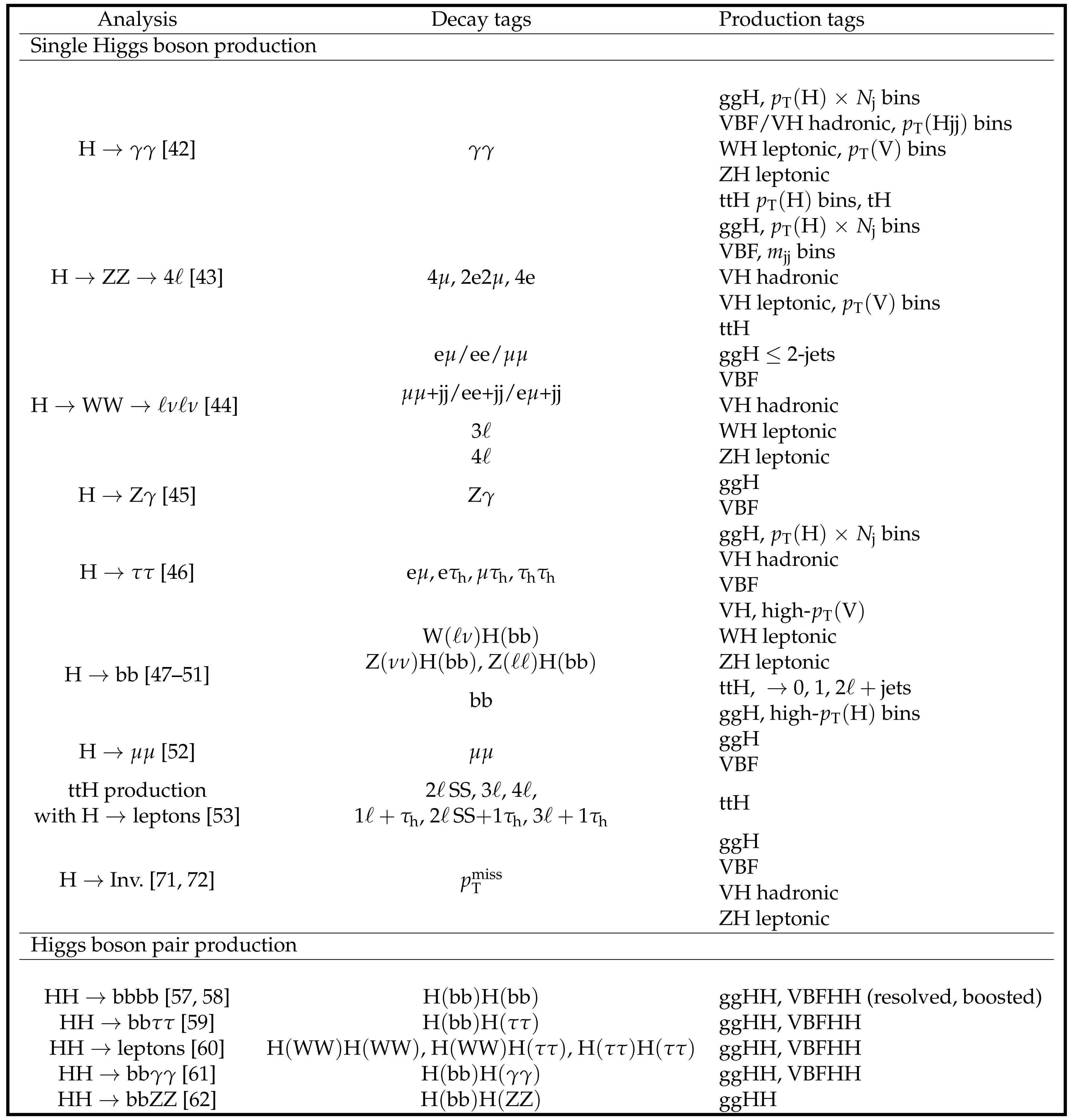

Analysis	Decay tags	Production tags
Single Higgs boson production		
H $\to \gamma\gamma$ [42]	$\gamma\gamma$	ggH, p_{T}(H) $\times$ N_{j} bins VBF/VH hadronic, p_{T}(Hjj) bins WH leptonic, p_{T}(V) bins ZH leptonic ttH p_{T}(H) bins, tH
H $\to$ ZZ $\to 4\ell$ [43]	4μ, $2e2\mu$, 4e	ggH, p_{T}(H) $\times$ N_{j} bins VBF, m_{jj} bins VH hadronic VH leptonic, p_{T}(V) bins ttH
H $\to$ WW $\to \ell\nu\ell\nu$ [44]	$e\mu/ee/\mu\mu$ $\mu\mu$+jj/ee+jj/$e\mu$+jj 3ℓ 4ℓ	ggH $\leq$ 2-jets VBF VH hadronic WH leptonic ZH leptonic
H $\to Z\gamma$ [45]	$Z\gamma$	ggH VBF
H $\to \tau\tau$ [46]	$e\mu, e\tau_{\mathrm{h}}, \mu\tau_{\mathrm{h}}, \tau_{\mathrm{h}}\tau_{\mathrm{h}}$	ggH, p_{T}(H) $\times$ N_{j} bins VH hadronic VBF
H $\to$ bb [47–51]	W($\ell\nu$)H(bb) Z($\nu\nu$)H(bb), Z($\ell\ell$)H(bb) bb	VH, high-p_{T}(V) WH leptonic ZH leptonic ttH, $\to 0, 1, 2\ell +$ jets ggH, high-p_{T}(H) bins
H $\to \mu\mu$ [52]	$\mu\mu$	ggH VBF
ttH production with H $\to$ leptons [53]	2ℓ SS, 3ℓ, 4ℓ, $1\ell + \tau_{\mathrm{h}}$, 2ℓ SS+$1\tau_{\mathrm{h}}$, $3\ell + 1\tau_{\mathrm{h}}$	ttH
H $\to$ Inv. [71, 72]	$p_{\mathrm{T}}^{\mathrm{miss}}$	ggH VBF VH hadronic ZH leptonic
Higgs boson pair production		
HH $\to$ bbbb [57, 58]	H(bb)H(bb)	ggHH, VBFHH (resolved, boosted)
HH $\to$ bb$\tau\tau$ [59]	H(bb)H($\tau\tau$)	ggHH, VBFHH
HH $\to$ leptons [60]	H(WW)H(WW), H(WW)H($\tau\tau$), H($\tau\tau$)H($\tau\tau$)	ggHH, VBFHH
HH $\to$ bb$\gamma\gamma$ [61]	H(bb)H($\gamma\gamma$)	ggHH, VBFHH
HH $\to$ bbZZ [62]	H(bb)H(ZZ)	ggHH

Input channels for couplings and STXS combination

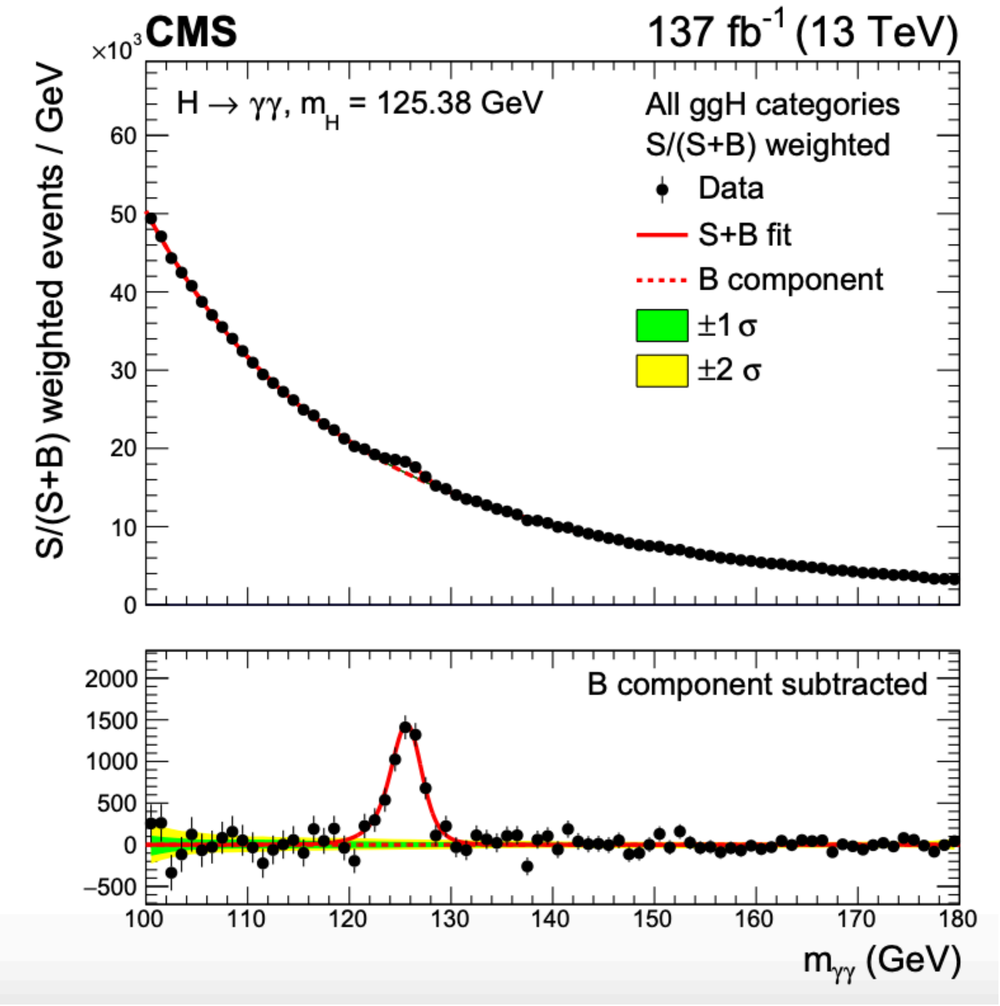

H→γγ

JHEP 07 027(2021)

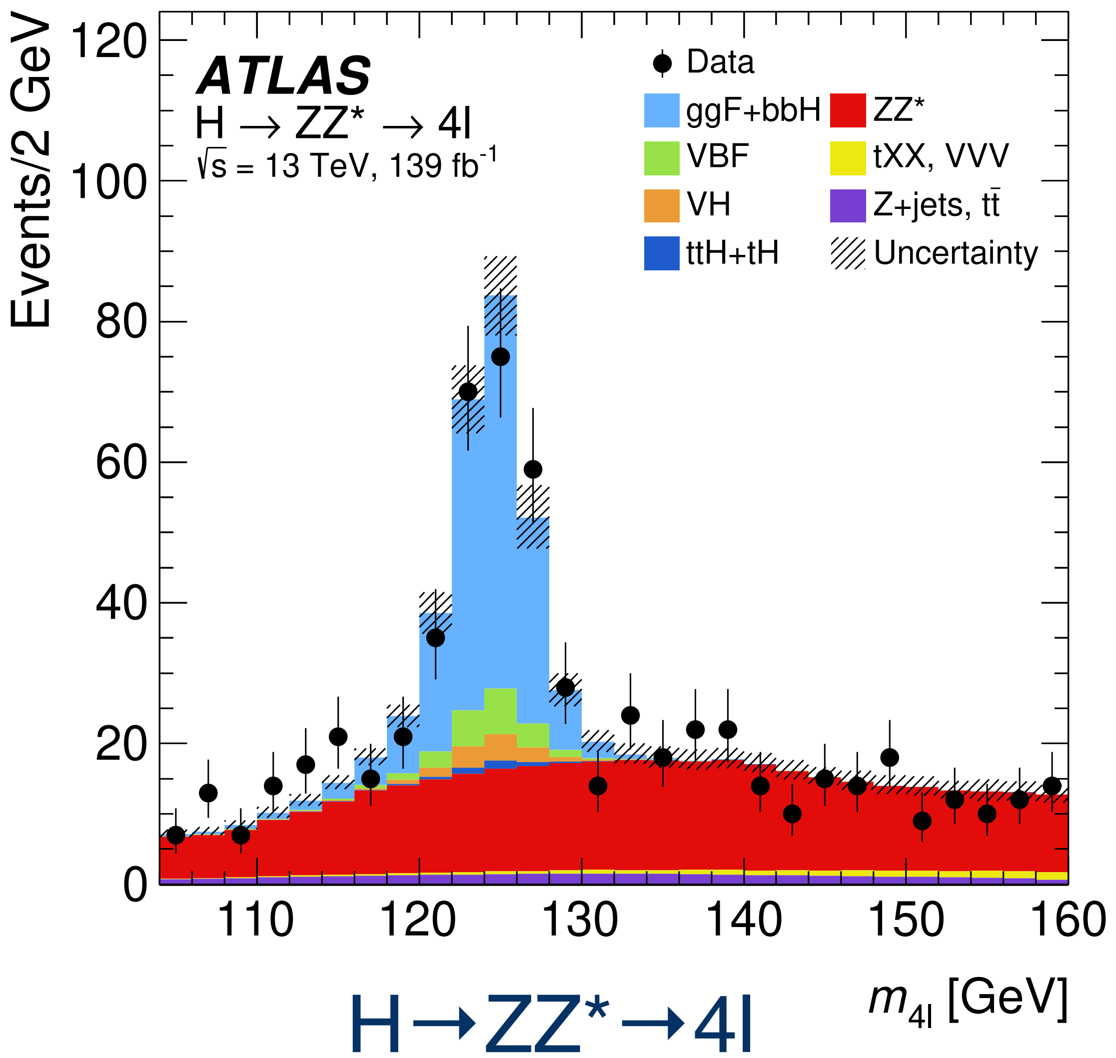

H→ZZ*→4l

EPJC 80 (2020) 957

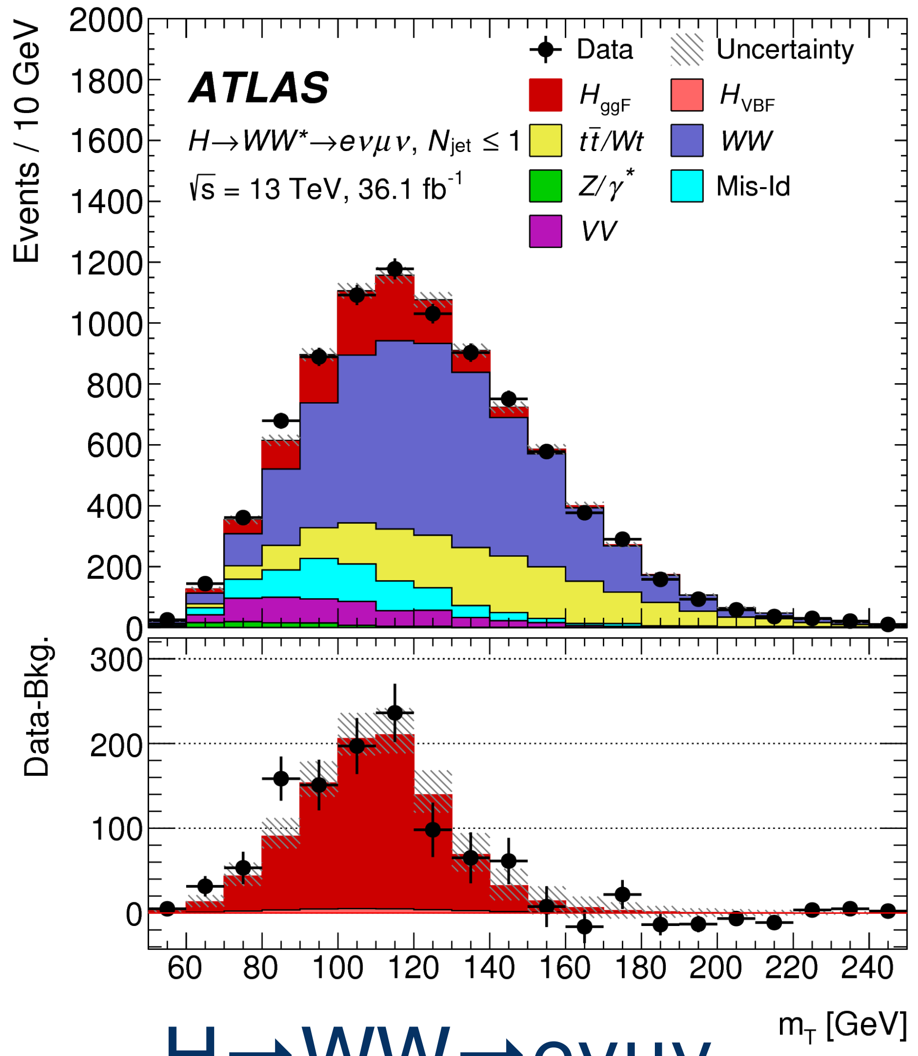

H→WW→eνμν

PLB 789 (2019) 508

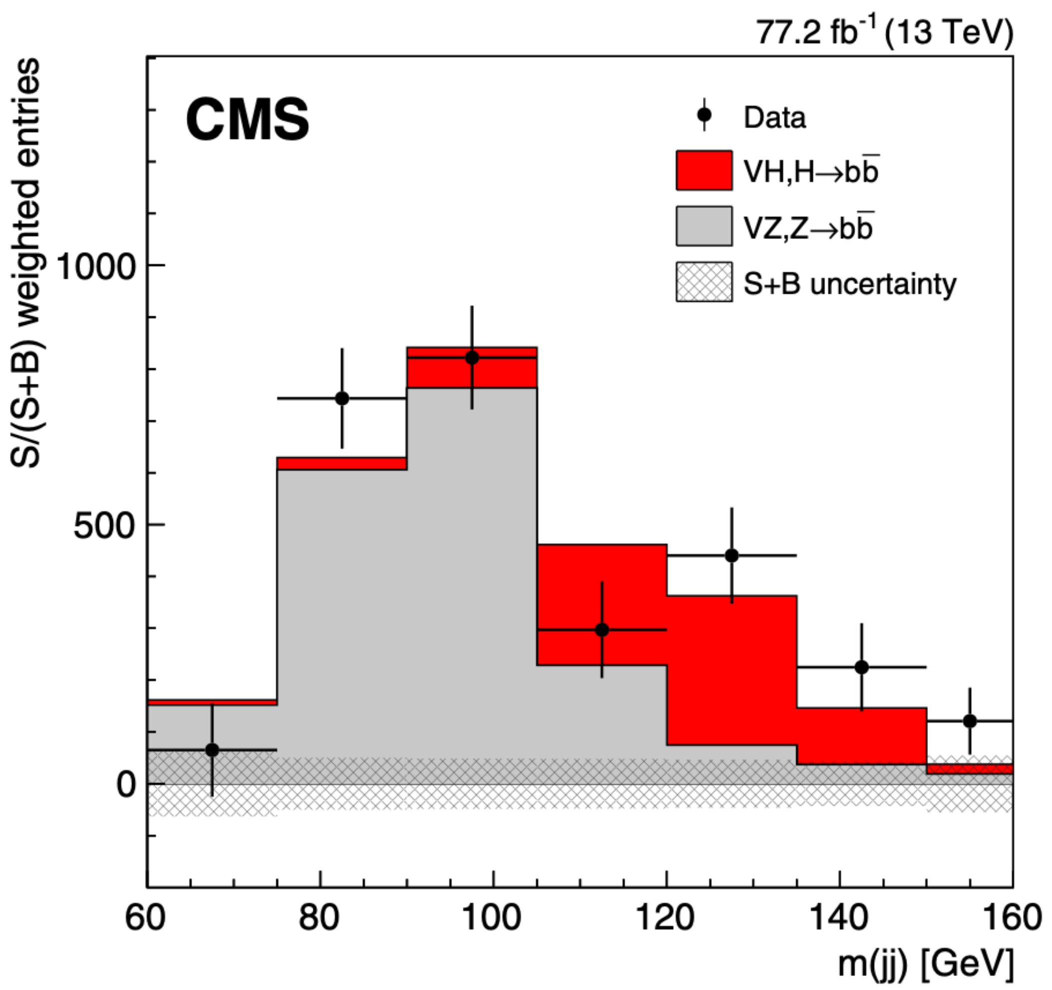

VH, H→bb

PRL 121 121801

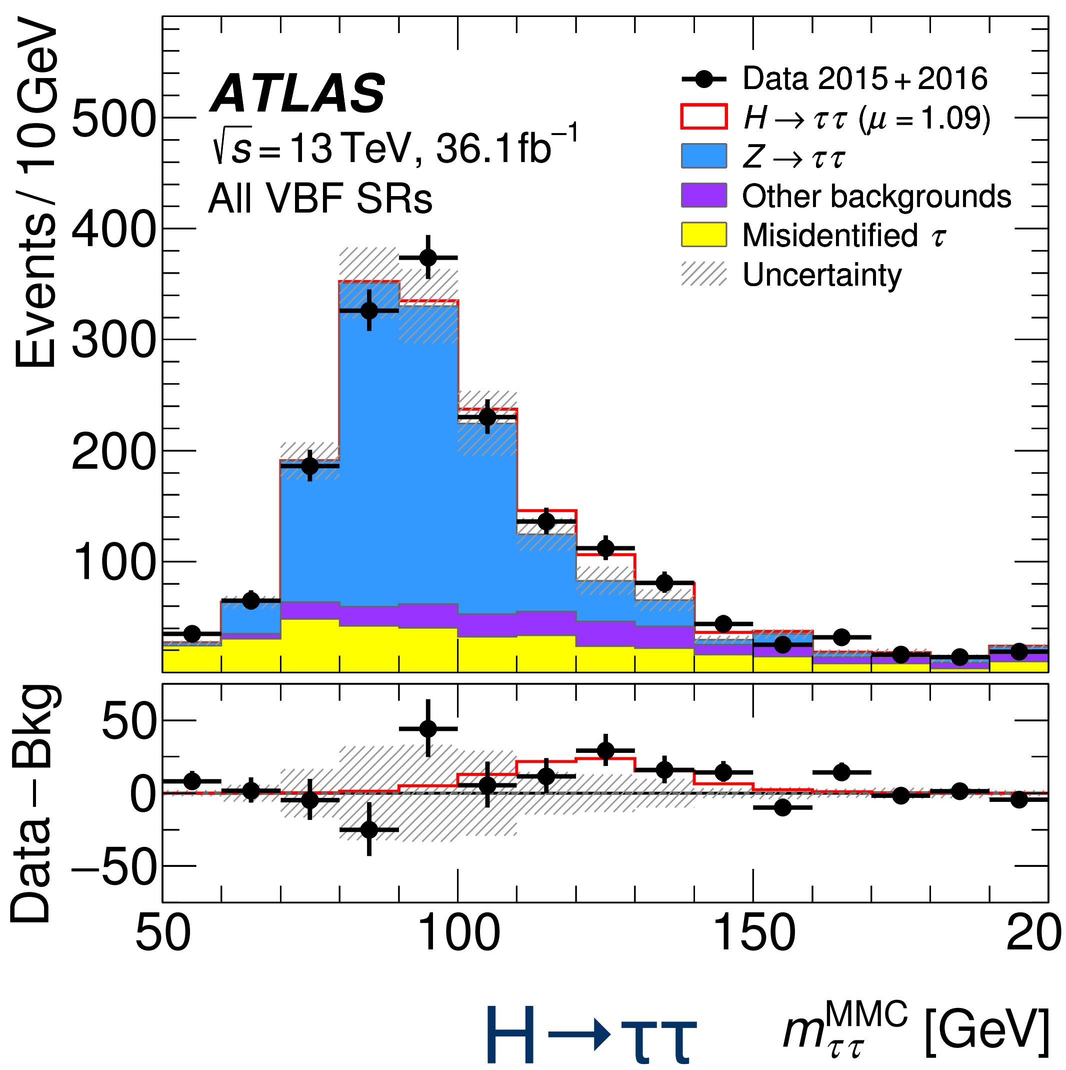

H→ττ

PRD 99 (2019) 072001

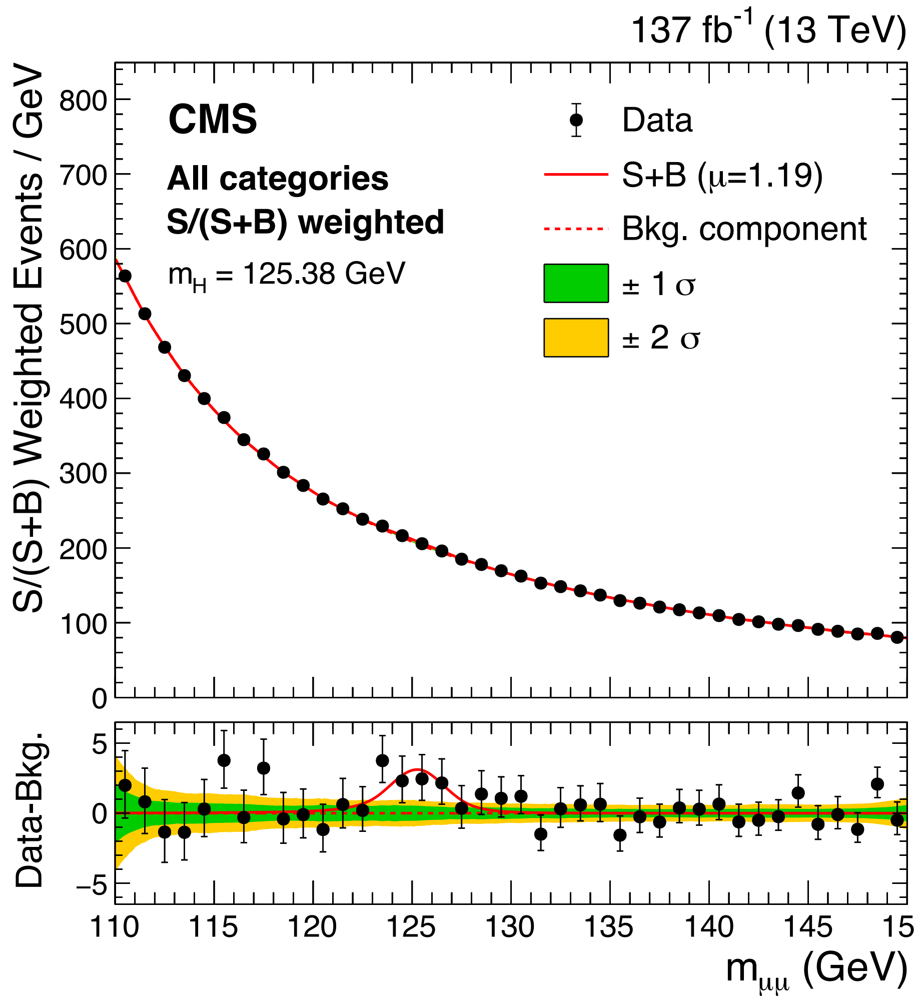

H→μμ

JHEP 01 (2021) 148

Input channels for couplings and STXS combination

ttH multi-lepton (H→ZZ, WW, ττ)
PRD 97 (2018) 072003

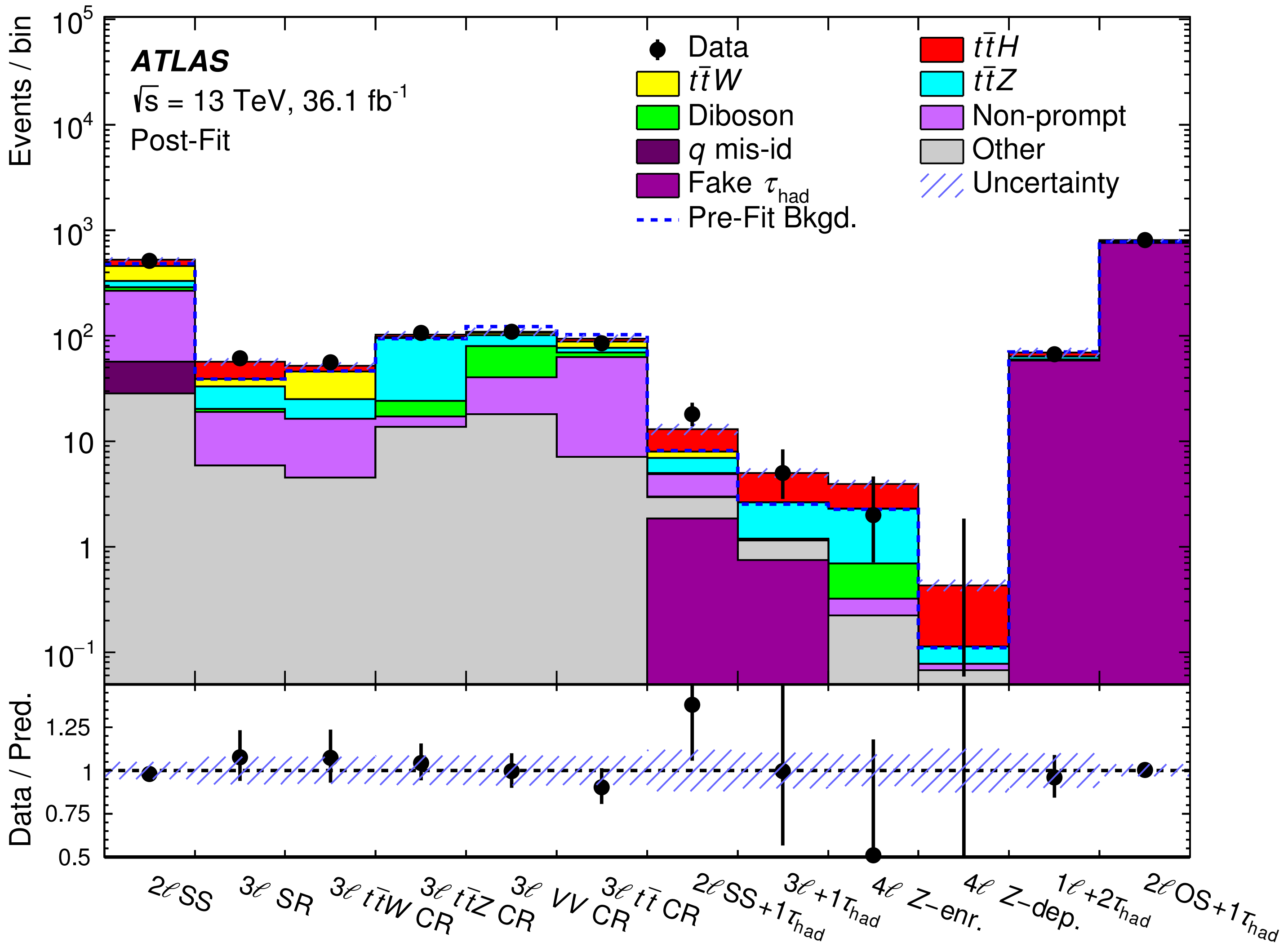

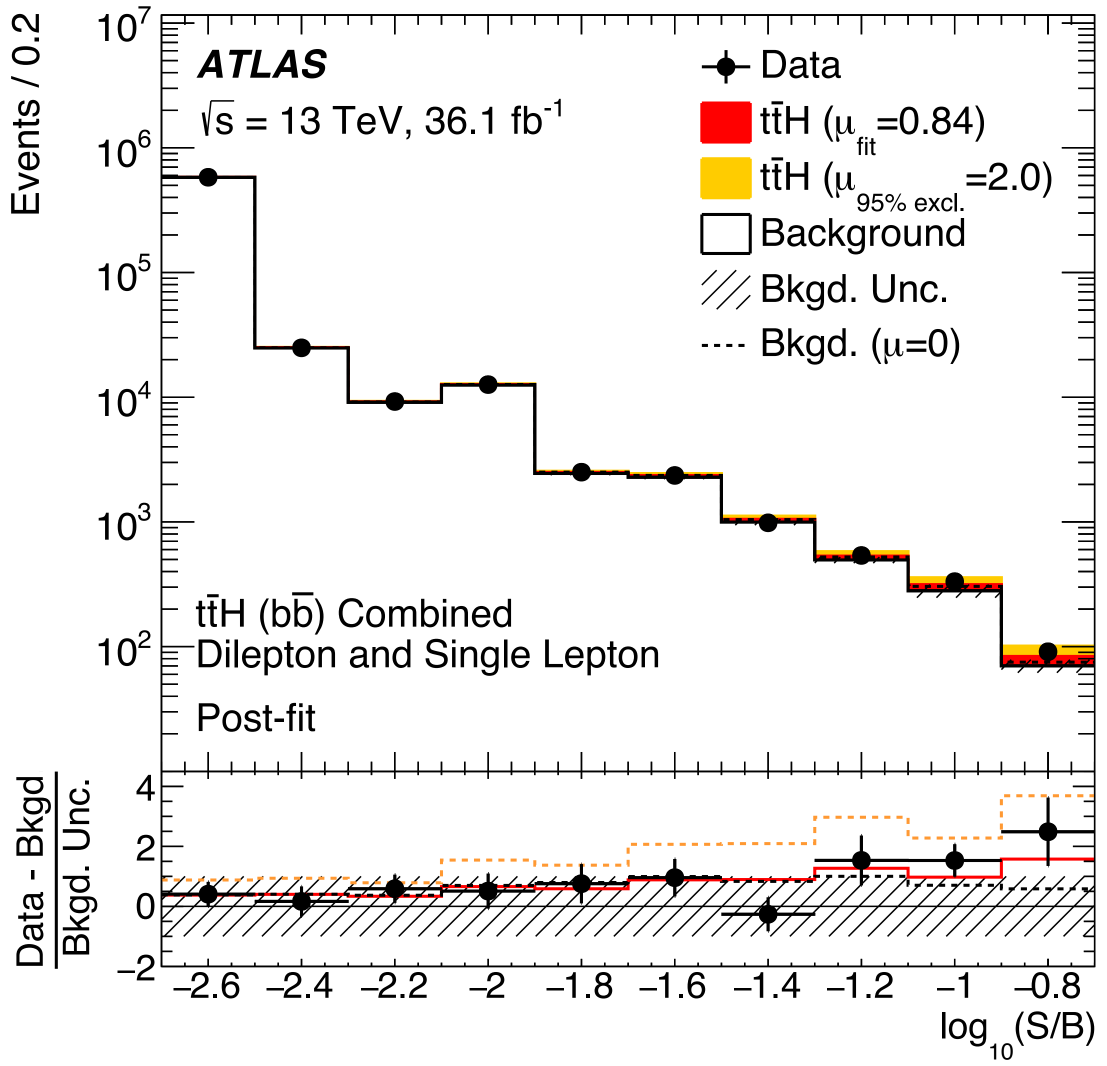

ttH, H→bb
PRD 97 (2018) 072016

H→Zγ
JHEP 01 (2021) 148

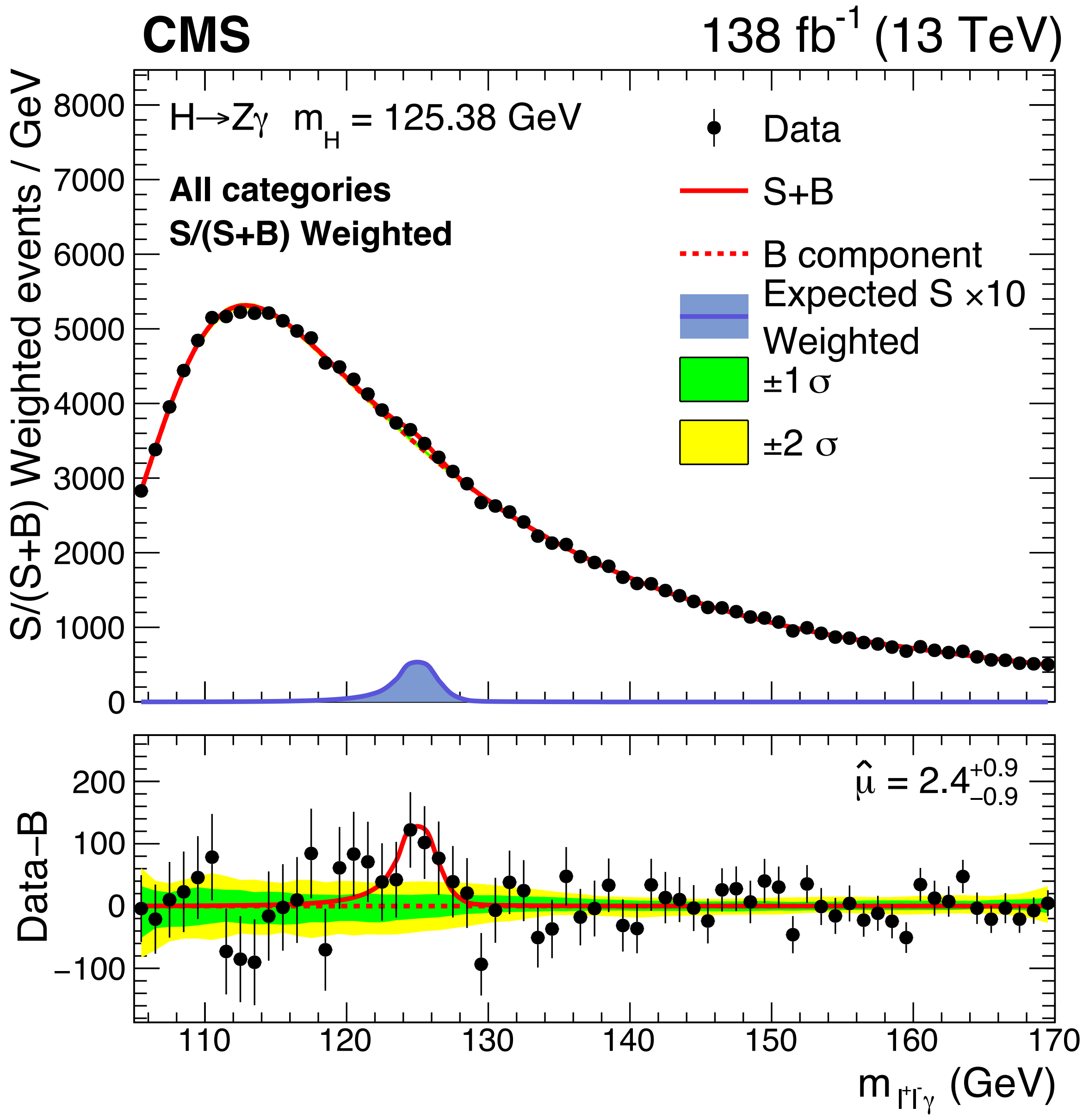

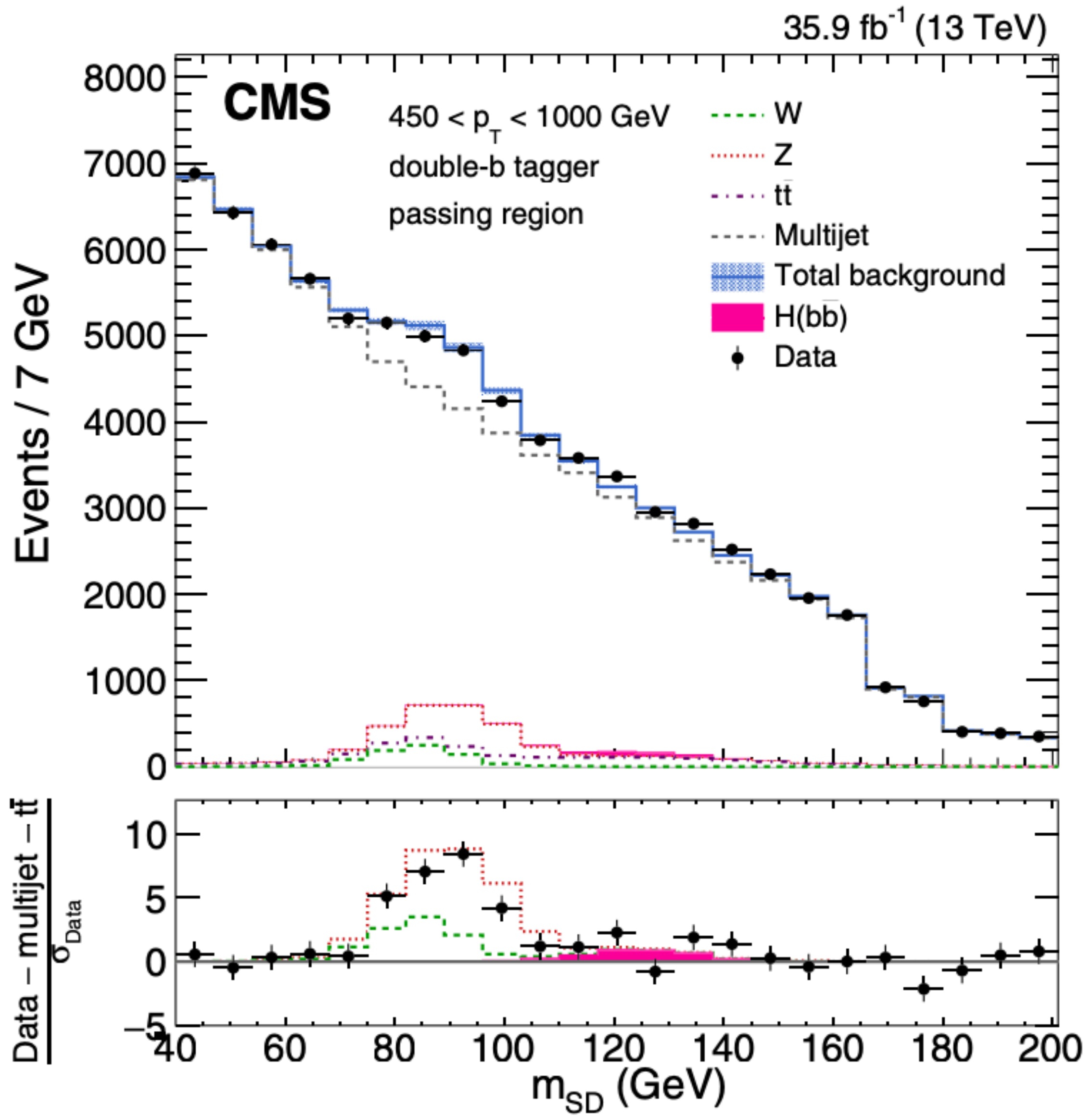

boosted H→bb
Phys. Rev. Lett. 120, 071802

Higgs boson production and decay rates

Signal strength: **$\mu = N_{\text{signal}}(\text{obs.})/N_{\text{signal}}(\text{exp.})$**

Nature 607, 52–59 (2022)

Inclusive signal strength:

$$\boxed{\mu = 1.05 \pm 0.06 = 1.05 \pm 0.03(\text{stat.}) \pm 0.03(\text{exp.}) \pm 0.04(\text{sig. th.}) \pm 0.02(\text{bkg. th.})}$$

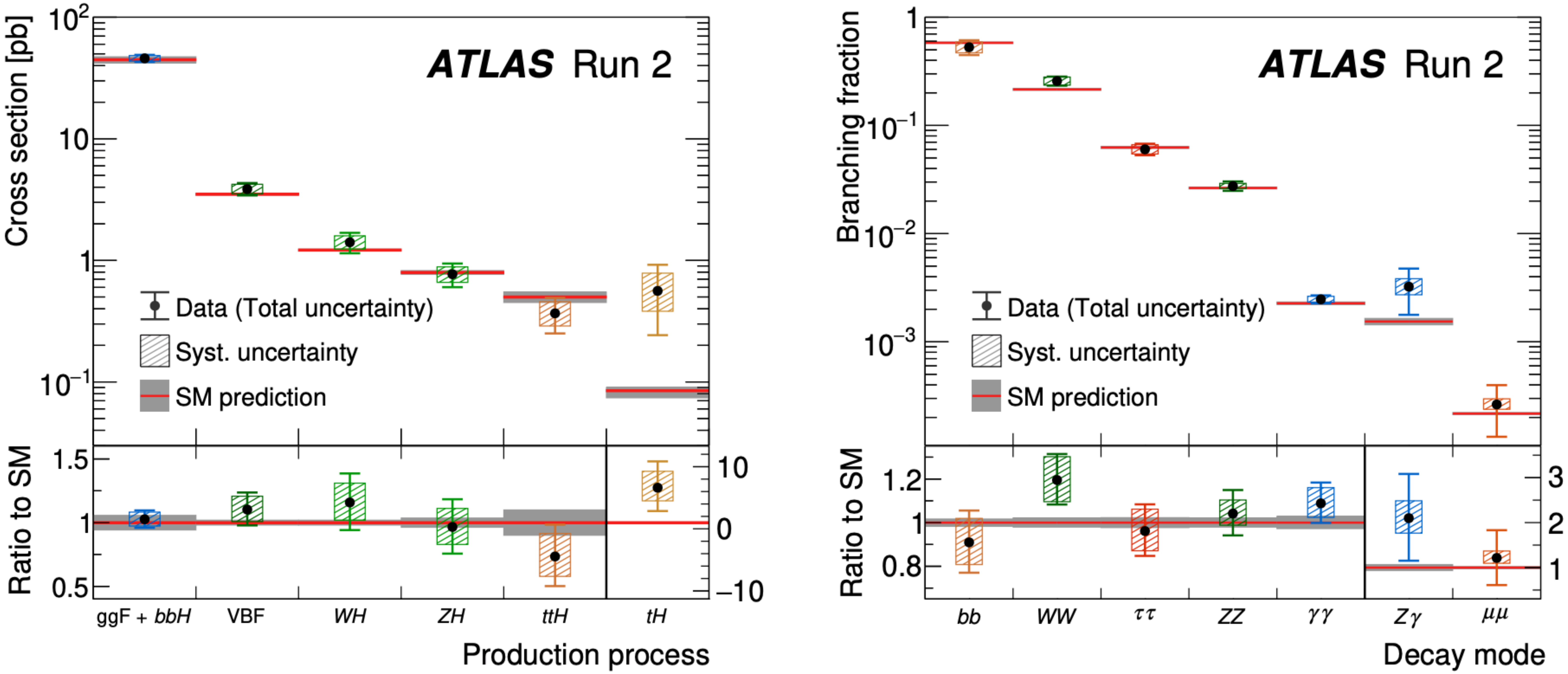

- Good compatibility among decay channels and with SM

Higgs boson production and decay rates

Inclusive signal strength: $\mu = 1.002 \pm 0.057$

Nature 607, 60–68 (2022)

- Good compatibility among decay channels and with SM

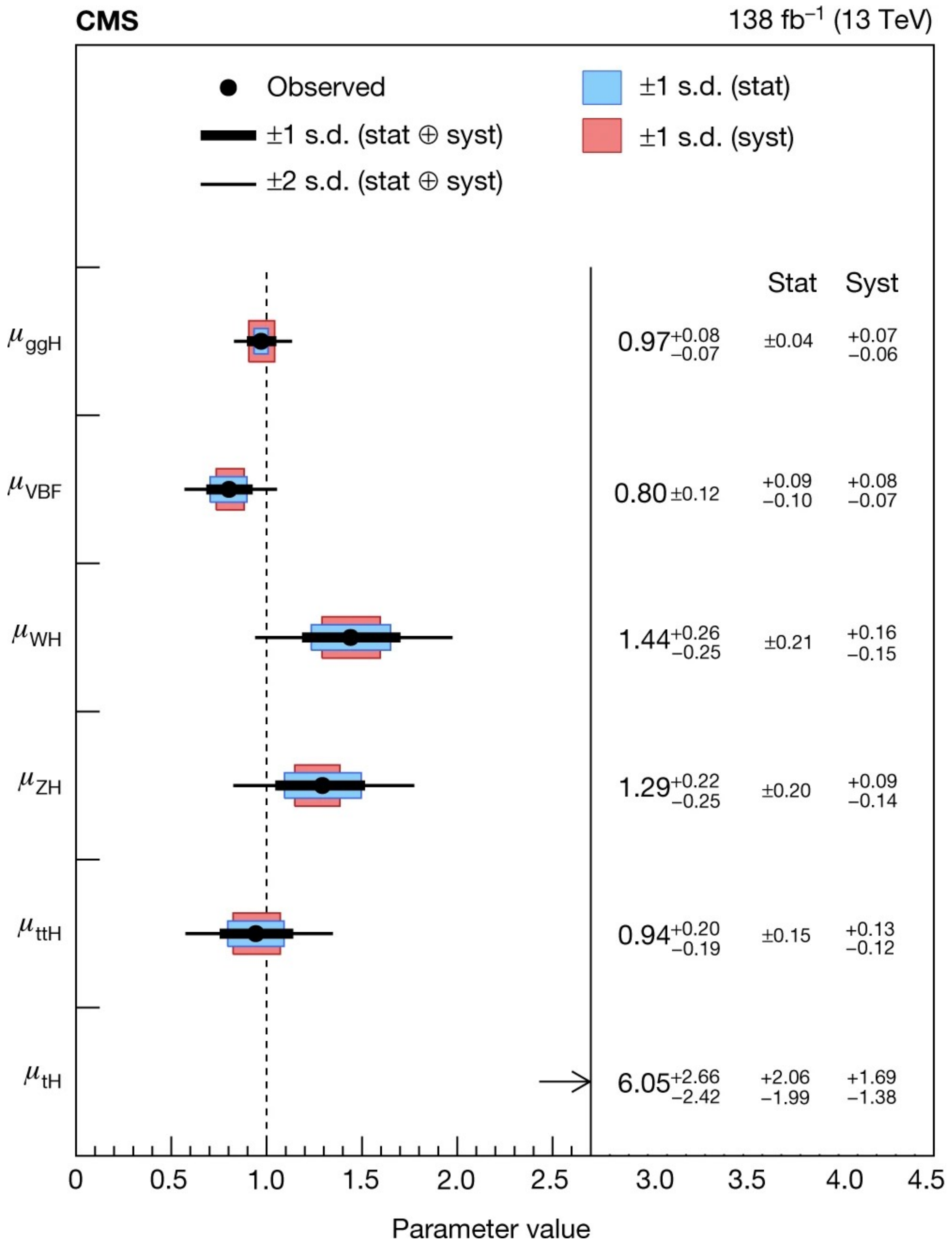

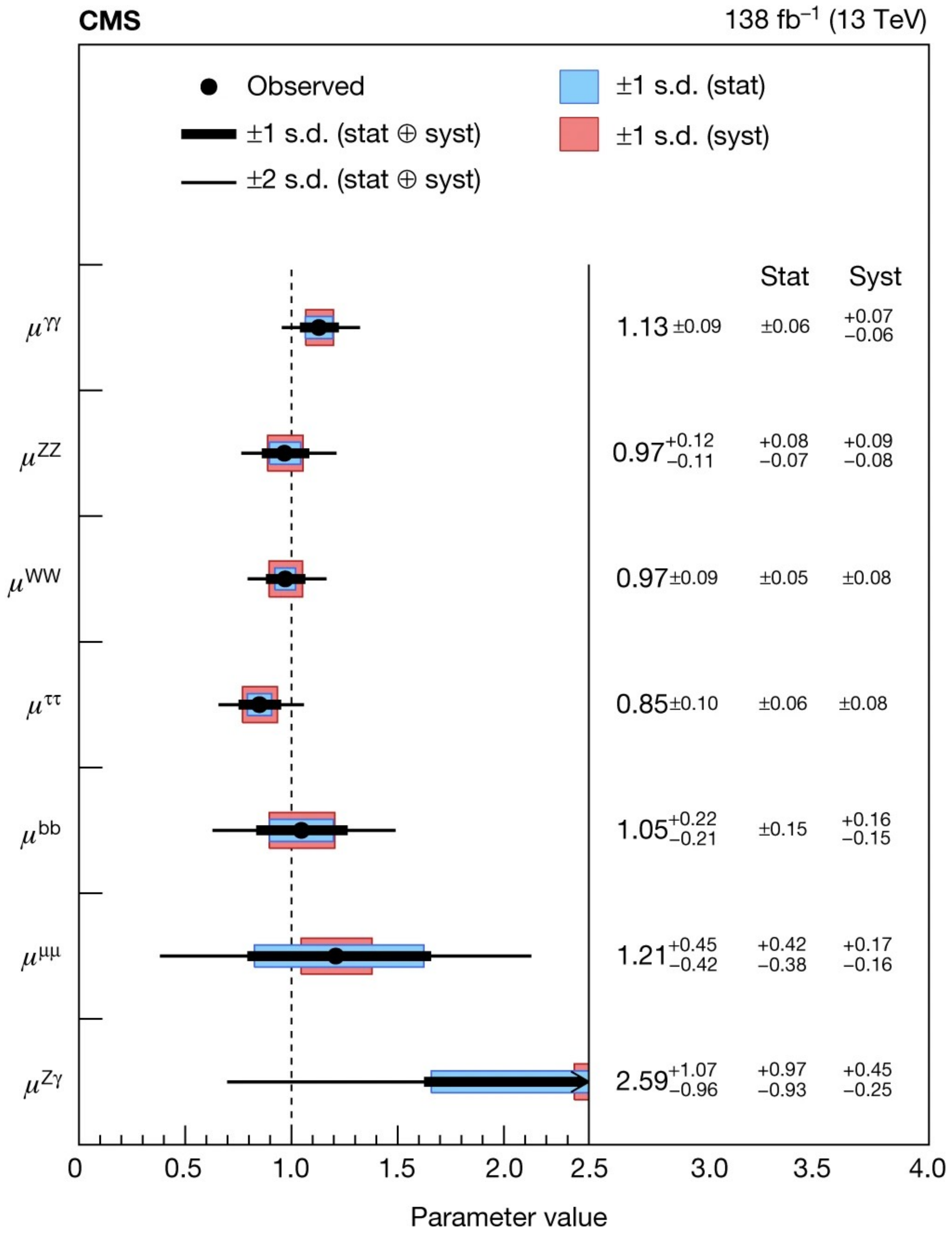

Higgs boson couplings: κ-framework

- Leading order framework to characterize possible deviations from the SM: assign coupling modifier to each (effective) interaction vertex (e.g. κ_W, κ_Z, κ_t…) and total width (κ_H)
- Assumptions: single resonance, zero width, SM tensor structure $J^P = 0^+$
- Coupling Compatibility Tests using κ and their ratios

Cross section for production and decay i→H→f parametrized as

SM cross sections and widths scaled by coupling modifiers

$$\sigma \cdot B(i \to H \to f) = \frac{\sigma_i \cdot \Gamma_f}{\Gamma_H} = \boxed{\frac{\sigma_i^{SM} \cdot \Gamma_f^{SM}}{\Gamma_H^{SM}}} \cdot \boxed{\left(\frac{\kappa_i^2 \kappa_f^2}{\kappa_H^2}\right)}$$

coupling modifiers: $\kappa_i^2 = \frac{\sigma_i}{\sigma_i^{SM}}$ Production $\kappa_f^2 = \frac{\Gamma_f}{\Gamma_f^{SM}}$ Decay $\kappa_H^2 = \frac{\sum \Gamma_f}{\sum \Gamma_f^{SM}}$ Total width

https://doi.org/10.5170/CERN-2013-004

Example: $gg \to H \to \gamma\gamma$

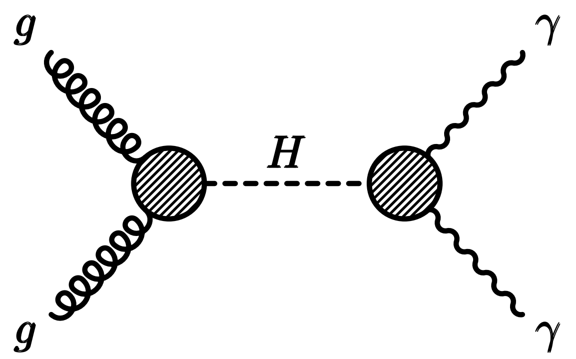

Assume only SM particles contribute in the loops

Nature 607, 52–59 (2022)

$$\frac{\sigma \times BR(gg \to H \to \gamma\gamma)}{\sigma \times BR(gg \to H \to \gamma\gamma)_{SM}} = \underline{\kappa_g^2}\frac{\kappa_\gamma^2}{\underline{\kappa_H^2}} = \underline{(1.040\kappa_t^2 + 0.002\kappa_b^2 - 0.038\kappa_t\kappa_b - 0.005\kappa_t\kappa_c)}\underline{\frac{1.589\kappa_W^2 + 0.072\kappa_t^2 - 0.674\kappa_W\kappa_t + 0.009\kappa_W\kappa_\tau + 0.008\kappa_W\kappa_b - 0.002\kappa_t\kappa_b - 0.002\kappa_t\kappa_\tau}{\kappa_H^2(\kappa_b, \kappa_W, \kappa_\tau, \ldots)}}$$

Higgs boson couplings to massive gauge bosons vs fermions

- κ_V and κ_F, scaling the Higgs boson couplings to massive gauge bosons and to fermions
- κ_V and κ_F measured to be in agreement with SM prediction, within ~10% uncertainty

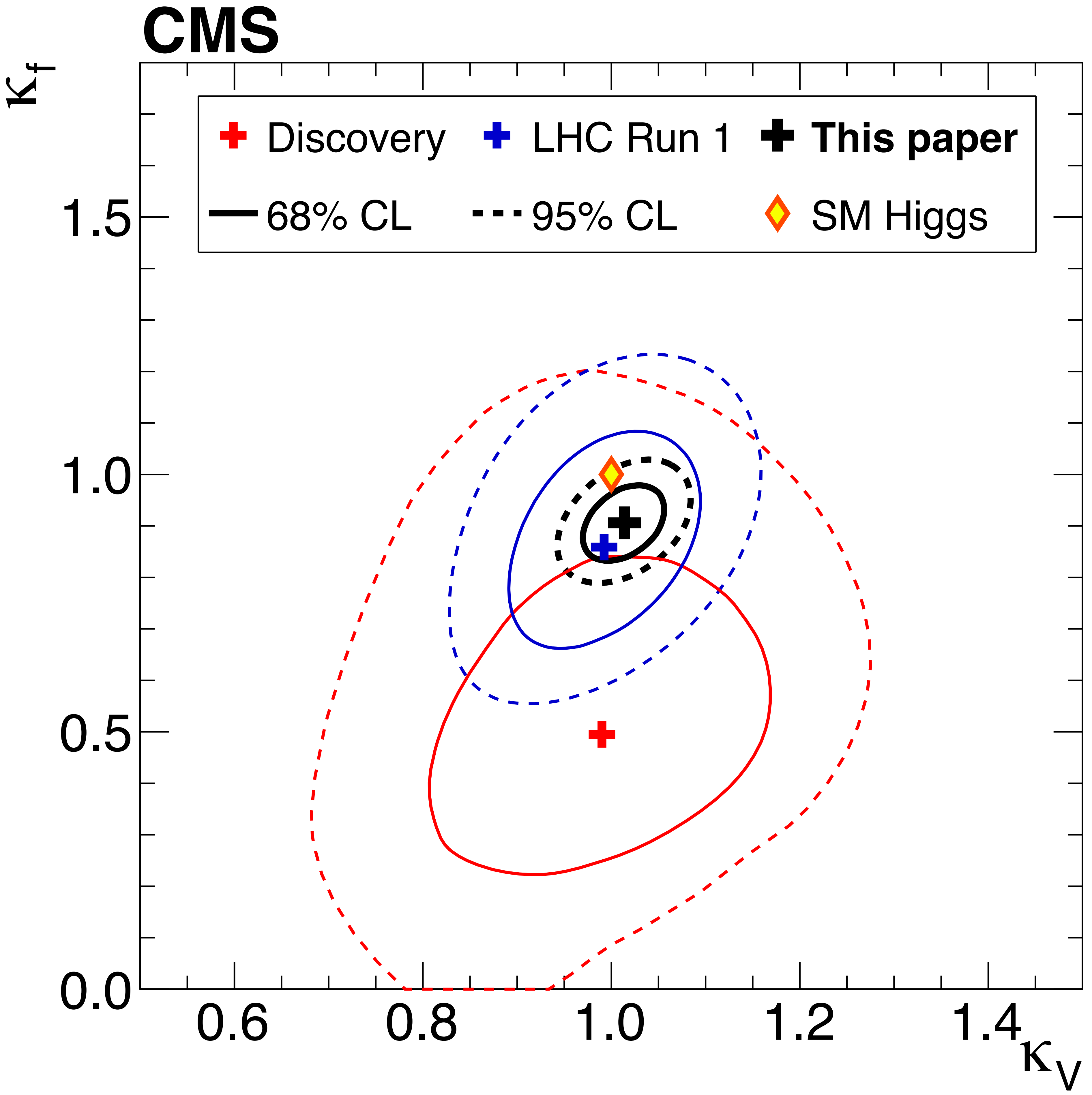

Nature 607, 60–68 (2022)

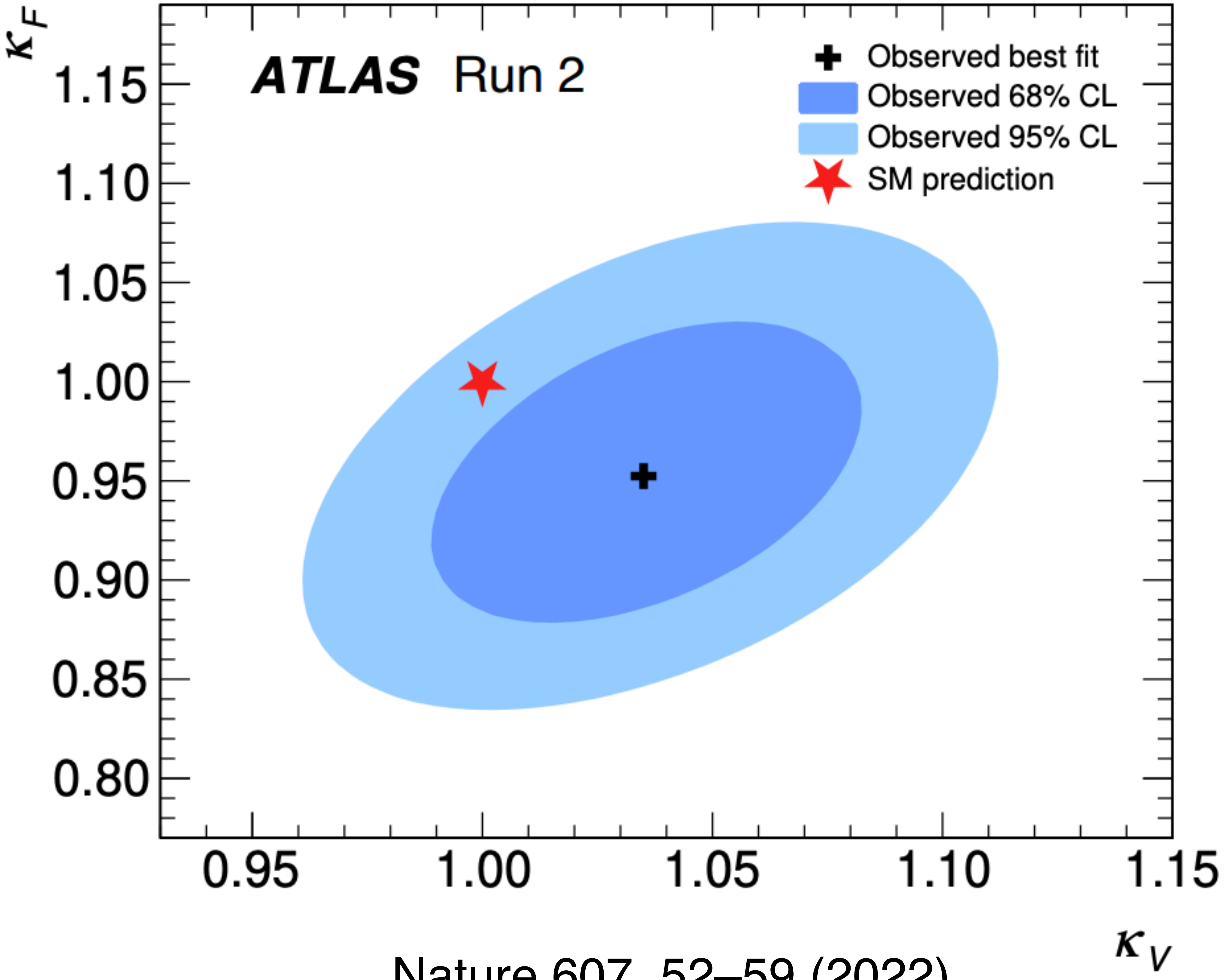

Nature 607, 52–59 (2022)

Higgs boson couplings vs particle mass

- Measure coupling modifiers κ for the massive gauge bosons (κ_W and κ_Z) and fermions probed in the present analyses (κ_t, κ_b, κ_τ, κ_μ and κ_c)
- Predictions for processes in SM occur via loops of intermediate virtual particles computed in terms of κ_i

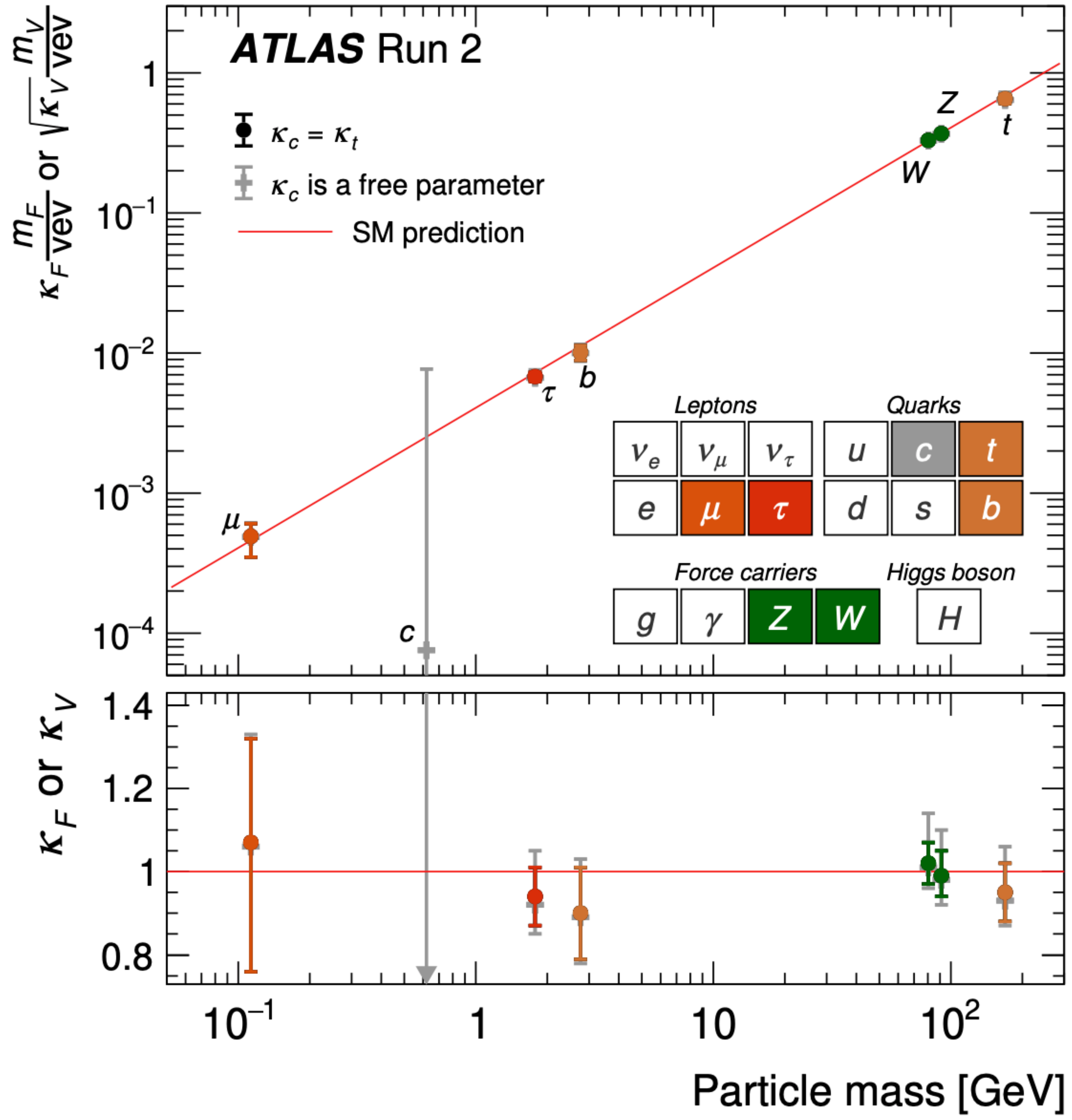

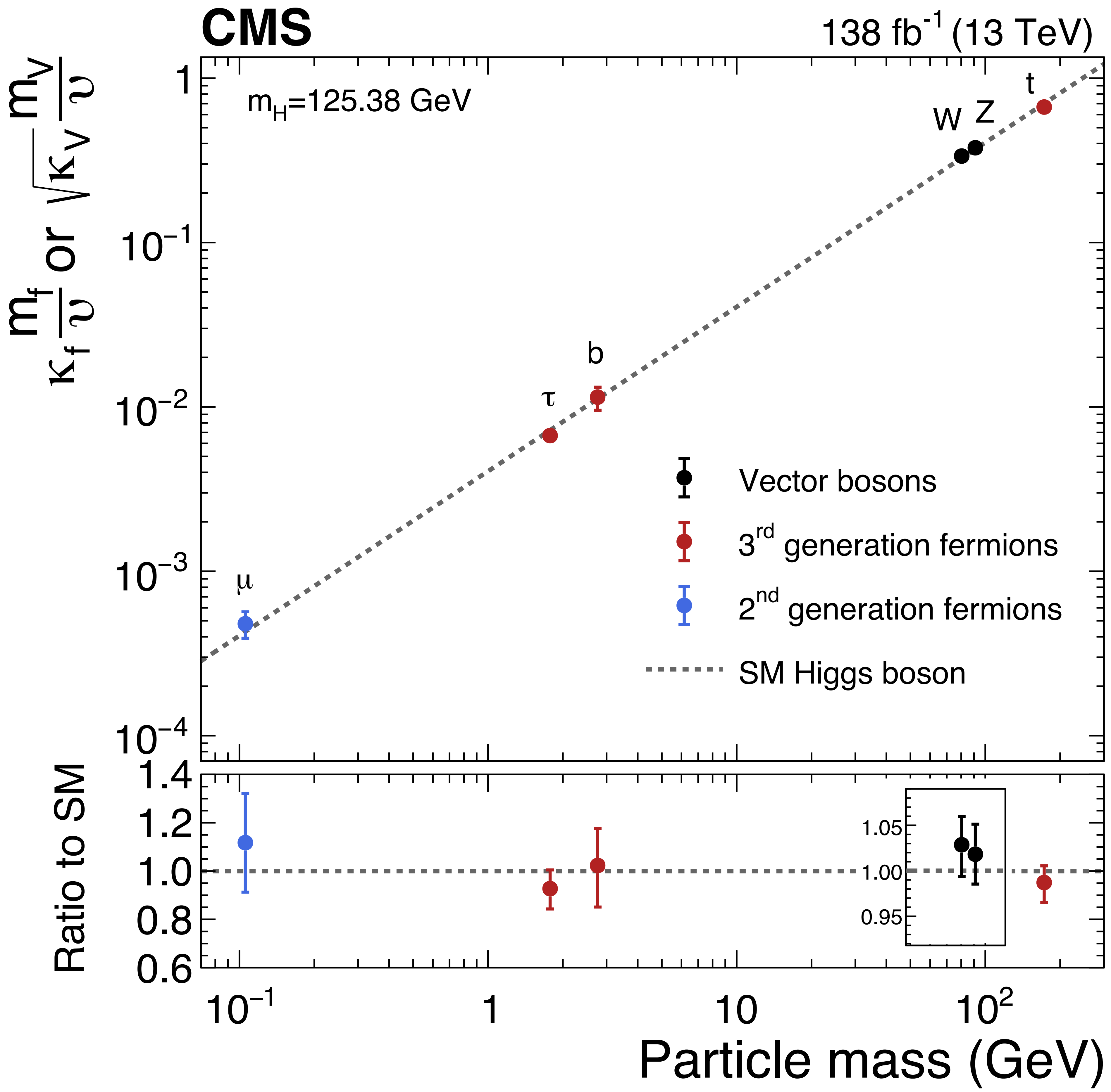

Higgs Boson coupling results

- Presence of non-SM particles in loop-induced process with effective coupling modifiers **$\kappa_g, \kappa_\gamma, \kappa_{Z\gamma}$**

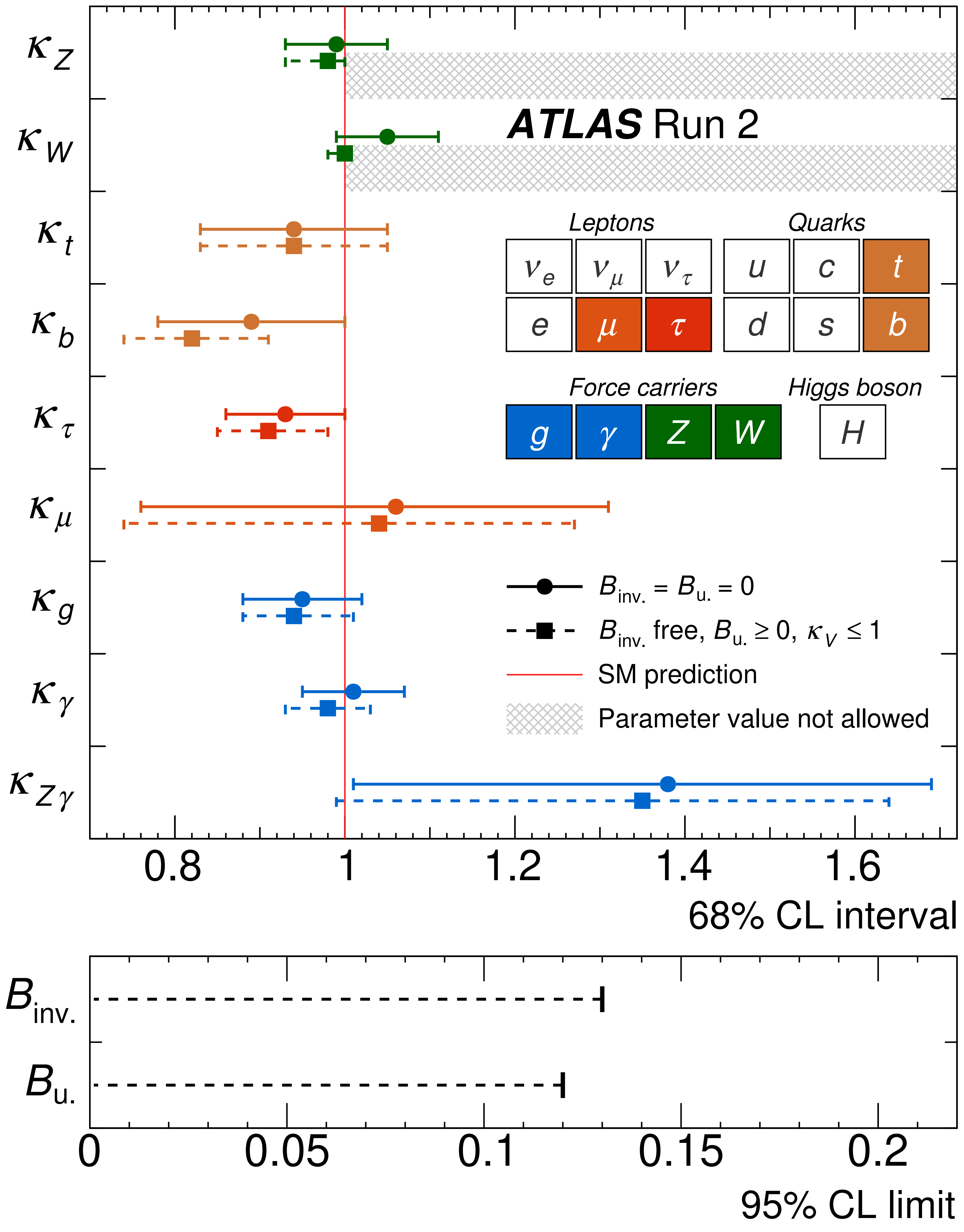

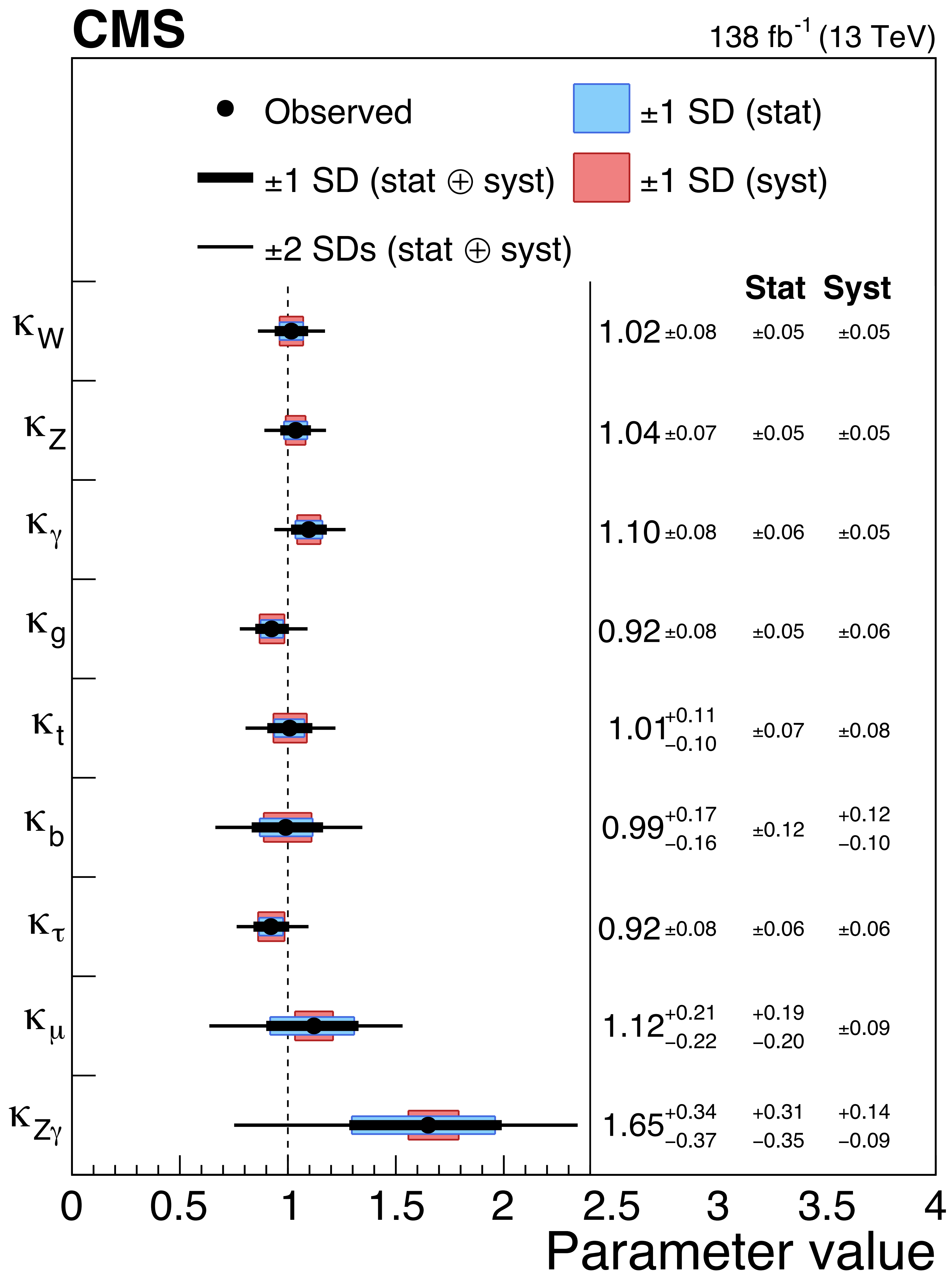

Probe High pT Higgs boson

Reconstruction of boosted Higgs as a tool to access very high-pT regime, sensitive to BSM physics

- Tagging the Higgs with machine learning based on the presence of two b quarks inside a fat jet.

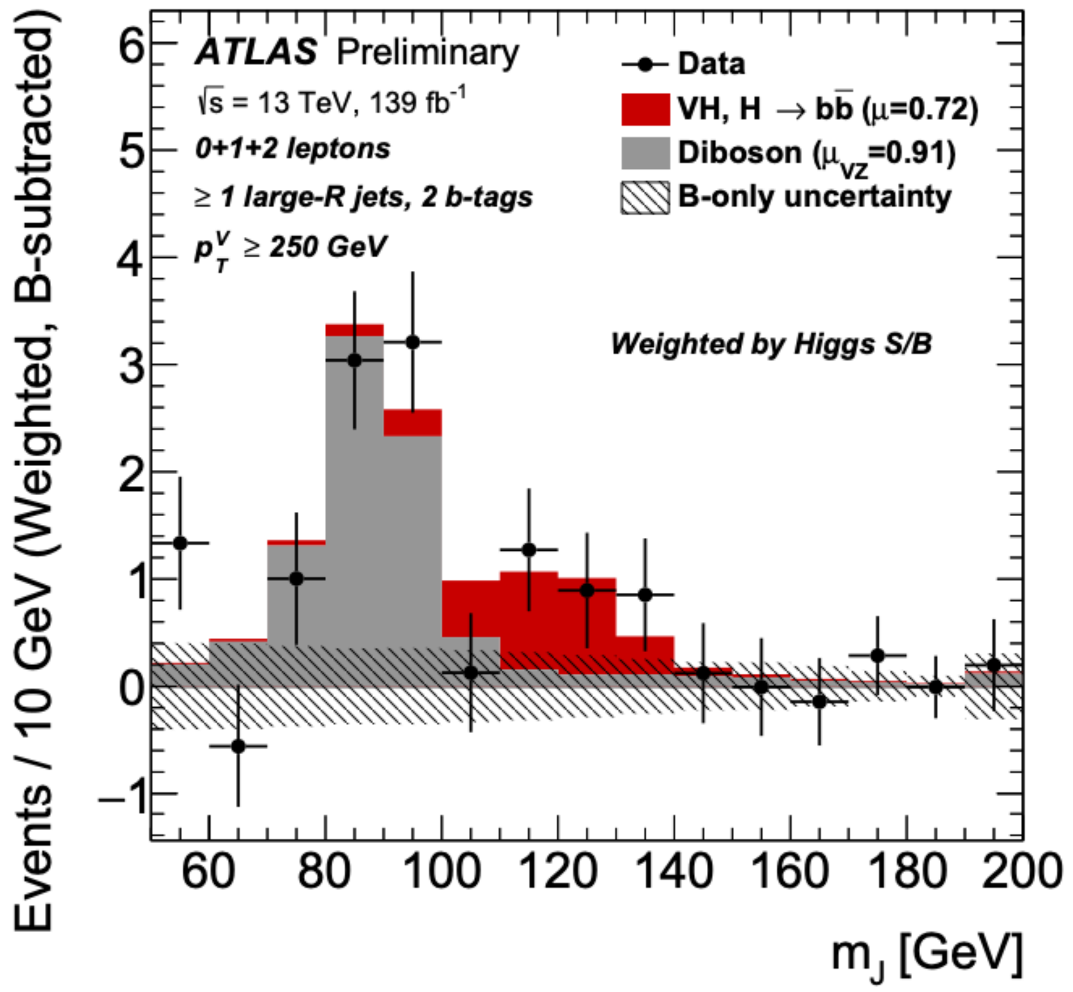

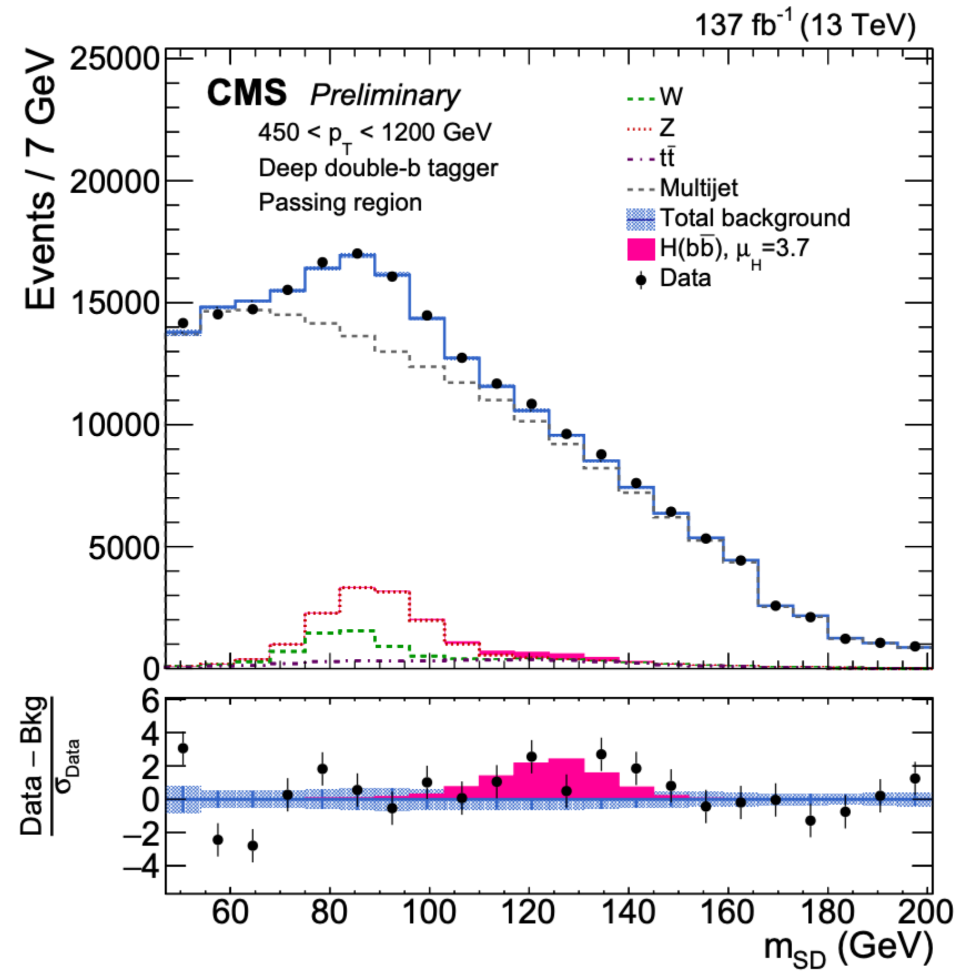

Unfolded differential cross section in pT(V) in simplified template cross section framework

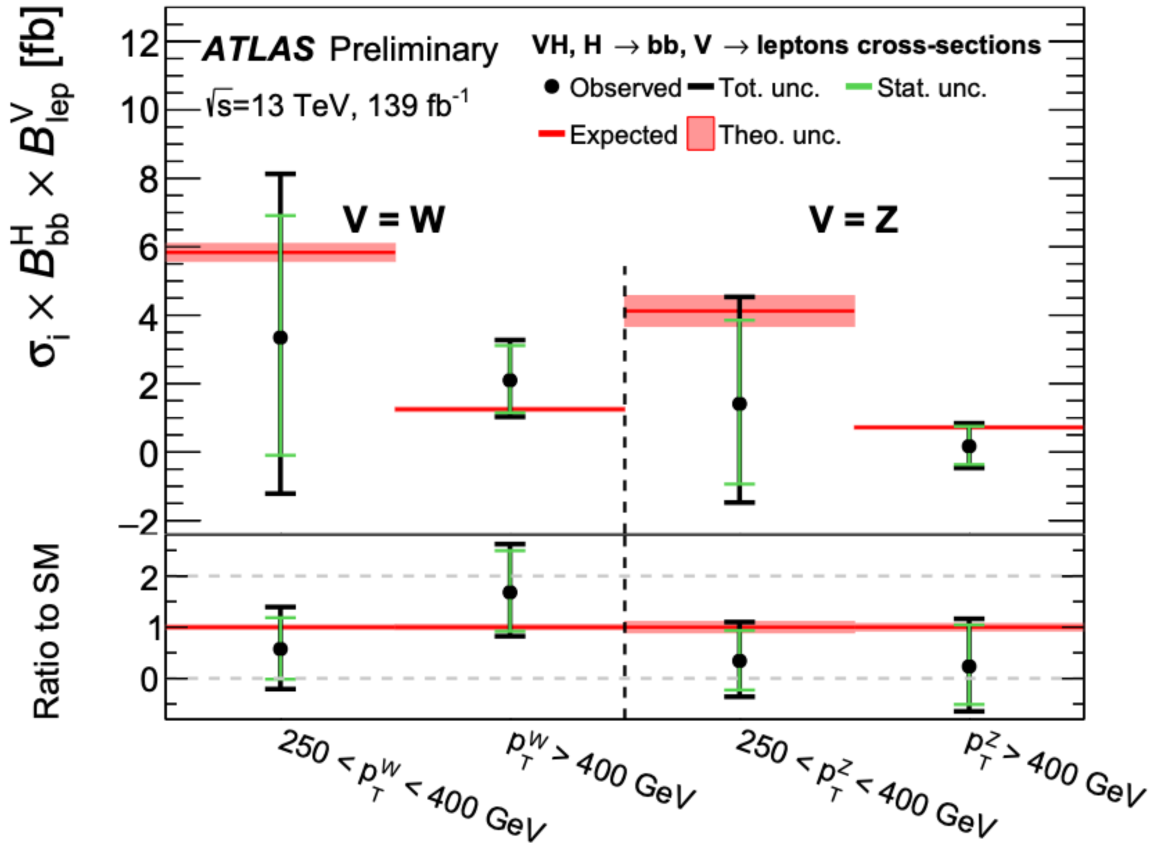

Unfolded differential cross section in pT(H)

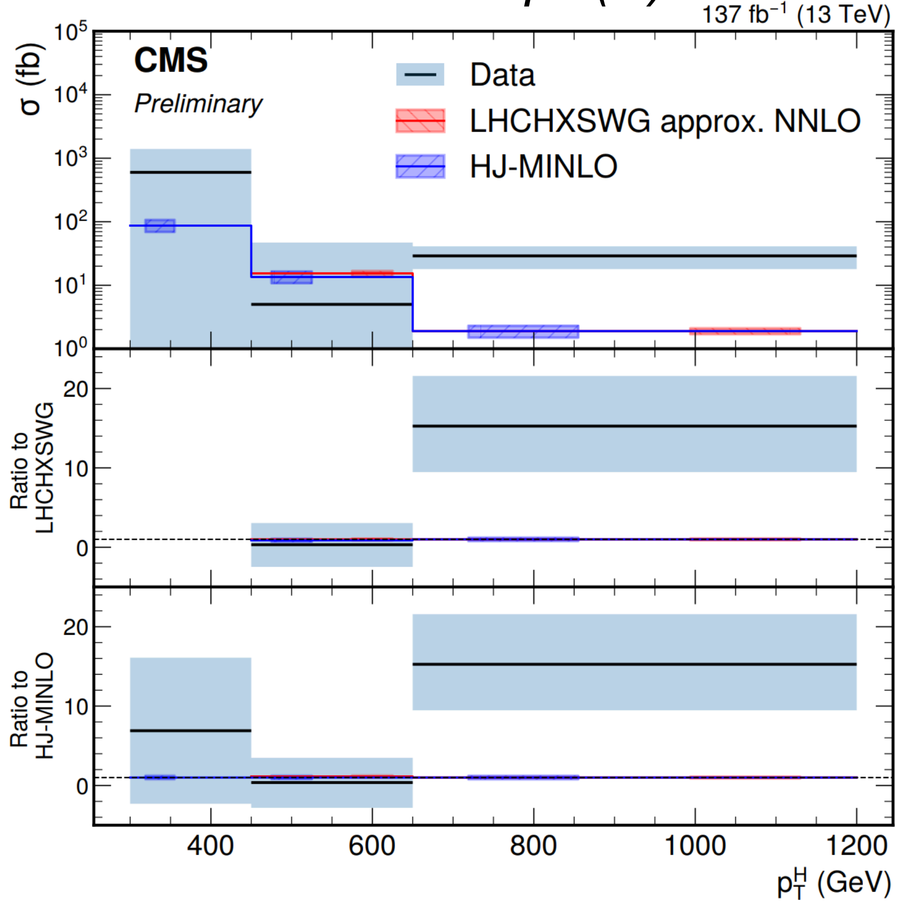

WH→lvbb event candidate

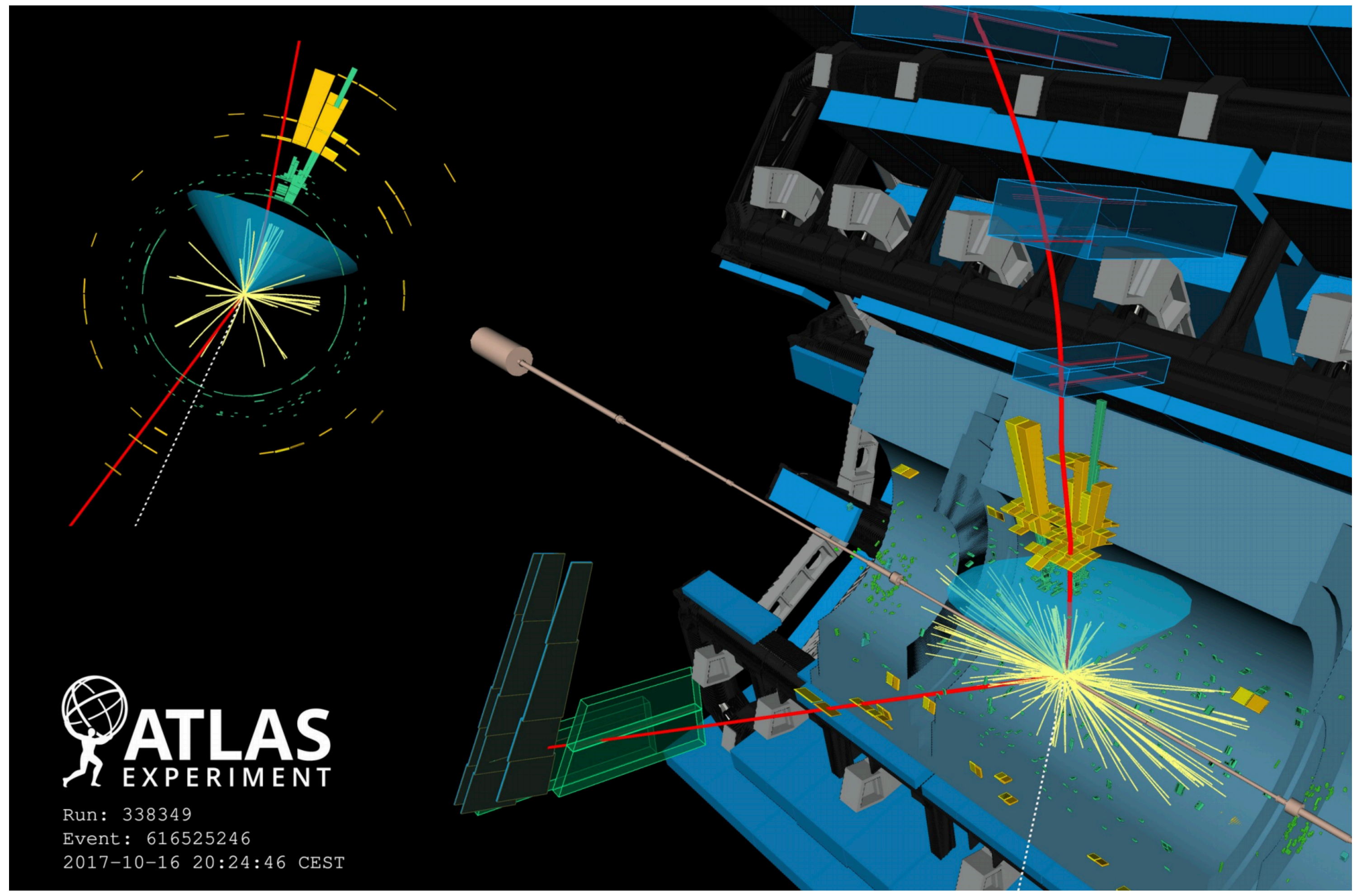

ATLAS-CONF-2020-007, CMS-PAS-HIG-19-003
CMS-BTV-15-002-PAS, Eur. Phys. J. C 79 (2019) 836

Simplified Template Cross Sections (STXS)

STXS: a natural evolution from Run 1 signal strength measurements

- Measure **production mode cross sections** in **exclusive phase space regions**
  - reduce theory dependence comparing to signal strength measurements
  - provide more finely-grained measurements
  - isolate BSM sensitive phase space
- Benefitting from **global combination**
  - Significant progress from ATLAS and CMS across accessible Higgs decays

Development initiated at Les Houches 2015

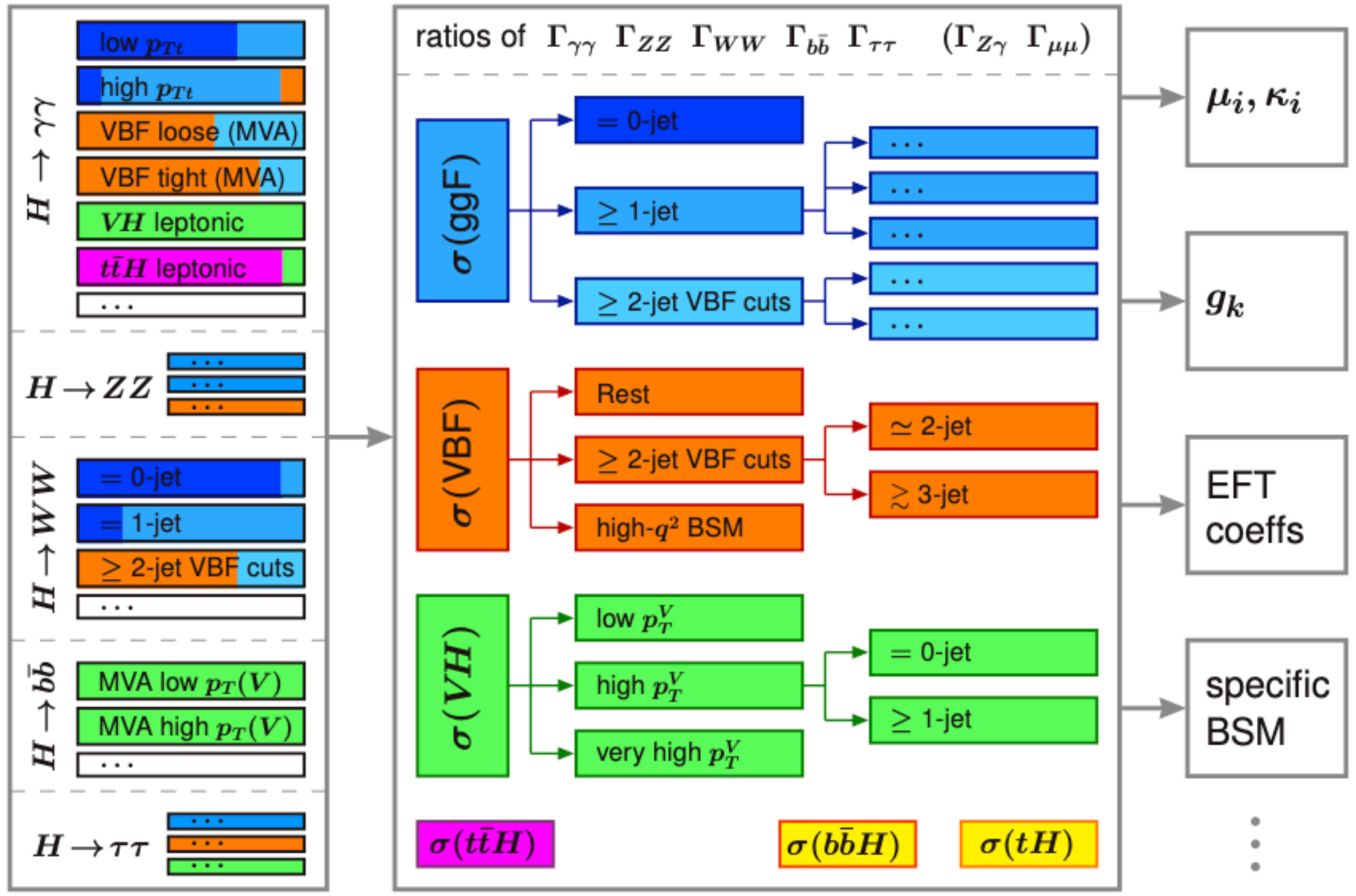

STXS stage 1.2 ggH production mode bins

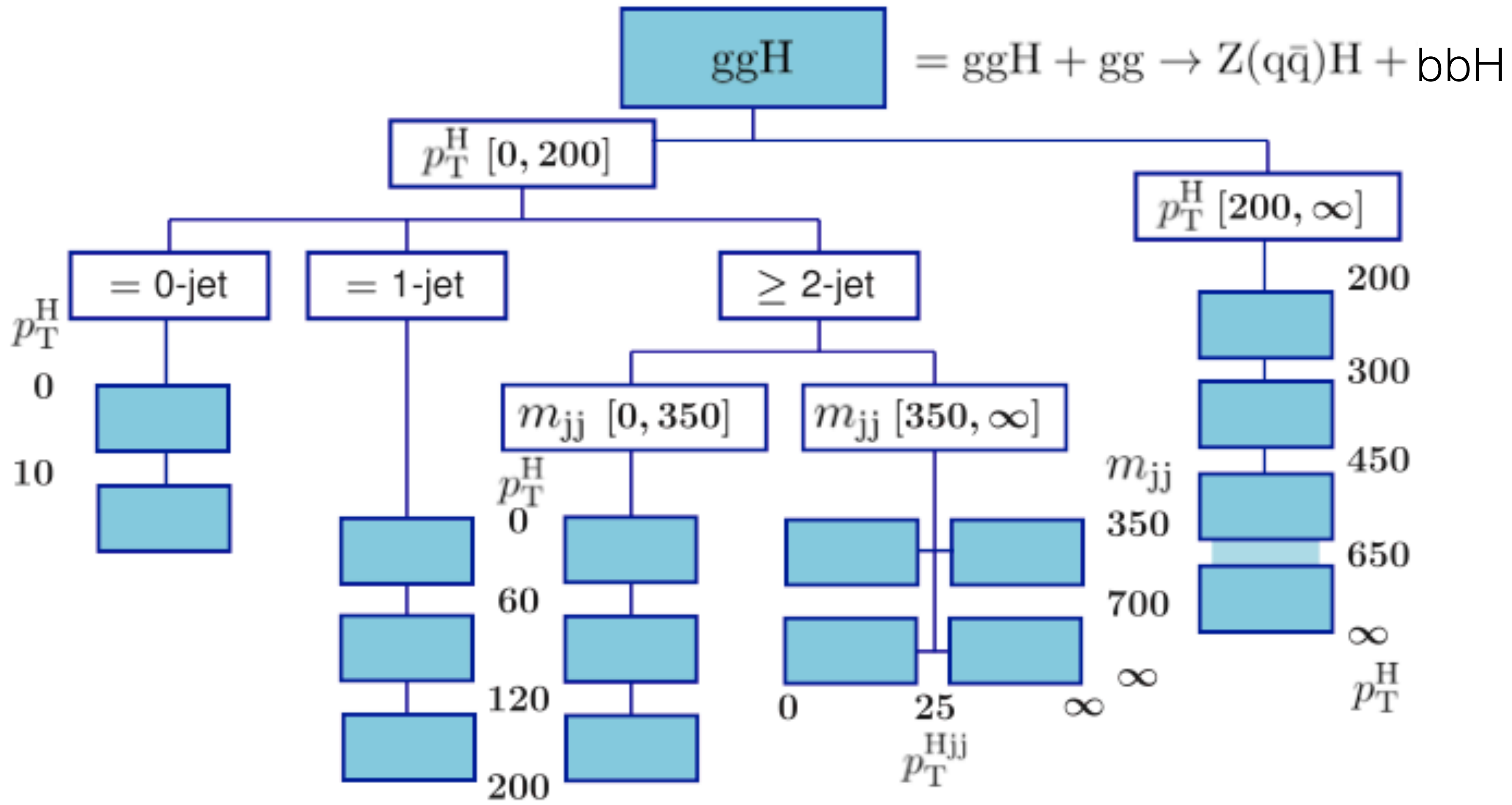

CMS STXS: recent result H→bb

Phys. Rev. D 109 (2024) 092011

- Full Run 2 measurement targeting VH production mechanism
- Dedicated category:
  - resolved topology: 2 b-tagged jets
  - boosted topology: large-radius H→bb jet

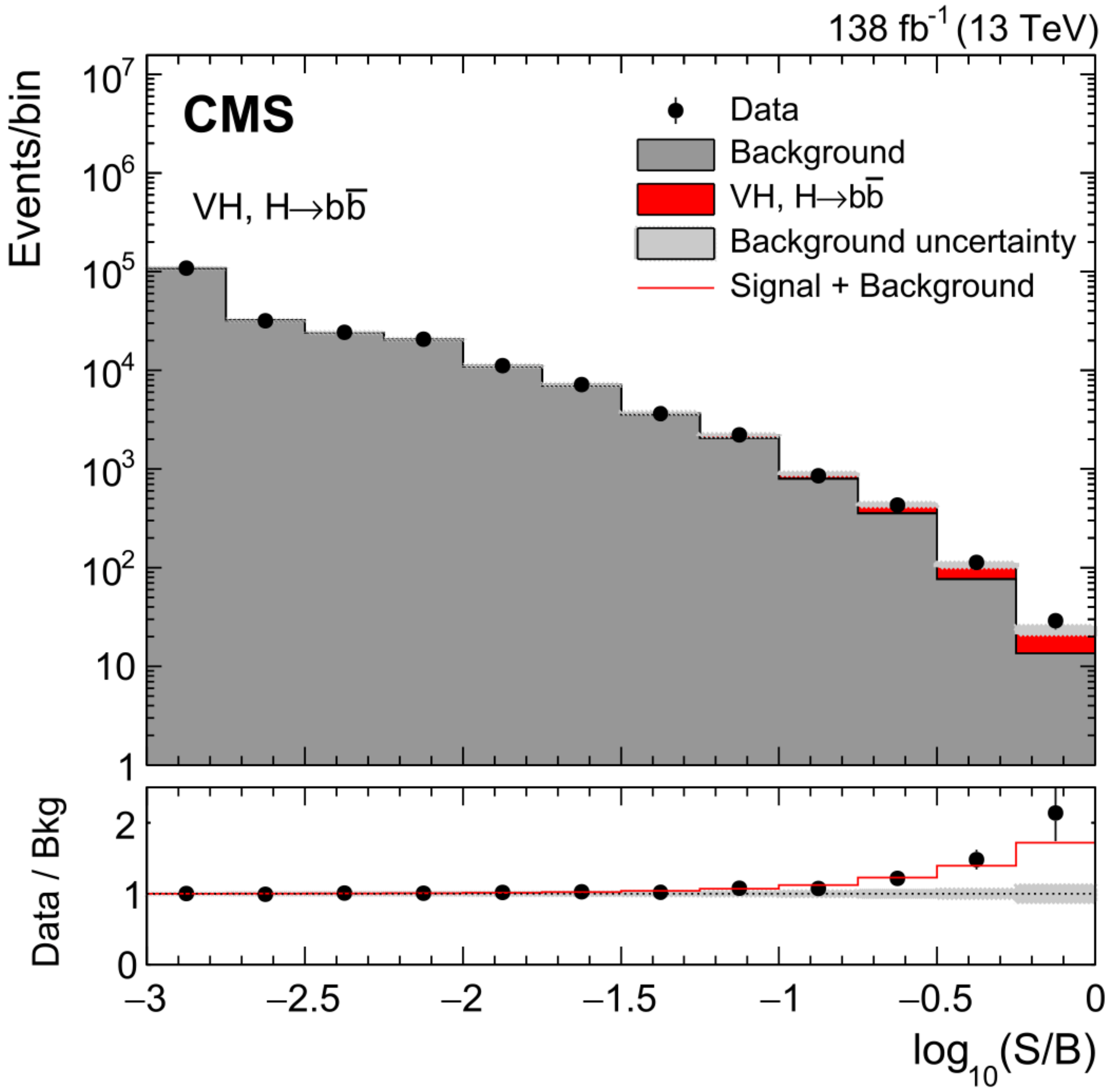

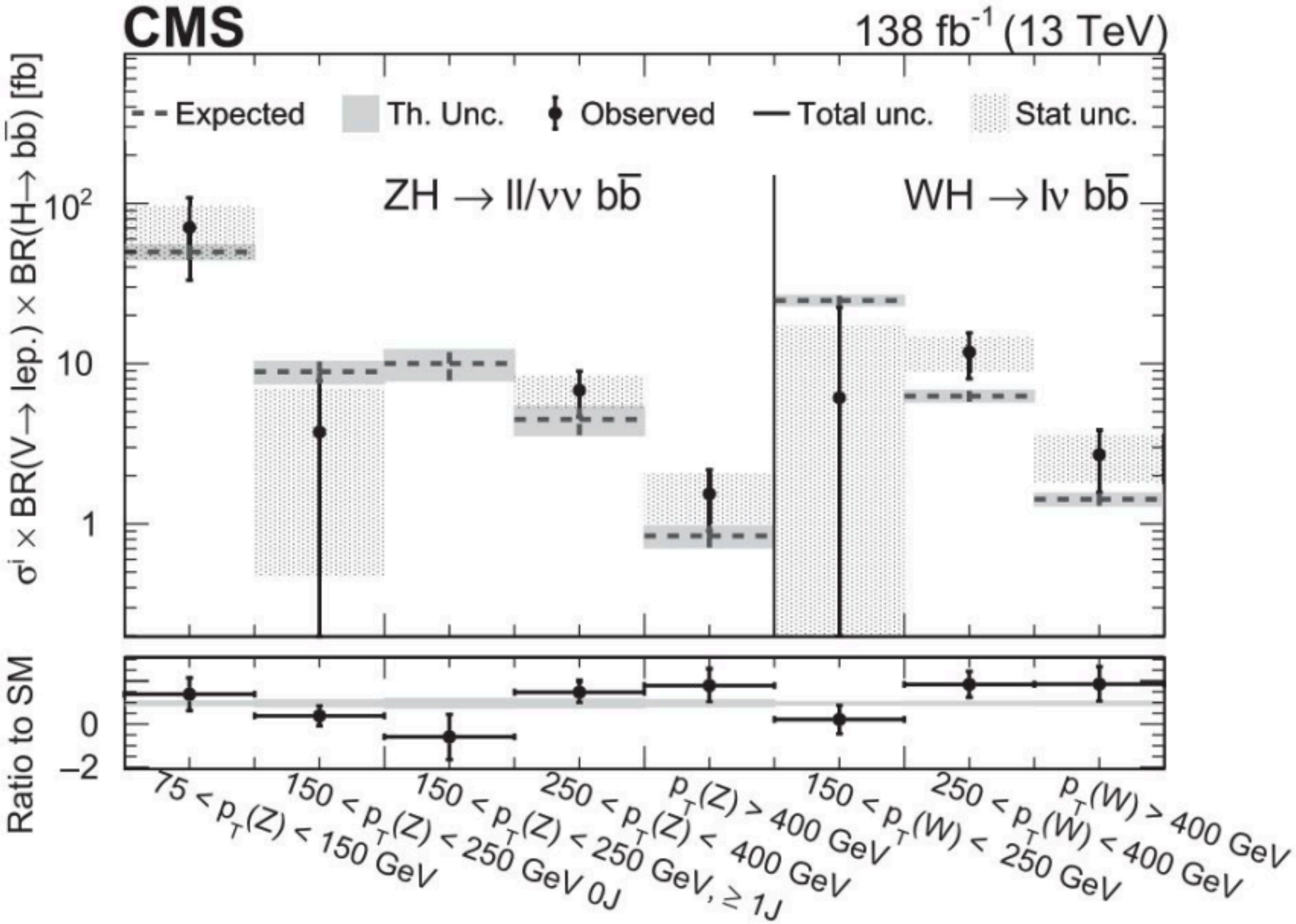

STXS Combination

Most precise measurements and interpretations obtained from statistical combination of STXS measurements in production modes and decay channels:

- Statistical precision, in particular in most BSM-sensitive regions is still limited: more data will help! [Nature volume 607, 52–59 (2022)]
- Provide an indirect constraint of the Higgs boson self-coupling through NLO EW corrections [PLB 843(2023)137745, CMS HIG-19-005]
- Measurements interpreted using EFT framework and BSM models: [arXiv:2402.05742, CMS-PAS-HIG-23-013]

- Example: STXS measurements in H→ZZ*, H→WW* decay channels, overall good compatibility with SM

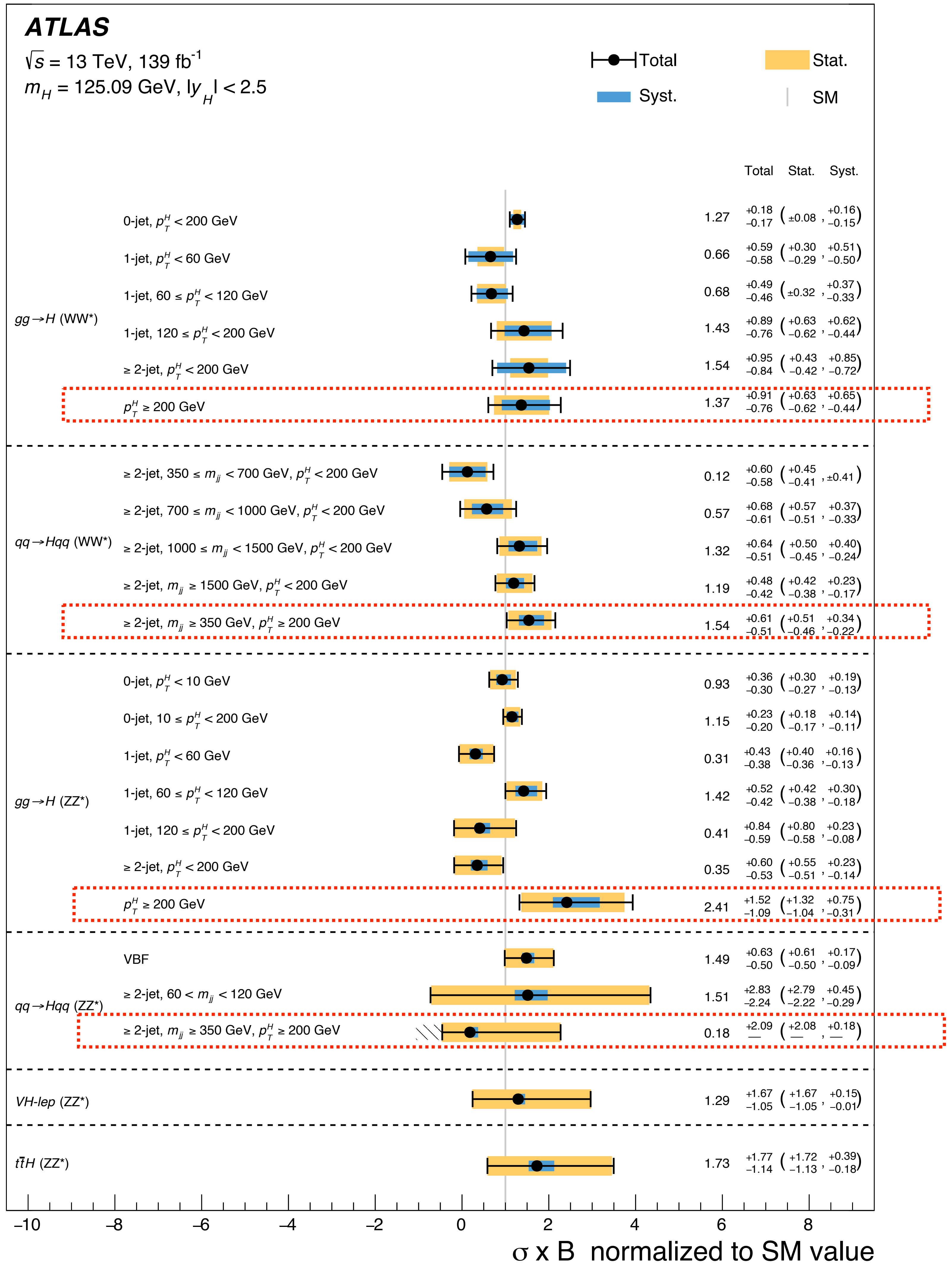

arXiv:2402.05742

ATLAS STXS Combination - ggH production

- ATLAS full Run 2 STXS combination [Nature volume 607, 52–59 (2022)]
- Input channels: $H\to\gamma\gamma$, $H\to ZZ^*$, $H\to WW^*$, $H\to Z\gamma$, $H\to bb$, $H\to\tau\tau$ and $H\to\mu\mu$

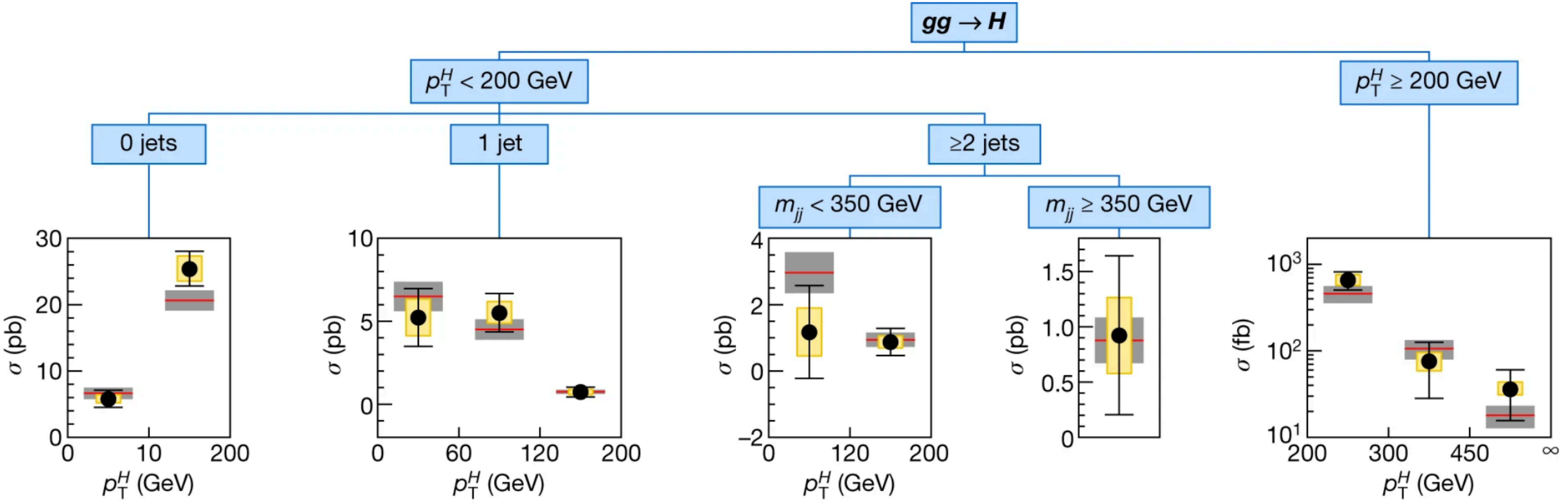

ATLAS STXS Combination: VBFH, VH, tt/tH

- ATLAS full Run 2 STXS combination [Nature volume 607, 52–59 (2022)]

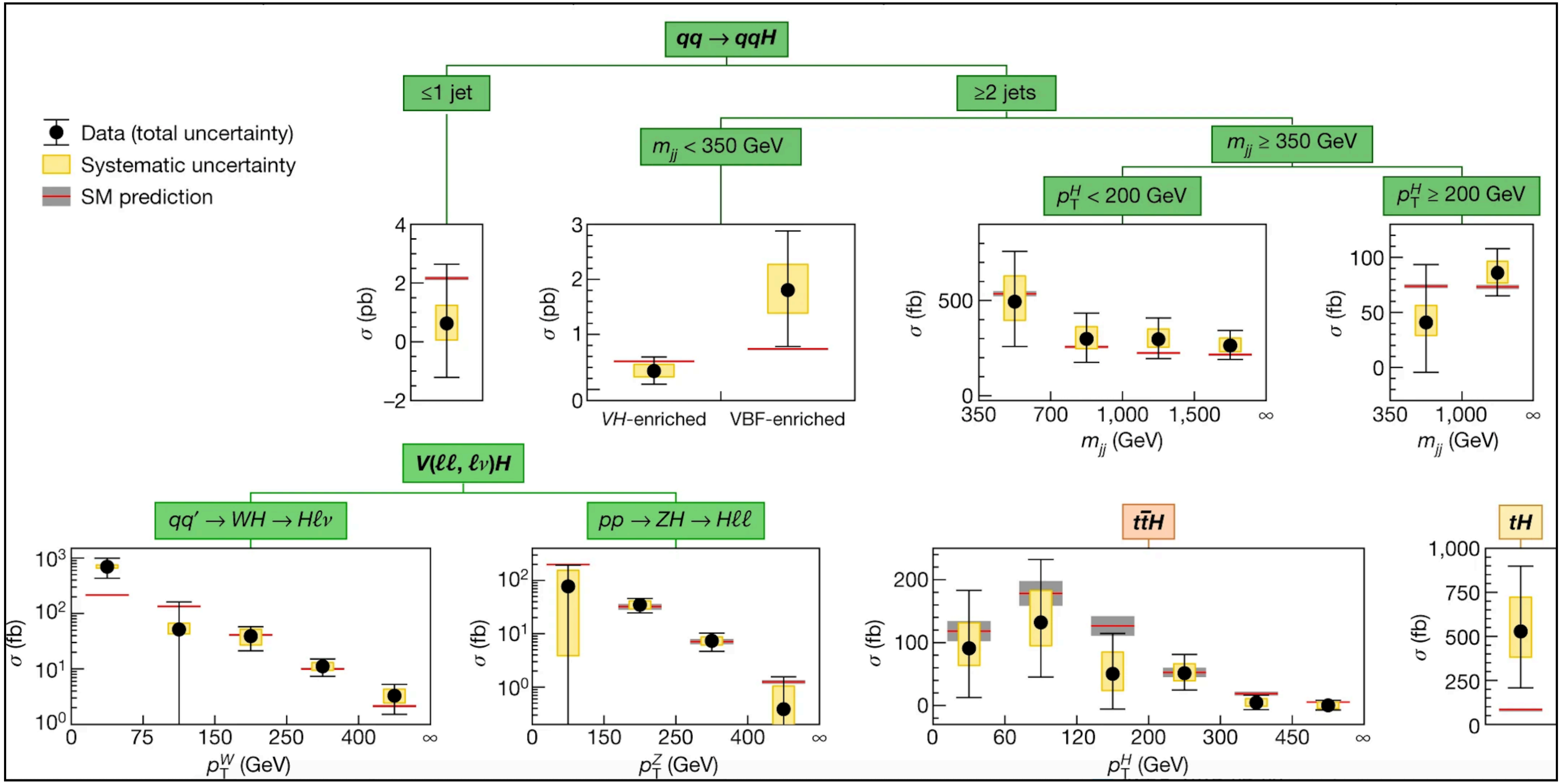

SMEFT and 2HDM and (h)MSSM interpretation of ATLAS STXS combination

arXiv:2402.05742 submitted to JHEP

Decay channel	Analysis Production mode	$\mathcal{L}$ [fb^{-1}]	Reference	Binning	SMEFT	2HDM and (h)MSSM
$H \to \gamma\gamma$	(ggF, VBF, WH, ZH, $t\bar{t}H$, tH)	139	[38]	STXS-1.2	✓	✓
			[19]	differential	✓(subset)	
$H \to ZZ^*$	($ZZ^* \to 4\ell$: ggF, VBF, $WH+ZH$, $t\bar{t}H+tH$)	139	[22]	STXS-1.2	✓	✓
			[18]	differential	✓(subset)	
	($ZZ^* \to \ell\ell\nu\bar{\nu}/\ell\ell q\bar{q}$: $t\bar{t}H$ multileptons)	36.1	[27]	STXS-0*		✓
$H \to \tau\tau$	(ggF, VBF, $WH+ZH$, $t\bar{t}H+tH$)	139	[39]	STXS-1.2	✓	✓
	($t\bar{t}H$ multileptons)	36.1	[27]	STXS-0*		✓
$H \to WW^*$	(ggF, VBF)	139	[40]	STXS-1.2	✓	✓
	(WH, ZH)	36.1	[41]	STXS-0*		✓
	($t\bar{t}H$ multileptons)	36.1	[27]	STXS-0*		✓
$H \to bb$	(WH, ZH)	139	[42,25]	STXS-1.2	✓	✓
	(VBF)	126	[43]	STXS-1.2	✓	✓
	($t\bar{t}H+tH$)	139	[44]	STXS-1.2	✓	✓
	(boosted Higgs bosons: inclusive production)	139	[45]	STXS-1.2	✓	✓
$H \to Z\gamma$	(inclusive production)	139	[46]	STXS-0*	✓	✓
$H \to \mu\mu$	(ggF $+ t\bar{t}H + tH$, VBF $+ WH + ZH$)	139	[47]	STXS-0*	✓	✓

SMEFT interpretation of STXS combination

arXiv:2402.05742 submitted to JHEP

- Standard Model Effective Field Theory (**SMEFT**) Effective Lagrangian :

$$\mathscr{L}_{\mathrm{SMEFT}} = \mathscr{L}_{\mathrm{SM}} + \sum_{i}^{N_{d=6}} \frac{c_i}{\Lambda^2}\mathcal{O}_i^{(6)} + \sum_{j}^{N_{d=8}} \frac{b_j}{\Lambda^4}\mathcal{O}_j^{(8)} + \dots$$

Only $d = 6$ operators are considered, impact of $d = 8$ operators might be non-negligible.

- Ratio of SMEFT cross section wrt SM prediction

$$\frac{\sigma_{\mathrm{EFT}}}{\sigma_{\mathrm{SM}}} = 1 + \sum_i A_i c_i + \sum_{ij} B_{ij} c_i c_j$$

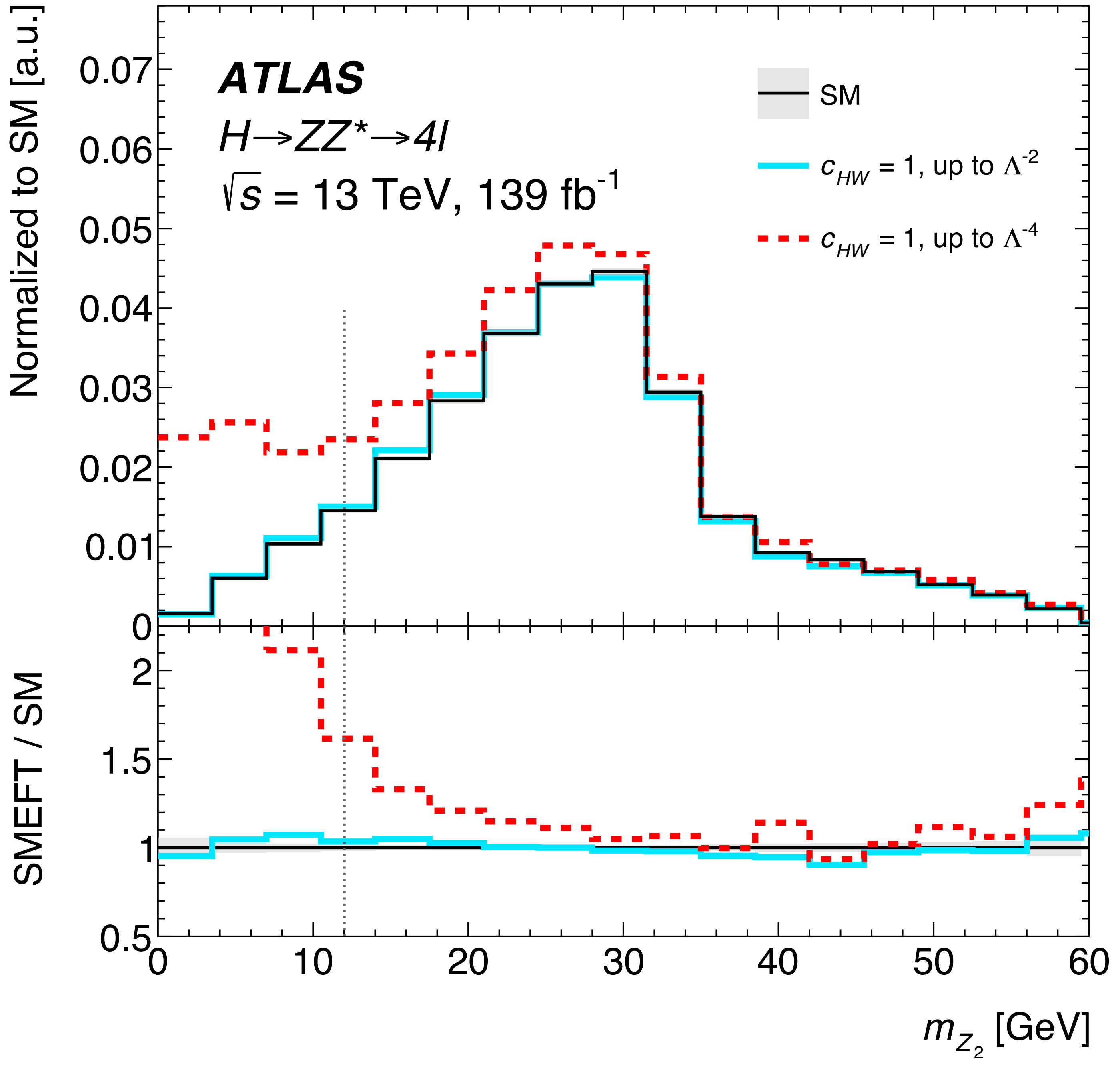

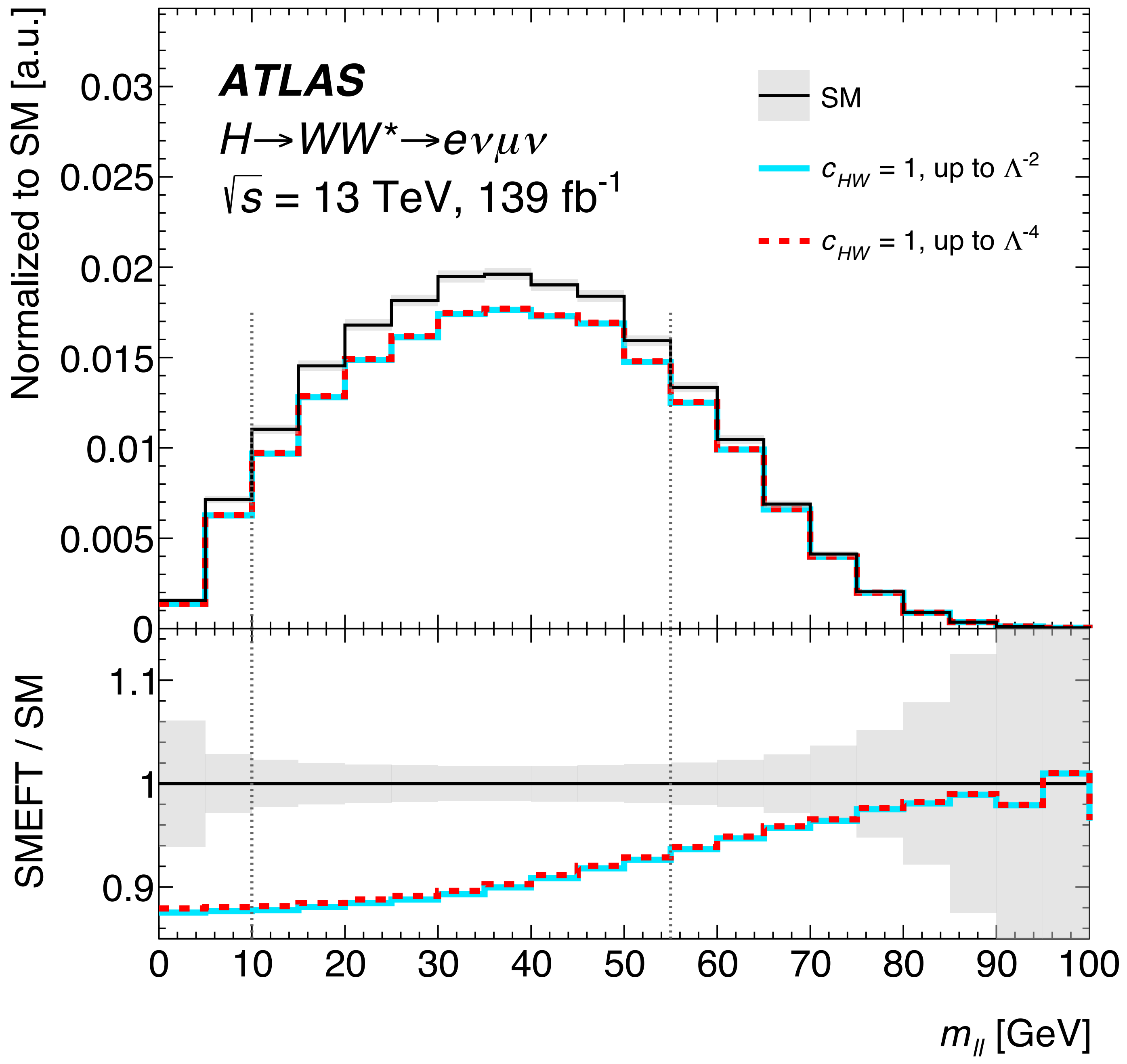

Taken into account the non-negligible acceptance effects for operator C_{HW}, C_{HB}, C_{HWB} and $C^{(3)}_{Hl}$ in the $H\rightarrow WW^*$ and $H\rightarrow ZZ^*$ decay modes

SMEFT interpretation of STXS combination

arXiv:2402.05742 submitted to JHEP

- SMEFT linear model vs SMEFT linear+quadratic results
- Linear+quadratic *p*-value **98.2%**, stronger constraints with linear+quadratic

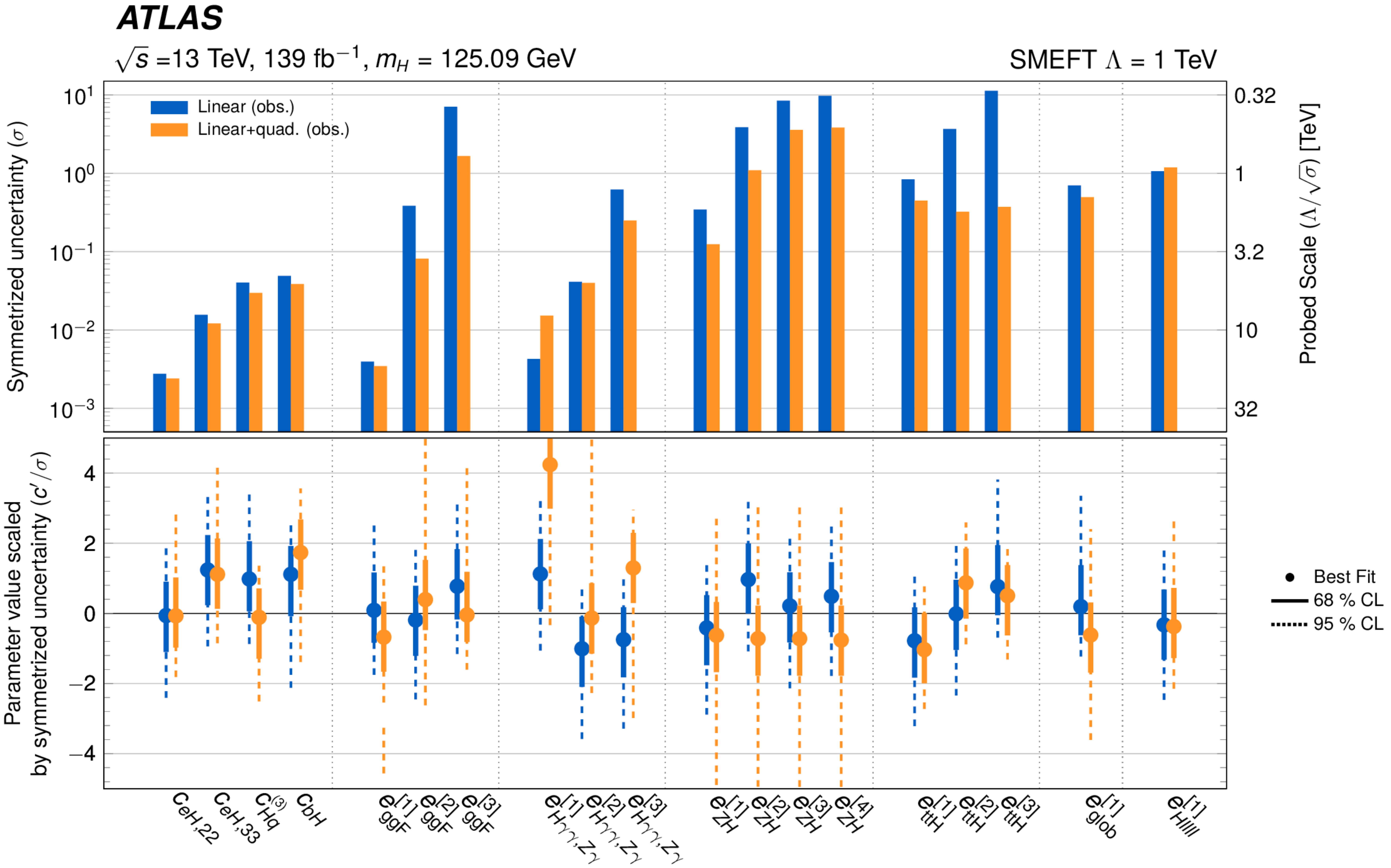

UV-complete models：2HDM

arXiv:2402.05742 submitted to JHEP

Comparison of the constraints in tanβ, cos(β-α) plane, from the κ- and EFT-interpretations of Higgs boson production and decay rates.

The κ_λ constraint is included in the Type-I model interpretation.

Type-I model

Type-II model

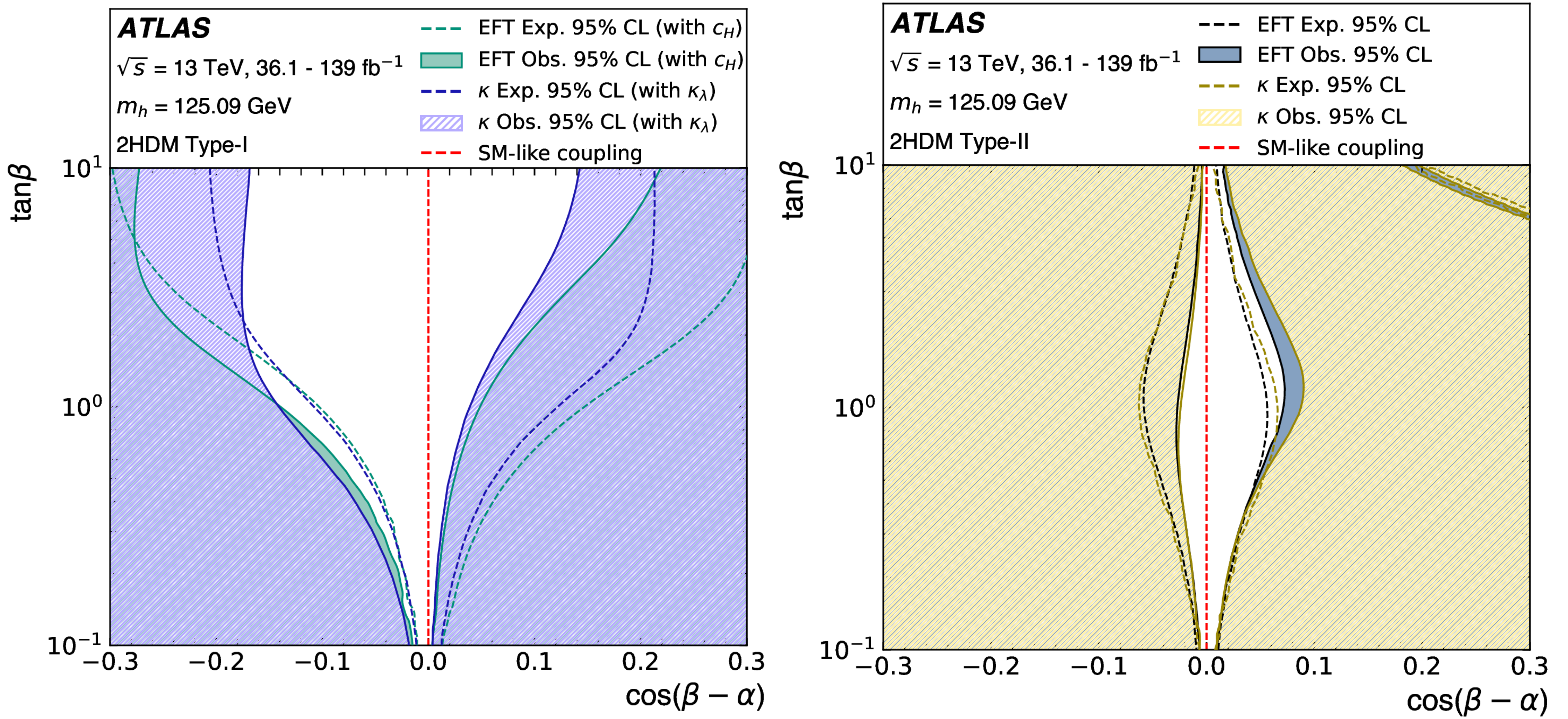

Higgs boson differential measurements combination and interpretation

Differential distributions are sensitive to Higgs couplings through distortions in the SM predicted spectra. Two interpretations: κ-framework and SMEFT

Higgs p_T sensitive to many BSM effects: physics in the ggF loops, perturbative QCD calculations, Higgs couplings to charm and bottom quarks, …

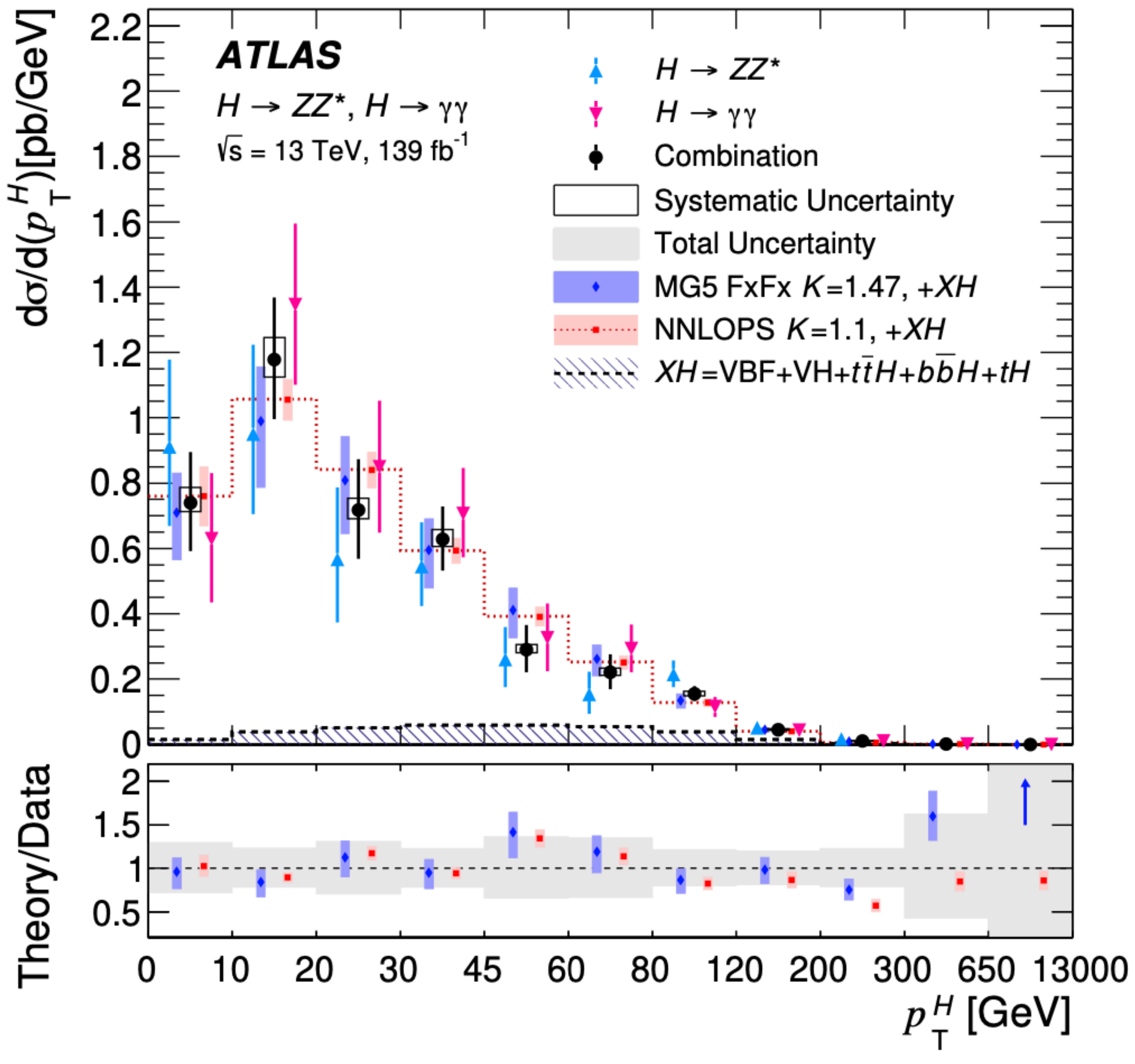

arXiv:2402.05742 submitted to JHEP

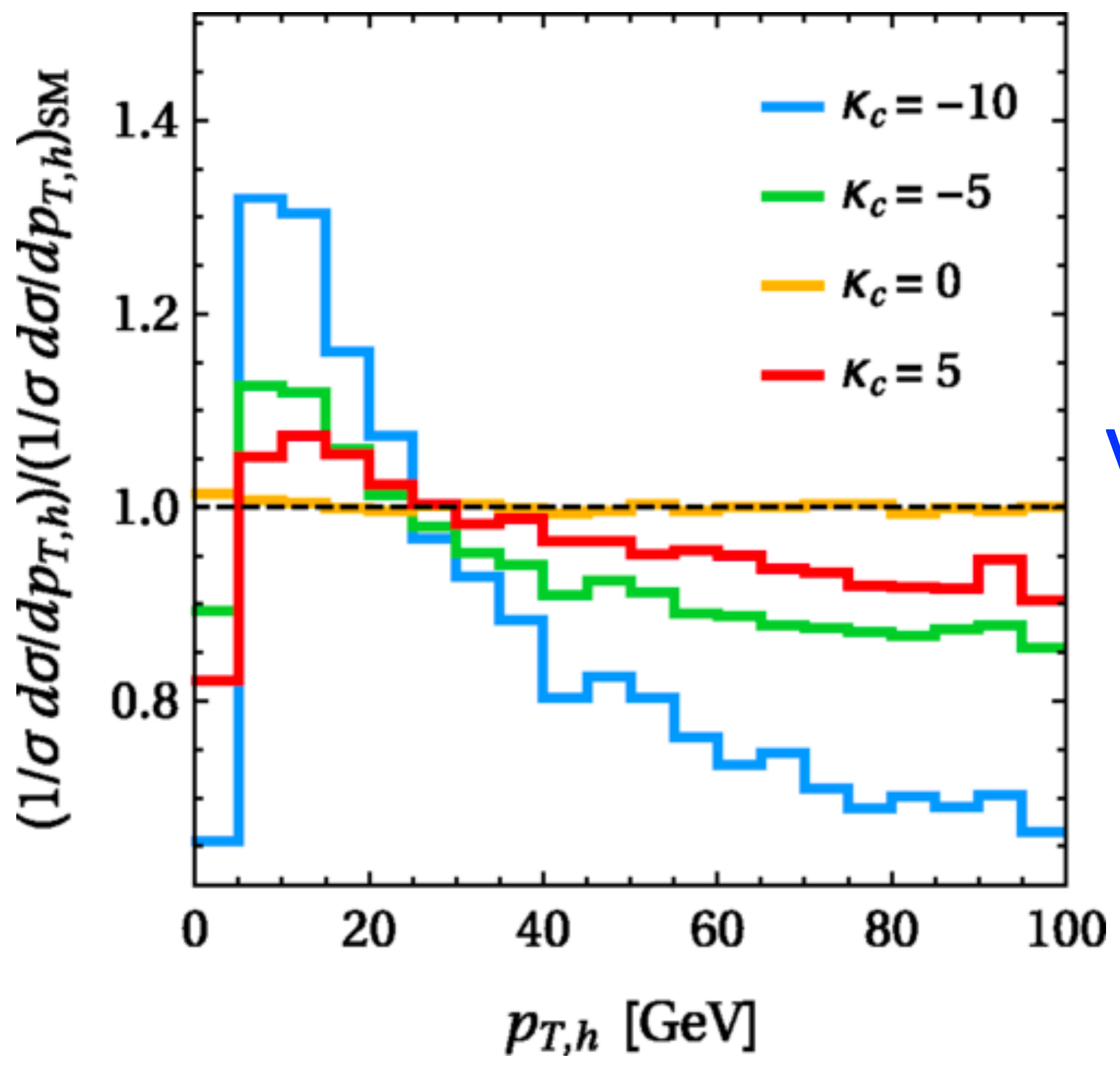

Phys. Rev. Lett. 118 (2017) 121801

Variations in $p_T(H)$ with κ_c

κ_c vs κ_b constraint from $p_T(H)$ shape

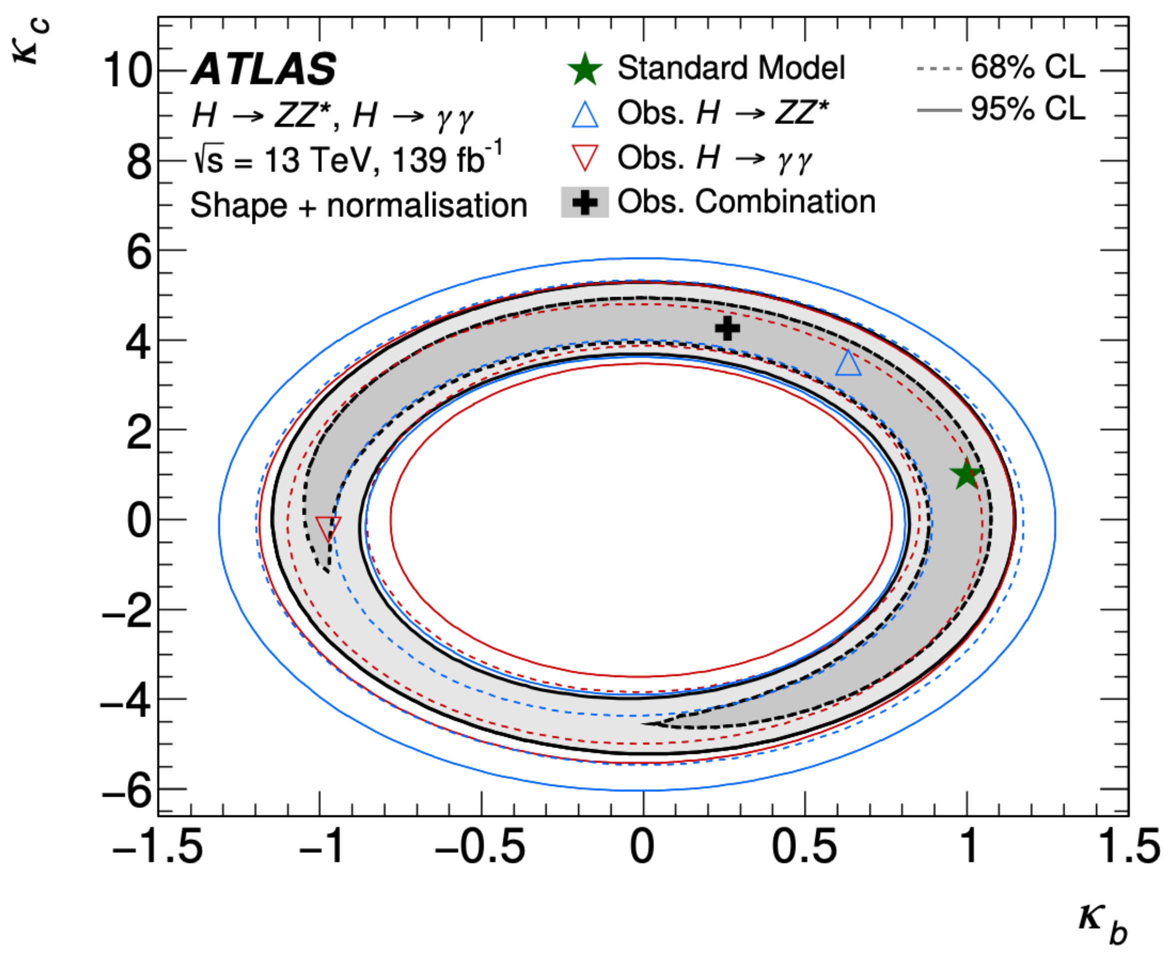

Higgs boson combined differential measurements

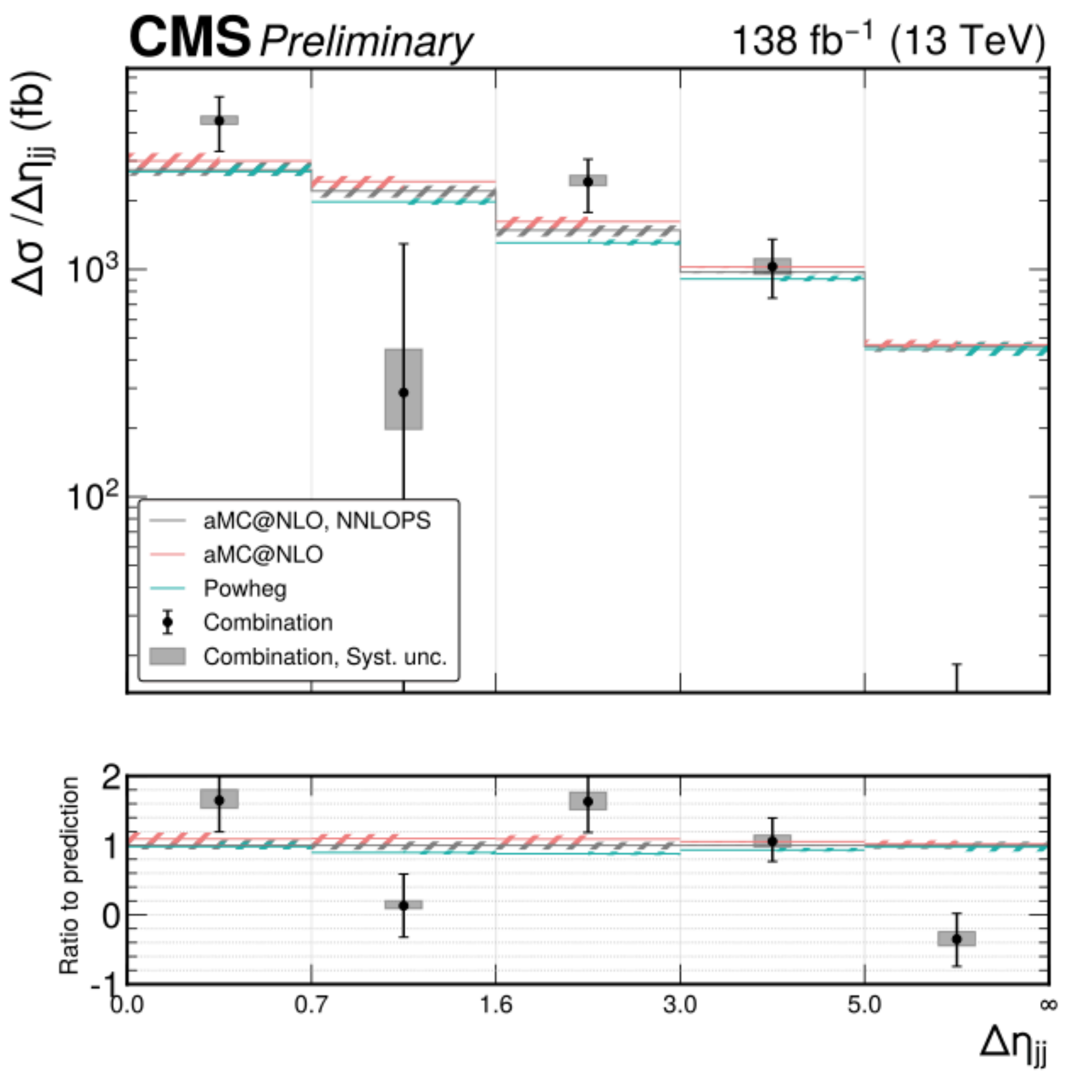

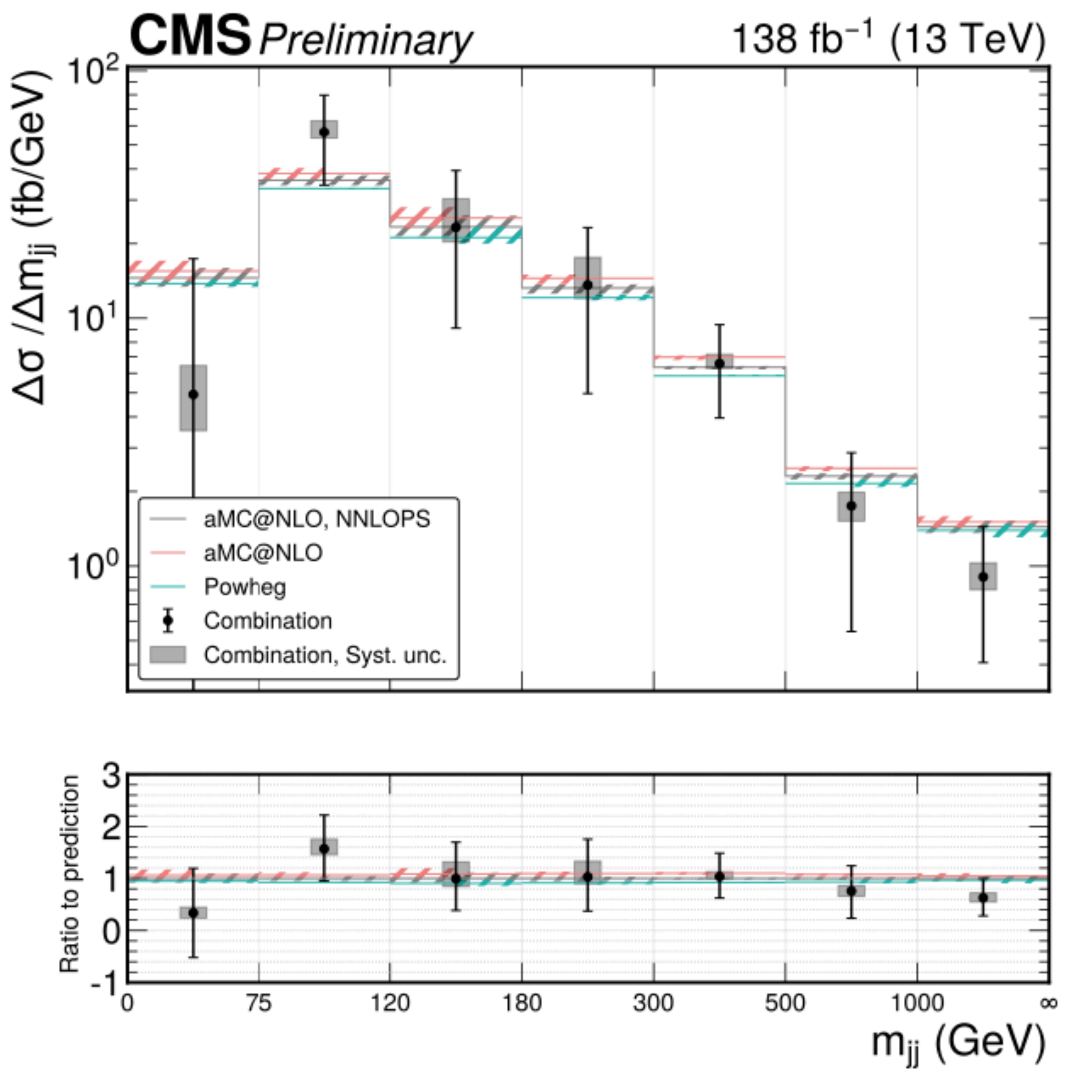

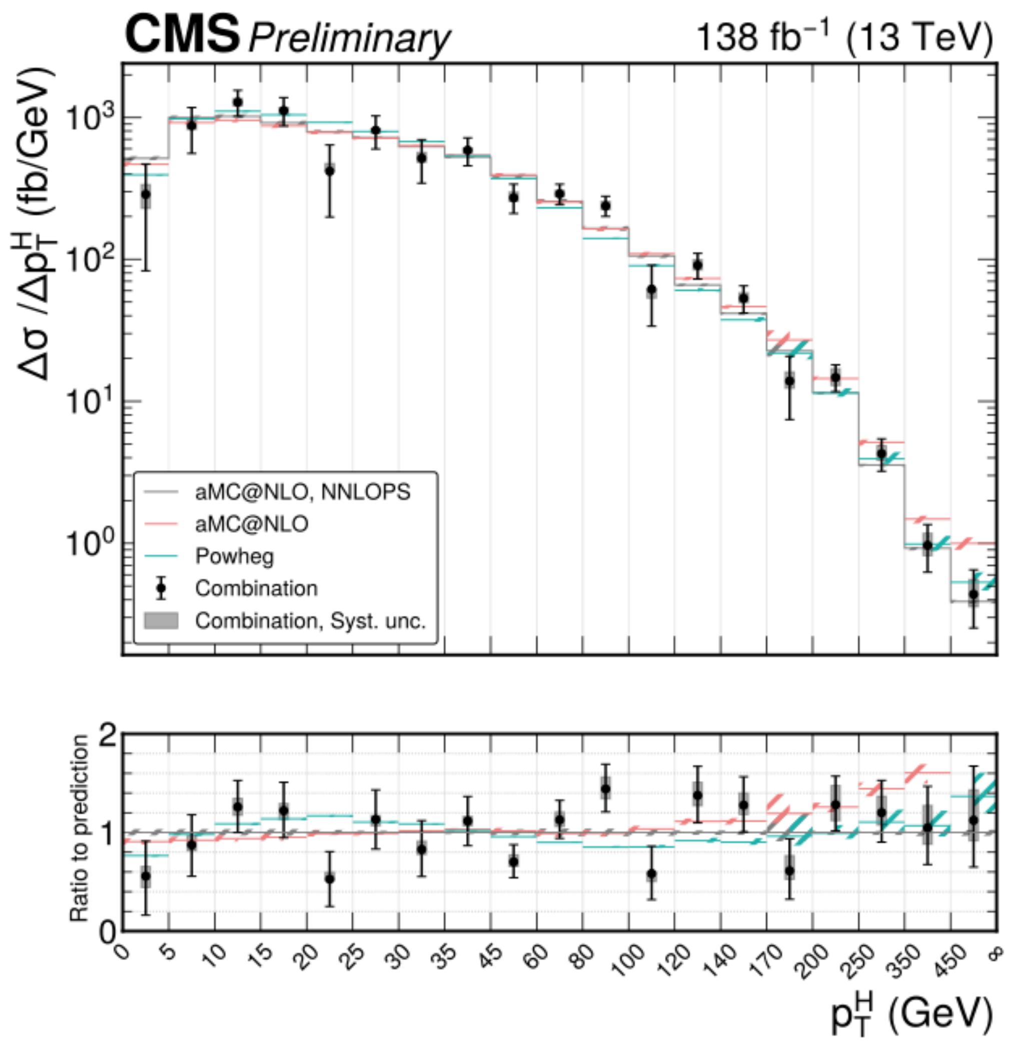

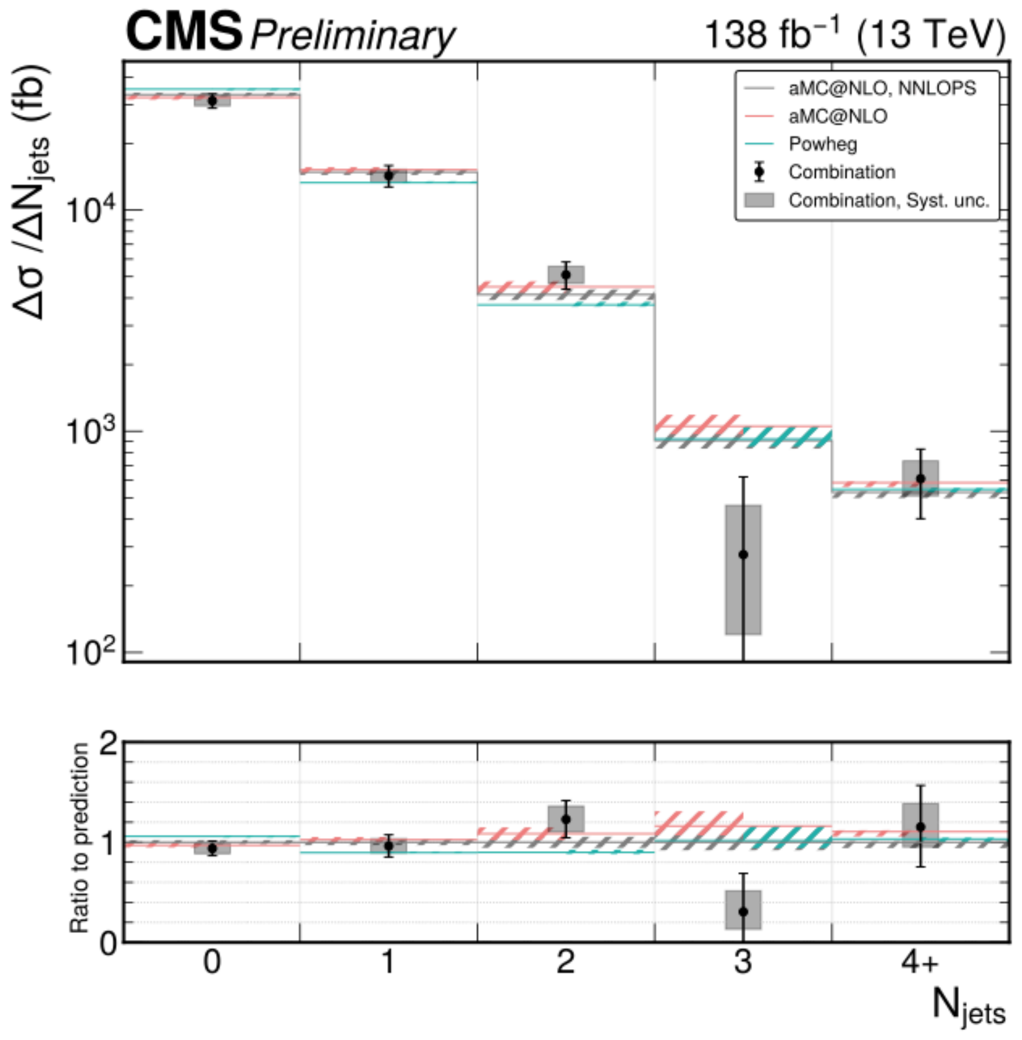

$$\tau_C^j = \max_{k\in\text{jets}}\left(\frac{\sqrt{E_k^2 - p_{z,k}^2}}{2\cosh\left(y_k - y_H\right)}\right)$$

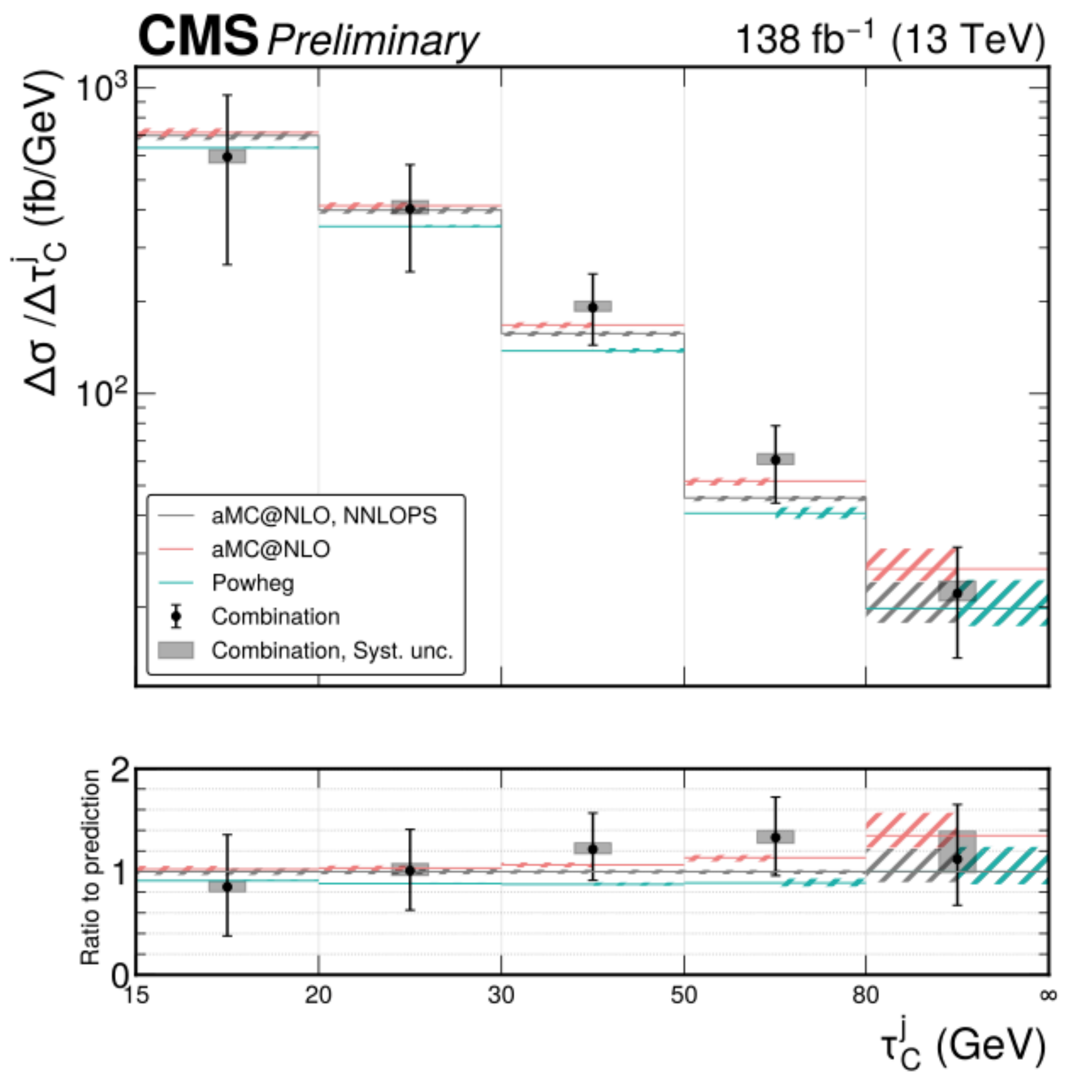

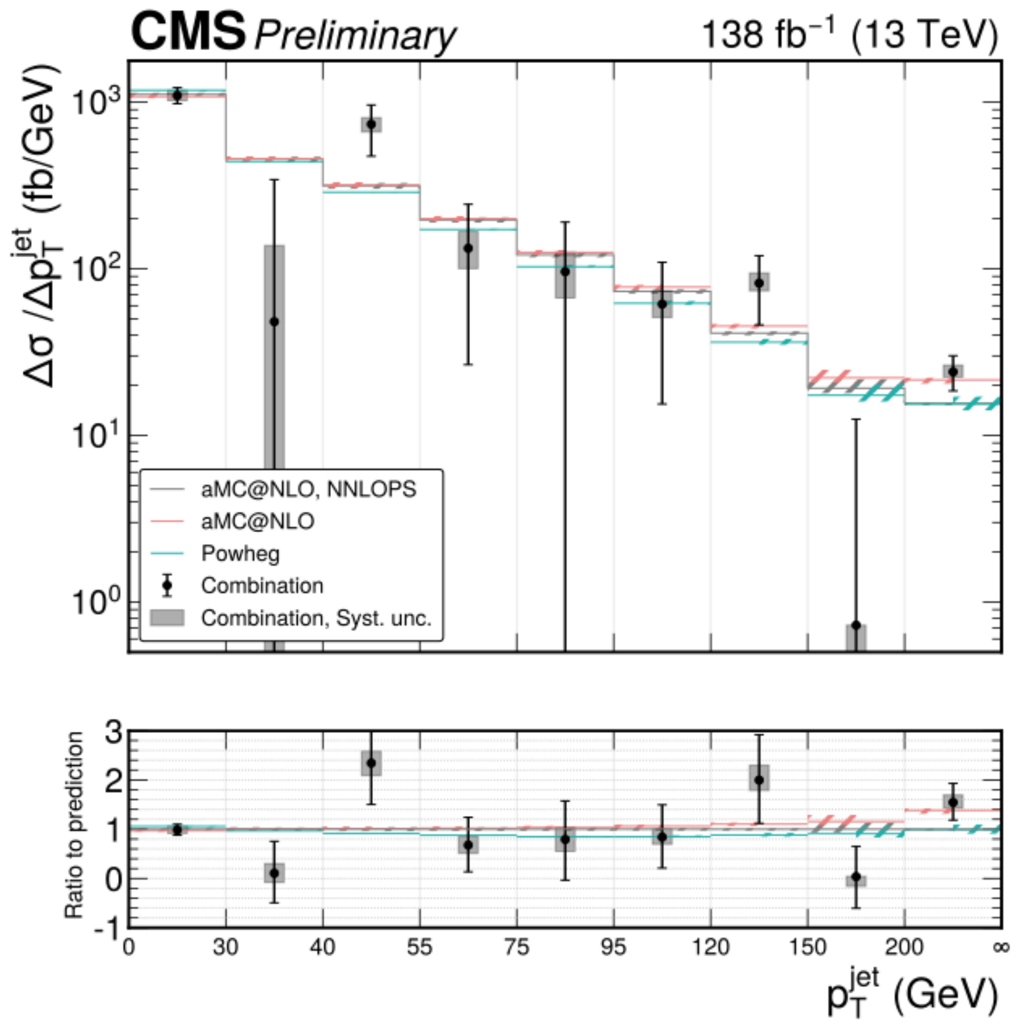

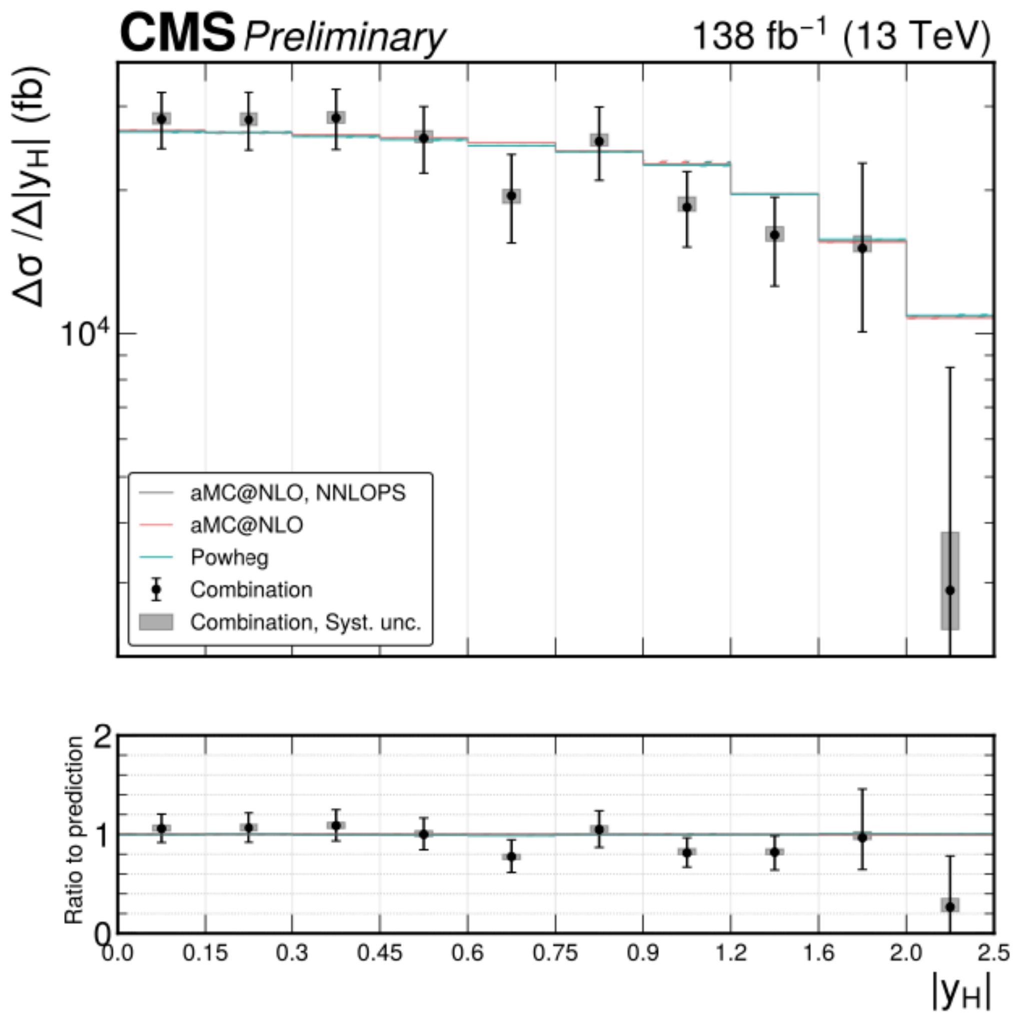

CMS-PAS-HIG-23-013

κ-framework interpretation of combined differential measurements

CMS-PAS-HIG-23-013

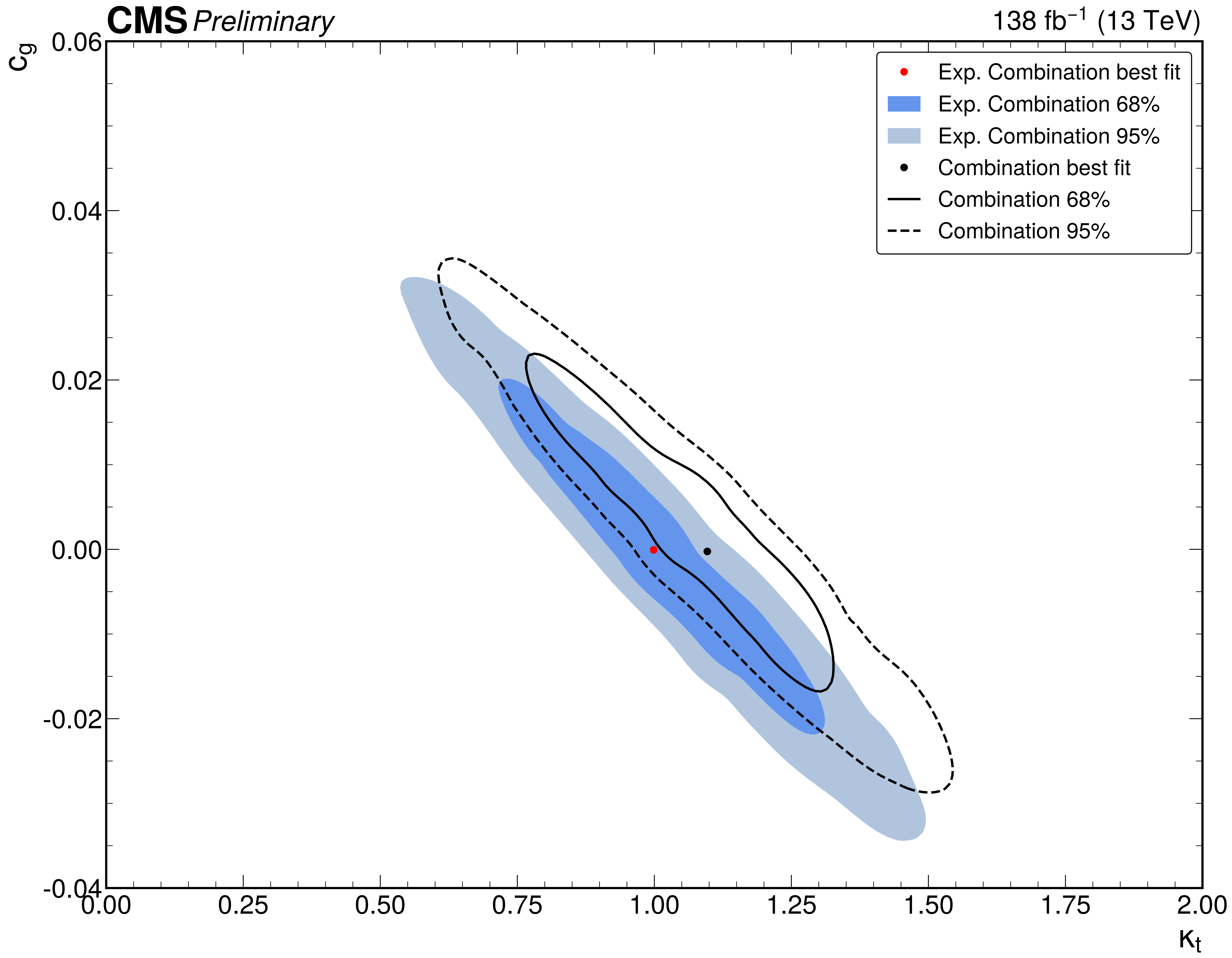

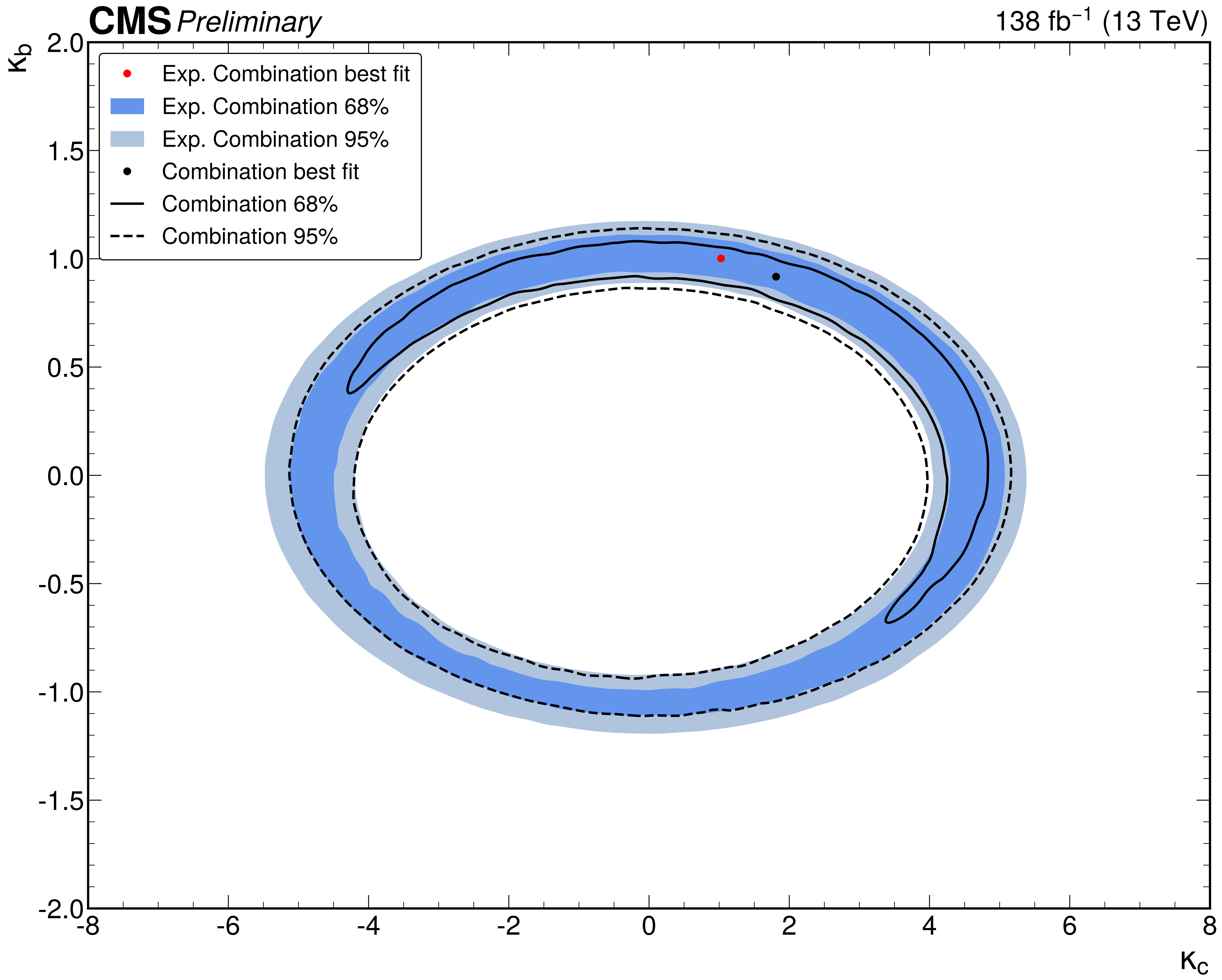

SMEFT interpretation of combined differential measurements

pT(H) 2D scans of Wilson coefficients

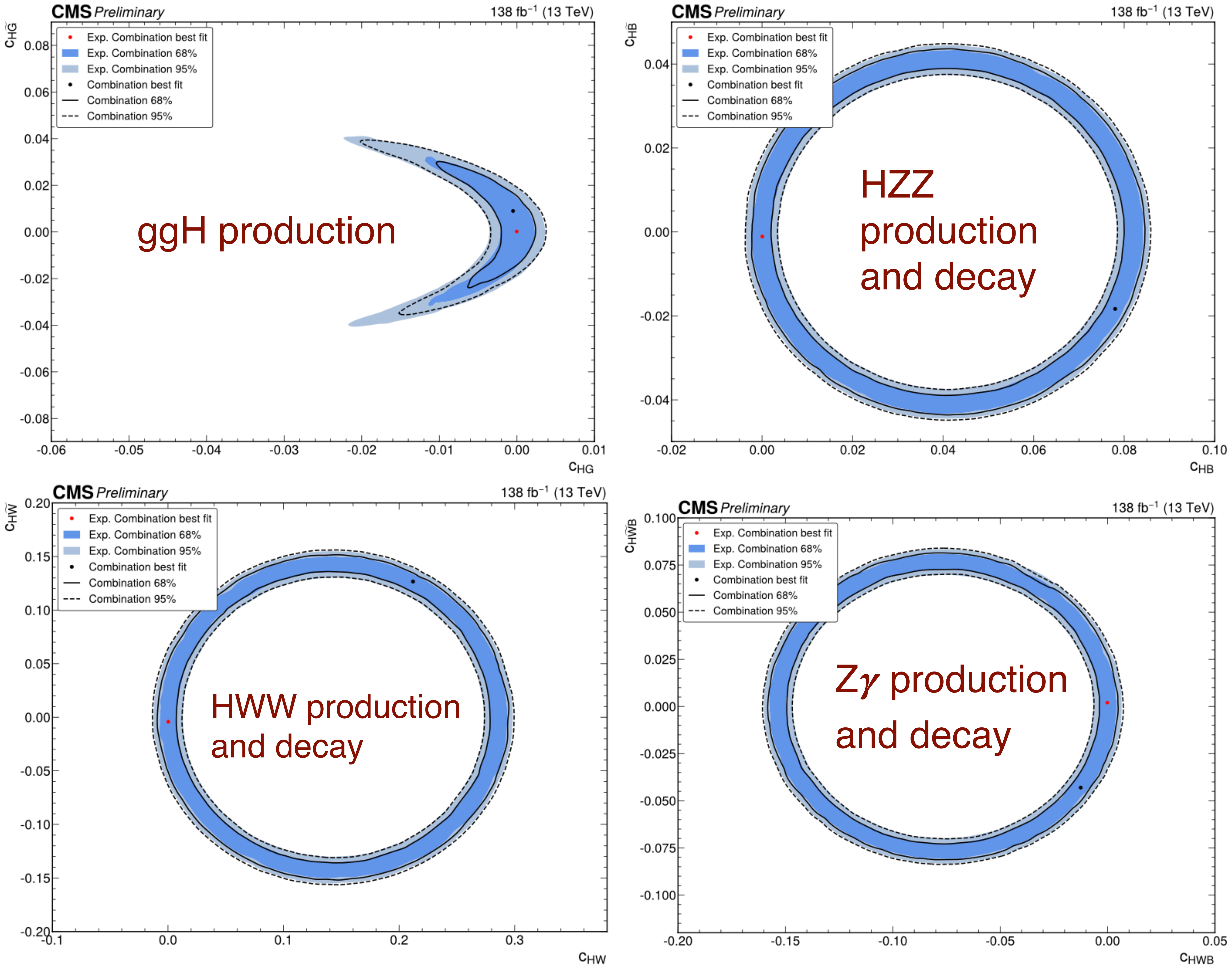

Class	Operator	Wilson coefficient	Example process
$\mathcal{L}_6^{(4)} - X^2H^2$	$H^\dagger H G^a_{\mu\nu} G^{a\mu\nu}$	c_{HG}	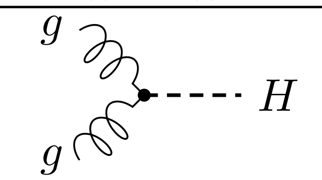
	$H^\dagger H \tilde{G}^a_{\mu\nu} G^{a\mu\nu}$	$\tilde{c}_{HG}$	
	$H^\dagger H B_{\mu\nu} B^{\mu\nu}$	c_{HB}	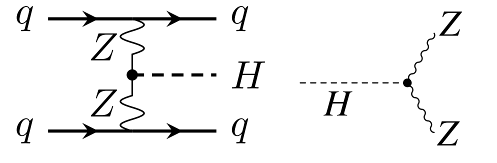
	$H^\dagger H \tilde{B}_{\mu\nu} B^{\mu\nu}$	$\tilde{c}_{HB}$	
	$H^\dagger H W^i_{\mu\nu} W^{i\mu\nu}$	c_{HW}	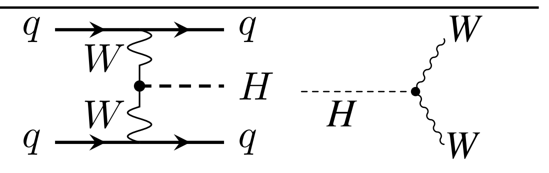
	$H^\dagger H \tilde{W}^i_{\mu\nu} W^{i\mu\nu}$	$\tilde{c}_{HW}$	
	$H^\dagger \sigma^i H W^i_{\mu\nu} B^{i\mu\nu}$	c_{HWB}	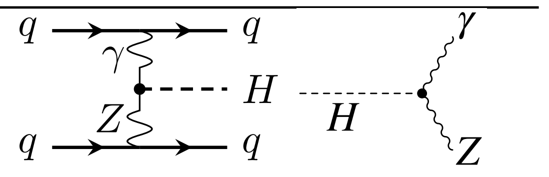
	$H^\dagger \sigma^i H \tilde{W}^i_{\mu\nu} B^{i\mu\nu}$	$\tilde{c}_{HWB}$	

Fit pairs of CP-even and CP-odd Wilson coefficients to assess their impact on Higgs production and decay, all other coefficients set to their SM values of zero.

CMS-PAS-HIG-23-013

Recent Higgs results: Higgs boson CP in Hff coupling

- Run 2 dataset allows to measure directly the **CP structure** of **Hff coupling via ttH+tH production**
  - CMS: 95% CL limit: $|f_{CP}^{Htt}| < 0.67$, CP odd rejected at 3.2σ.
  - ATLAS: $|\alpha| > 43°$ excluded at 95% CL. CP odd rejected at 3.9σ.

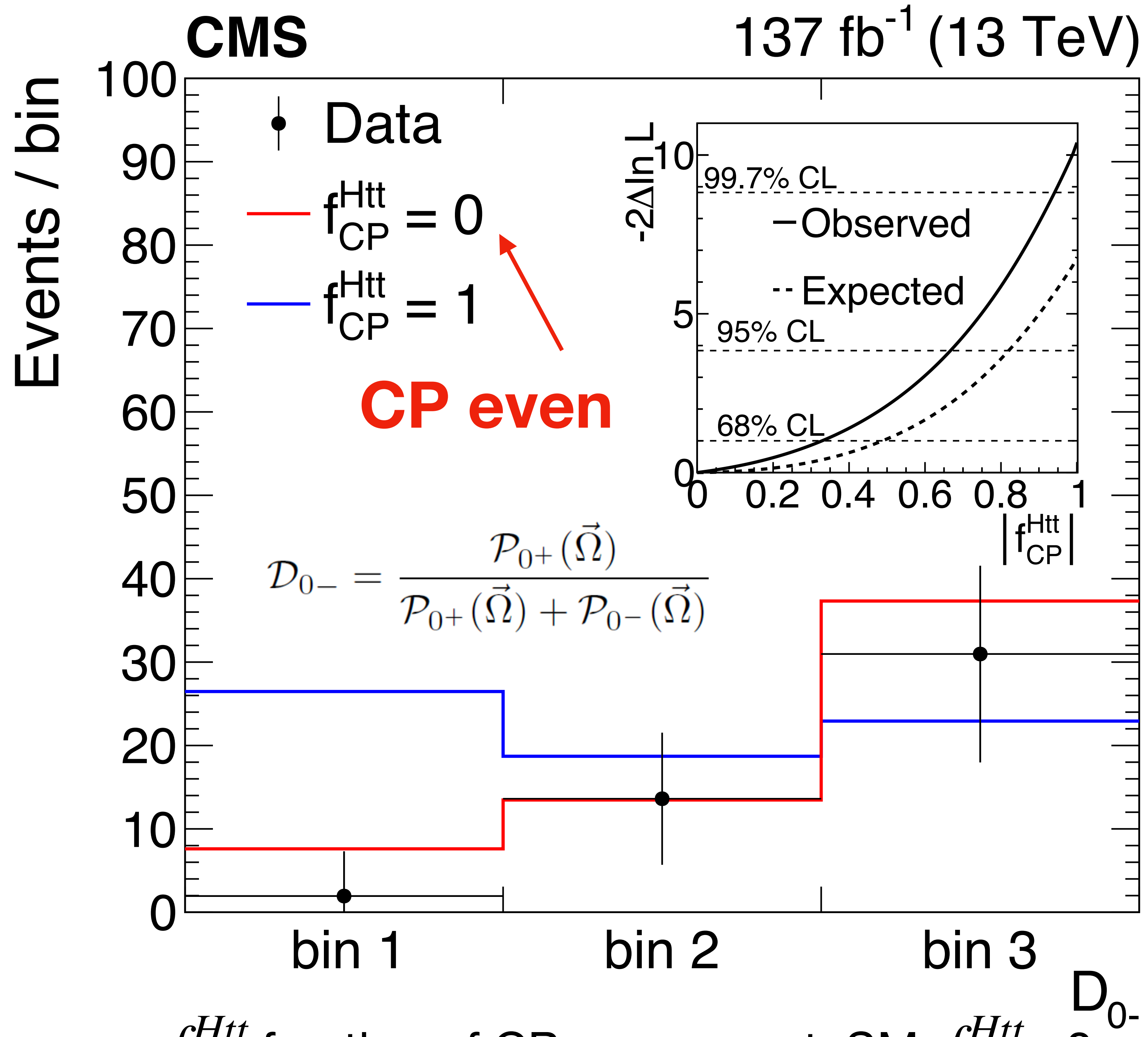

f_{CP}^{Htt} fraction of CP component. SM f_{CP}^{Htt} =0 SM, CP odd f_{CP}^{Htt} =1.

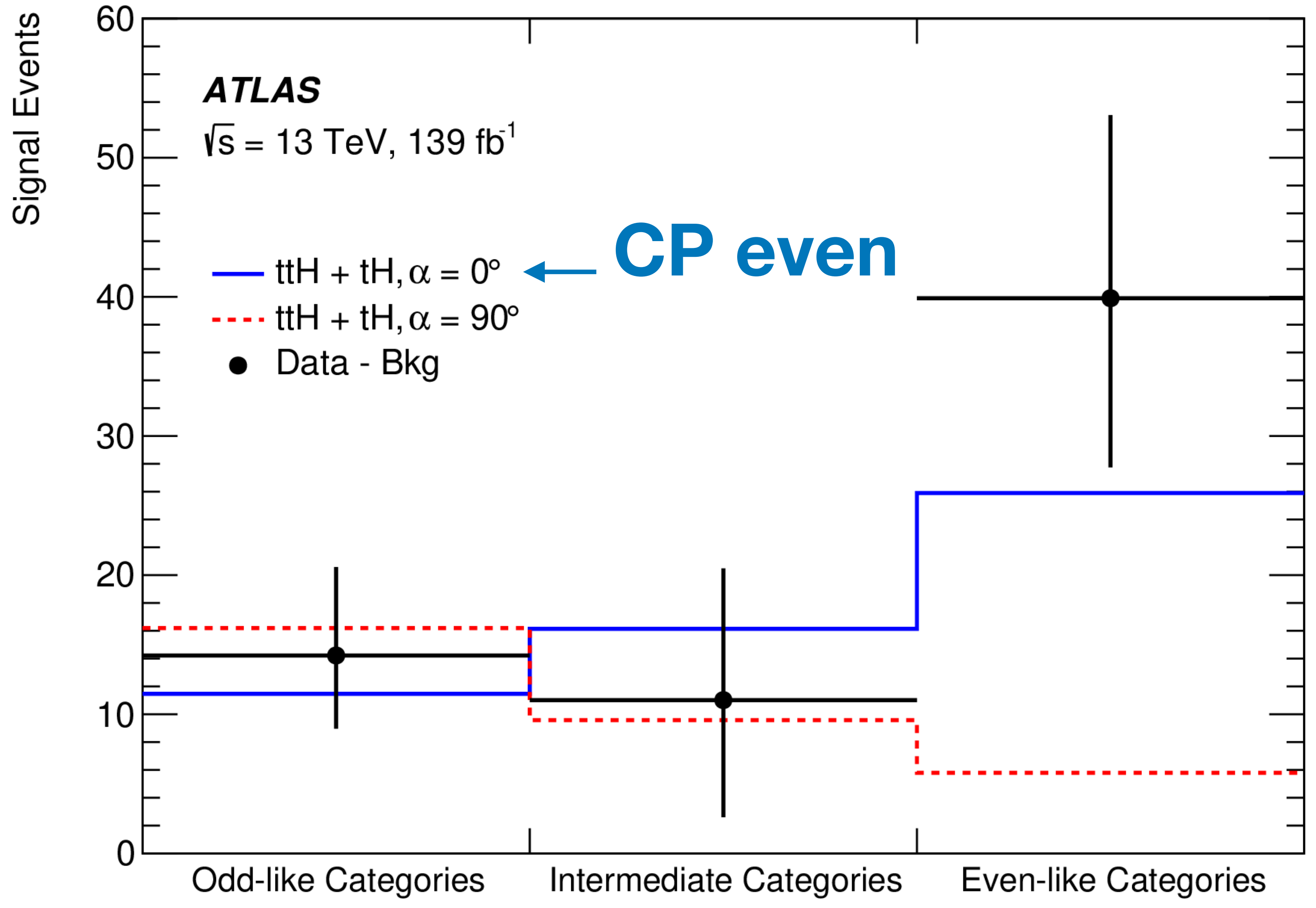

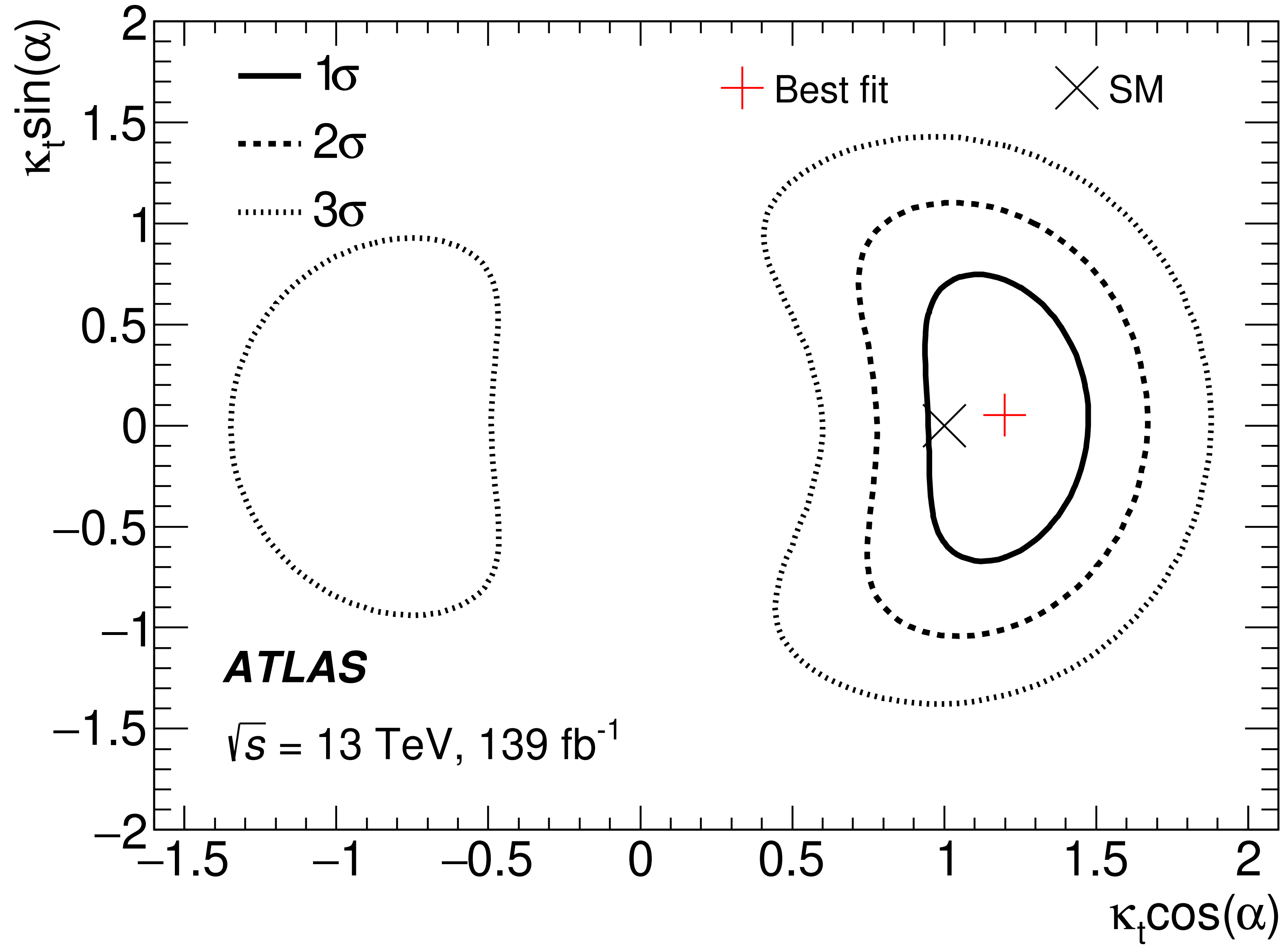

κt: topYukawa coupling, α CP mixing angle, SM κ=1,α=0°, CP odd:α=90°

nonresonant di-Higgs and Higgs self-coupling

- The potential energy of the Higgs field

$$V(\phi) = \frac{1}{2}\mu^2\phi^2 + \frac{1}{4}\lambda\phi^4 \quad (\mu^2 < 0,\ \lambda > 0)$$

- The potential has a minimum which is not at <ϕ>= 0, known as the vacuum expectation value v = 246 GeV

The Higgs potential has the shape of a “mexican hat”

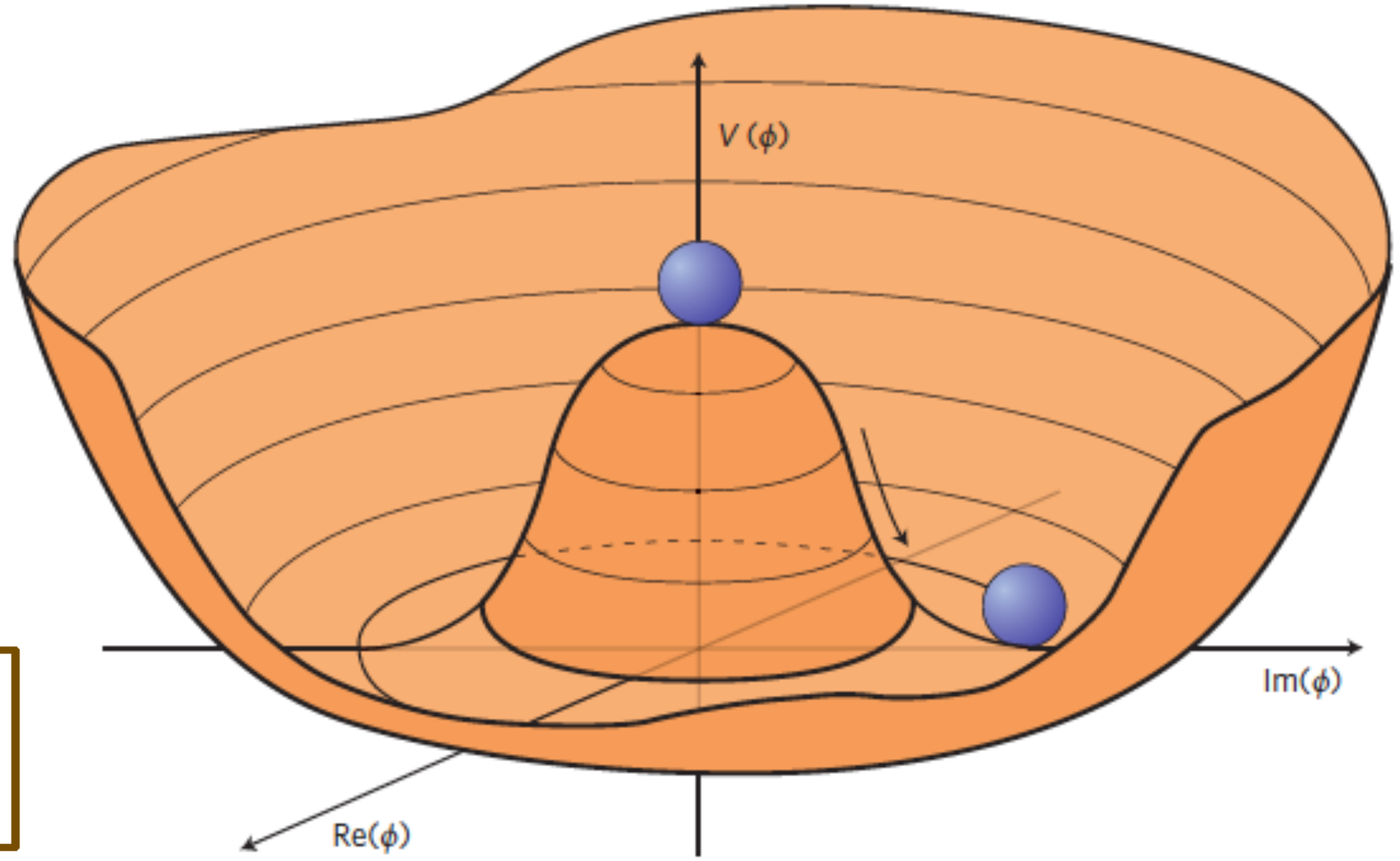

- Expand around the vacuum expectation value: $V(\varphi) \to V(v + h)$
- $V(h) = V_0 + \lambda v^2 h^2 + \lambda v h^3 + \frac{1}{4}\lambda h^4 + \cdots$
- $V(h) = V_0 + \underbrace{\frac{1}{2}{m_h}^2 h^2}_{\text{Mass term}} + \underbrace{\lambda v h^3}_{\text{Higgs trilinear self-coupling}} + \underbrace{\frac{1}{4}\lambda h^4}_{\text{Higgs quadratic self-coupling}} + \cdots$

Double Higgs production → Higgs trilinear self-coupling

This is what this talk is about

$\upsilon = \frac{\mu}{\sqrt{\lambda}}$ and $\mu = \frac{{m_h}^2}{2}$

In the SM υ=246 GeV

$$\lambda = \frac{{m_h}^2}{2\upsilon^2} \approx 0.13$$

nonresonant di-Higgs and Higgs self-coupling

- trilinear self-coupling (λ_3) can be probed directly via HH production, extremely challenging to measure at LHC

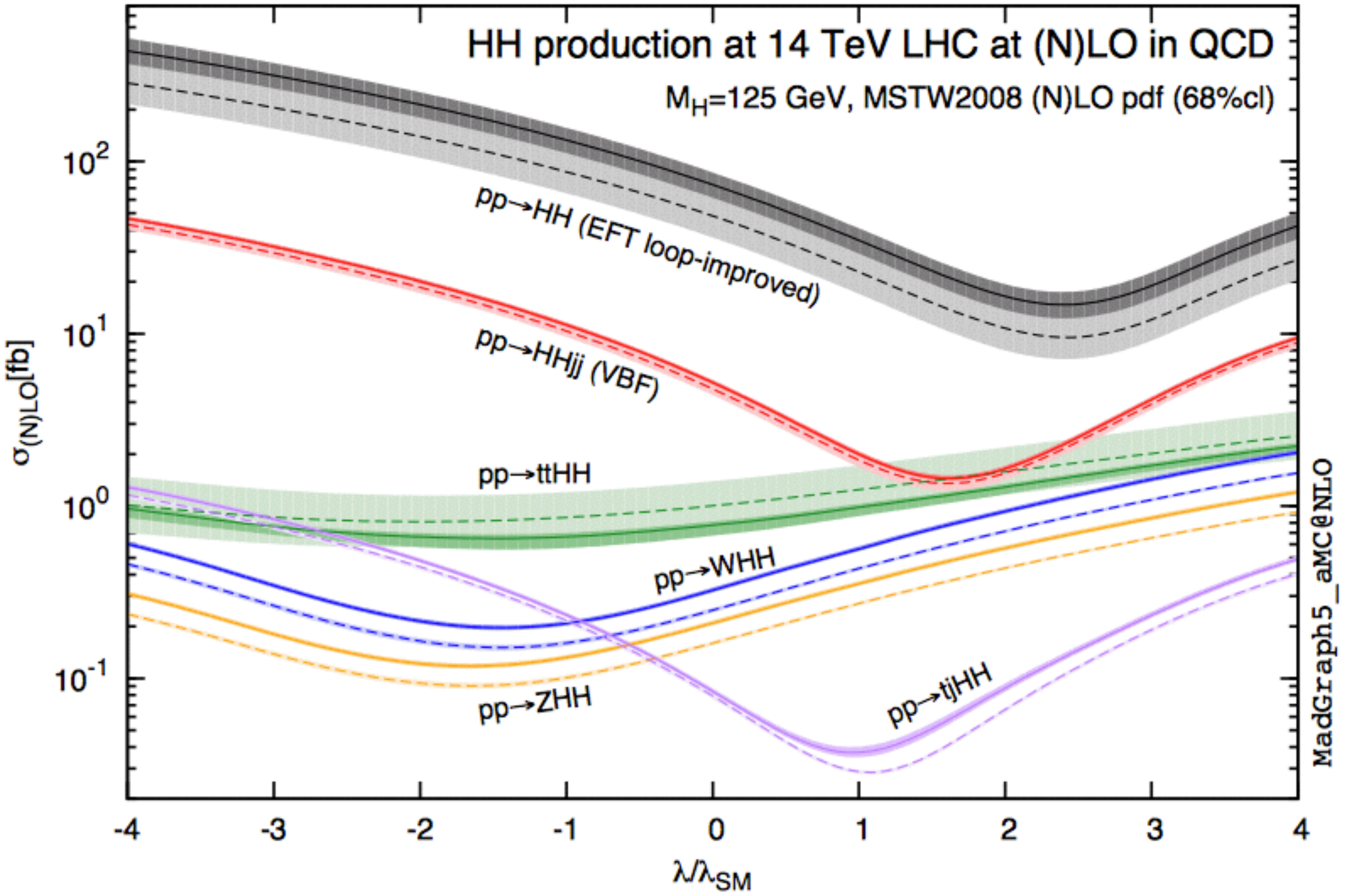

R.Frederix et al: Phys.Lett. B732 (2014) 142-149

gluon fusion HH production at the LHC

- Dominant gluon-gluon fusion (ggF) production mode (σ_{ggF} = 31.05 fb NNLO FTapprox) gives best access to H self-coupling (κ_λ)

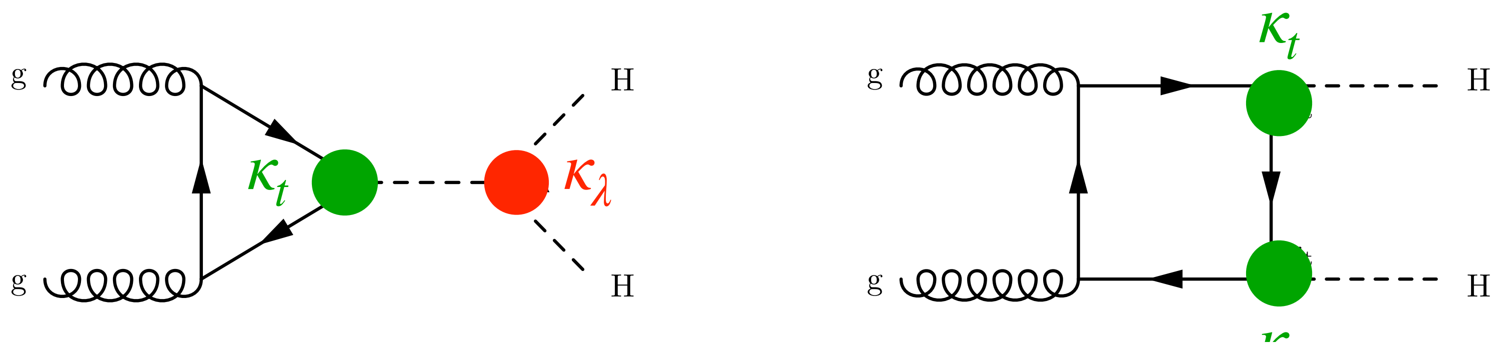

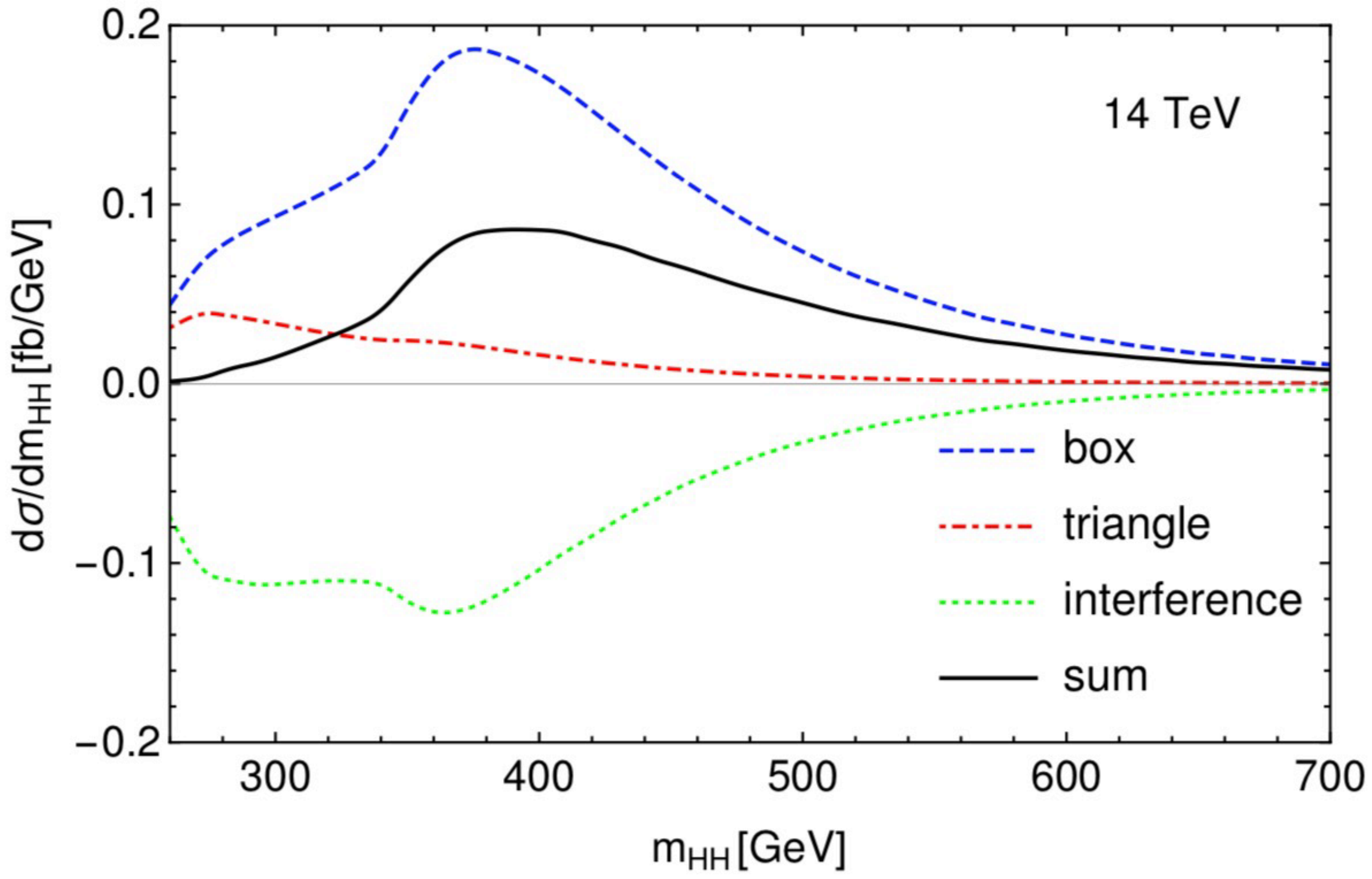

- Spectrum of m_{HH} depends on κ_λ

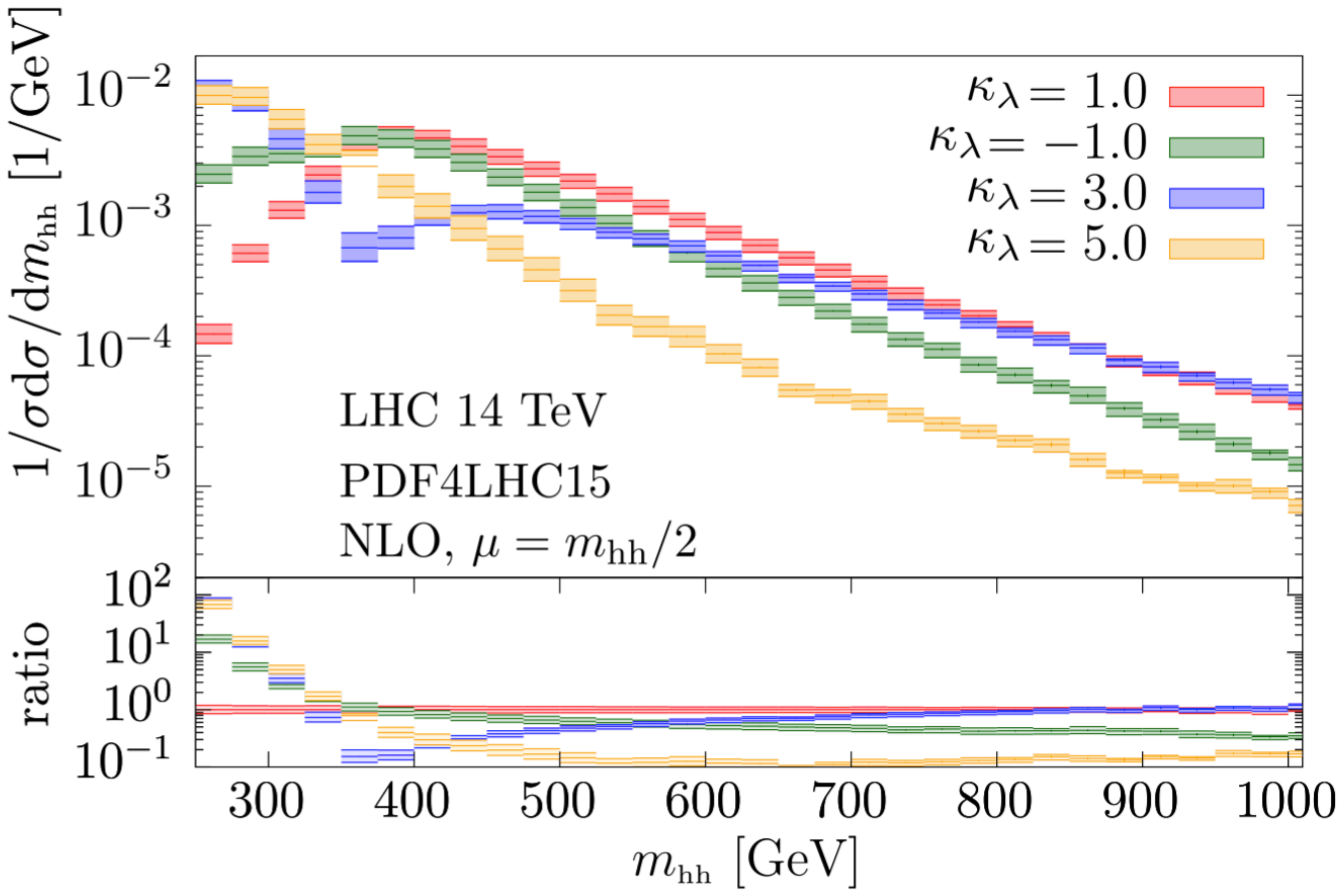

VBF HH Production at the LHC

- Vector boson fusion (VBF) (σ_{VBF} = 1.73 fb N^{3}LO) sensitive to HHVV coupling (κ_{2V})

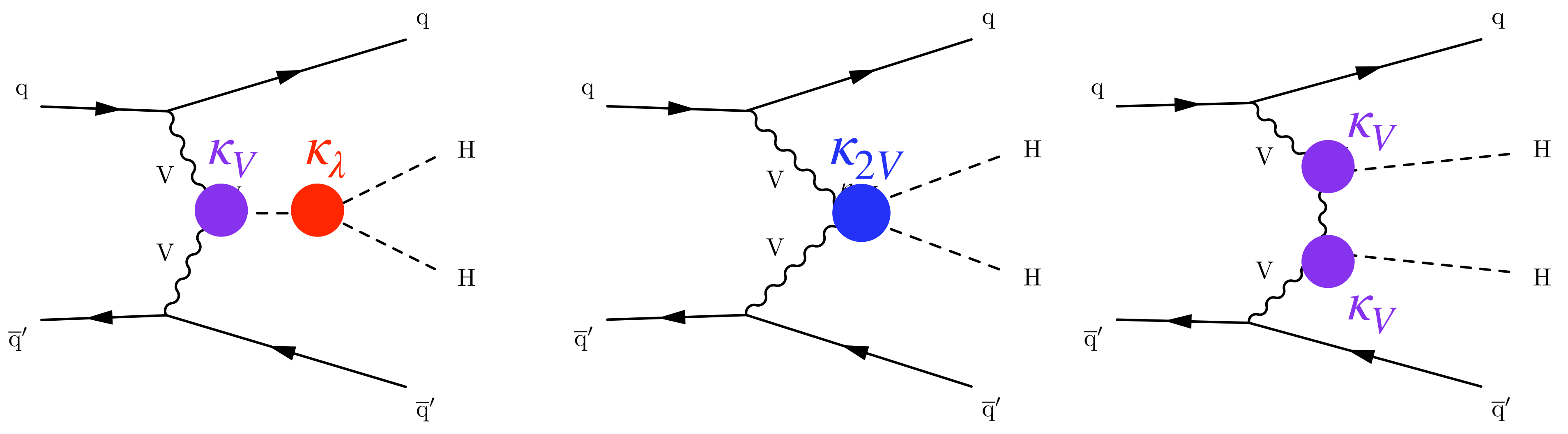

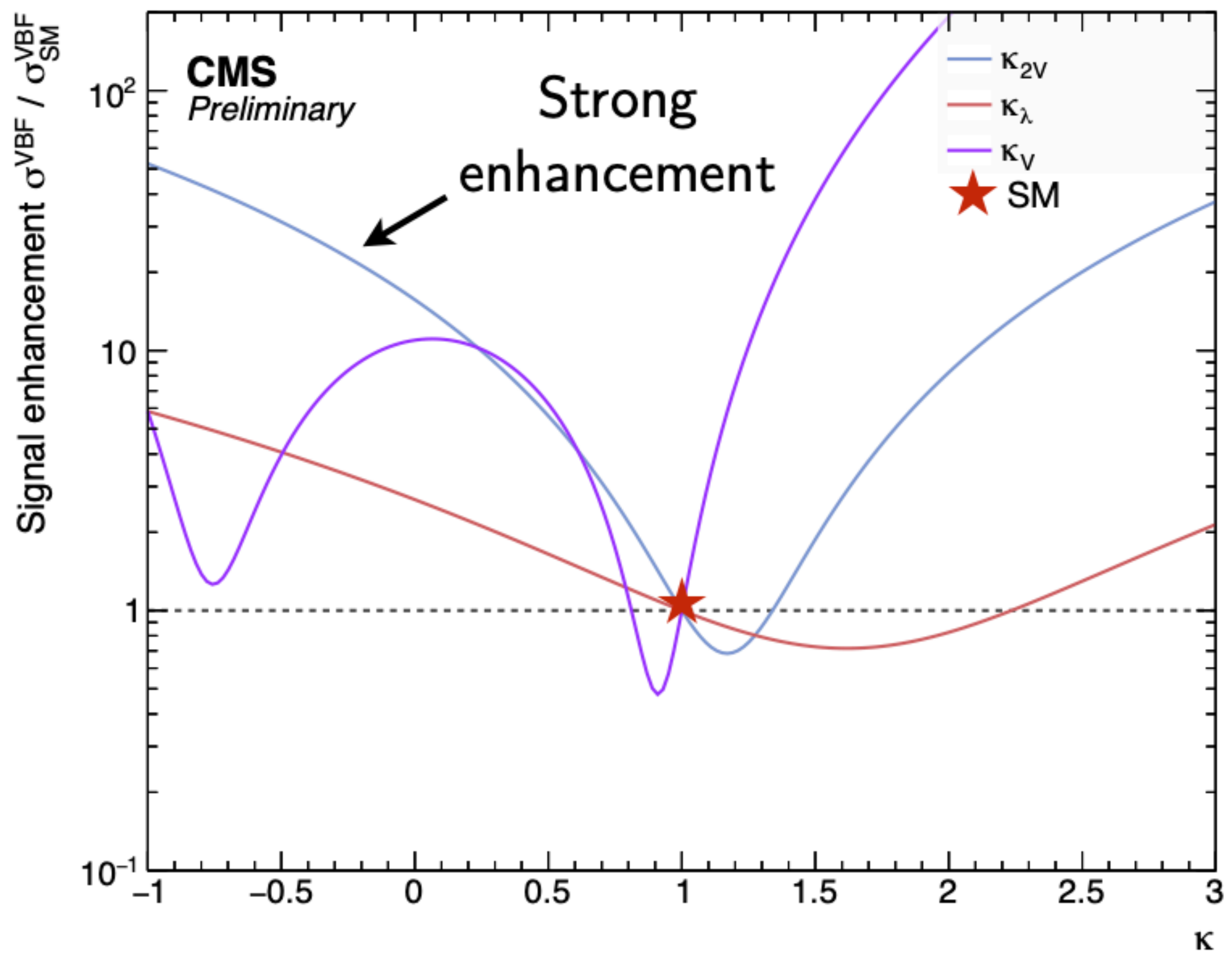

- smaller κ_{2V} => larger cross section, harder m_{HH} spectrum, boosted VBF signatures

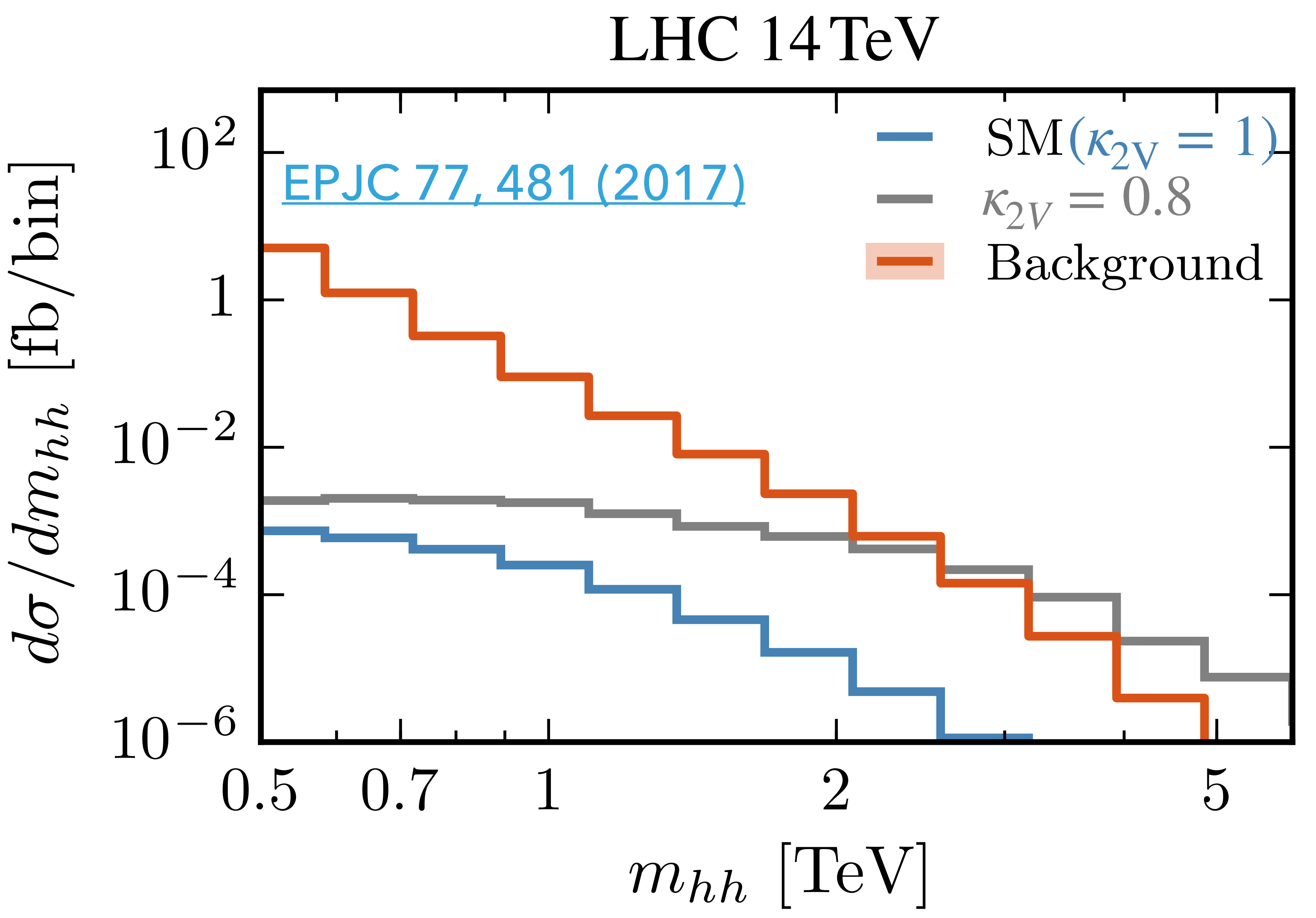

HEFT studies with di-Higgs

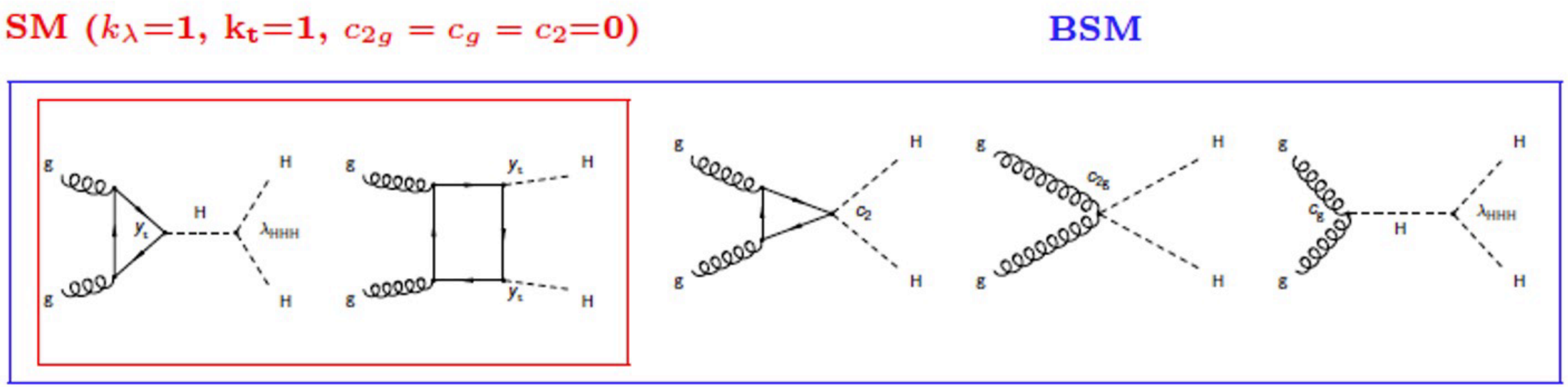

- **HEFT** ggF cross section modeling with three new contact interactions (couplings): ttHH (C_2), ggHH (C_{2g}) and ggH (C_g)
- HEFT benchmarks: JHEP 09 (2018) 057, JHEP 04 (2016) 126, JHEP 03 (2020) 091
  - Extract cross section upper limit on the benchmarks to explore HEFT sensitivity

	1	2	3	4	5	6	7	8	9	10	11	12	SM
κ_λ	7.5	1.0	1.0	−3.5	1.0	2.4	5.0	15.0	1.0	10.0	2.4	15.0	1.0
κ_t	1.0	1.0	1.0	1.5	1.0	1.0	1.0	1.0	1.0	1.5	1.0	1.0	1.0
c_2	−1.0	0.5	−1.5	−3.0	0.0	0.0	0.0	0.0	1.0	−1.0	0.0	1.0	0.0
c_g	0.0	−0.8	0.0	0.0	0.8	0.2	0.2	−1.0	−0.6	0.0	1.0	0.0	0.0
c_{2g}	0.0	0.6	−0.8	0.0	−1.0	−0.2	−0.2	1.0	0.6	0.0	−1.0	0.0	0.0

nonresonant HH searches in Run 2 CMS

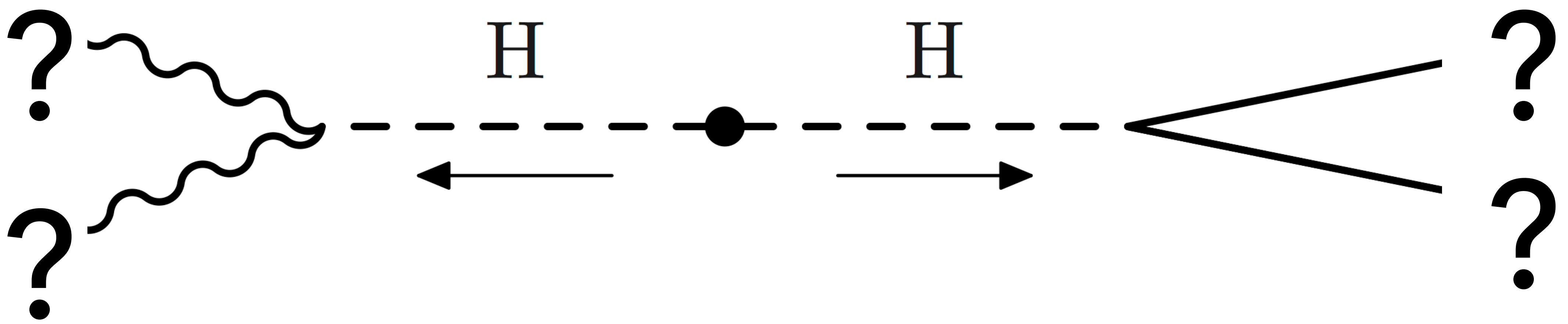

- ggF and VBF HH → bbbb boosted (Phys. Rev. Lett. 131 (2023) 041803) resolved (PRL. 129, 081802) , VH (rXiv:2404.08462 Accepted for publication in JHEP)
- HH → bbττ (Phys. Lett. B 842 (2023) 137531)
- HH → bbWW (JHEP07(2024)293)
- HH → ττγγ (CMS-PAS-HIG-22-012)
- HH → bbZZ(4l) (JHEP 06 (2023) 130)
- HH → bbγγ (JHEP03(2021)257)
- multilepton (e, μ, τ_h), HH → WWWW + WWττ + ττττ (JHEP 07 (2023) 095)
- HH → WWγγ (CMS-PAS-HIG-21-014)

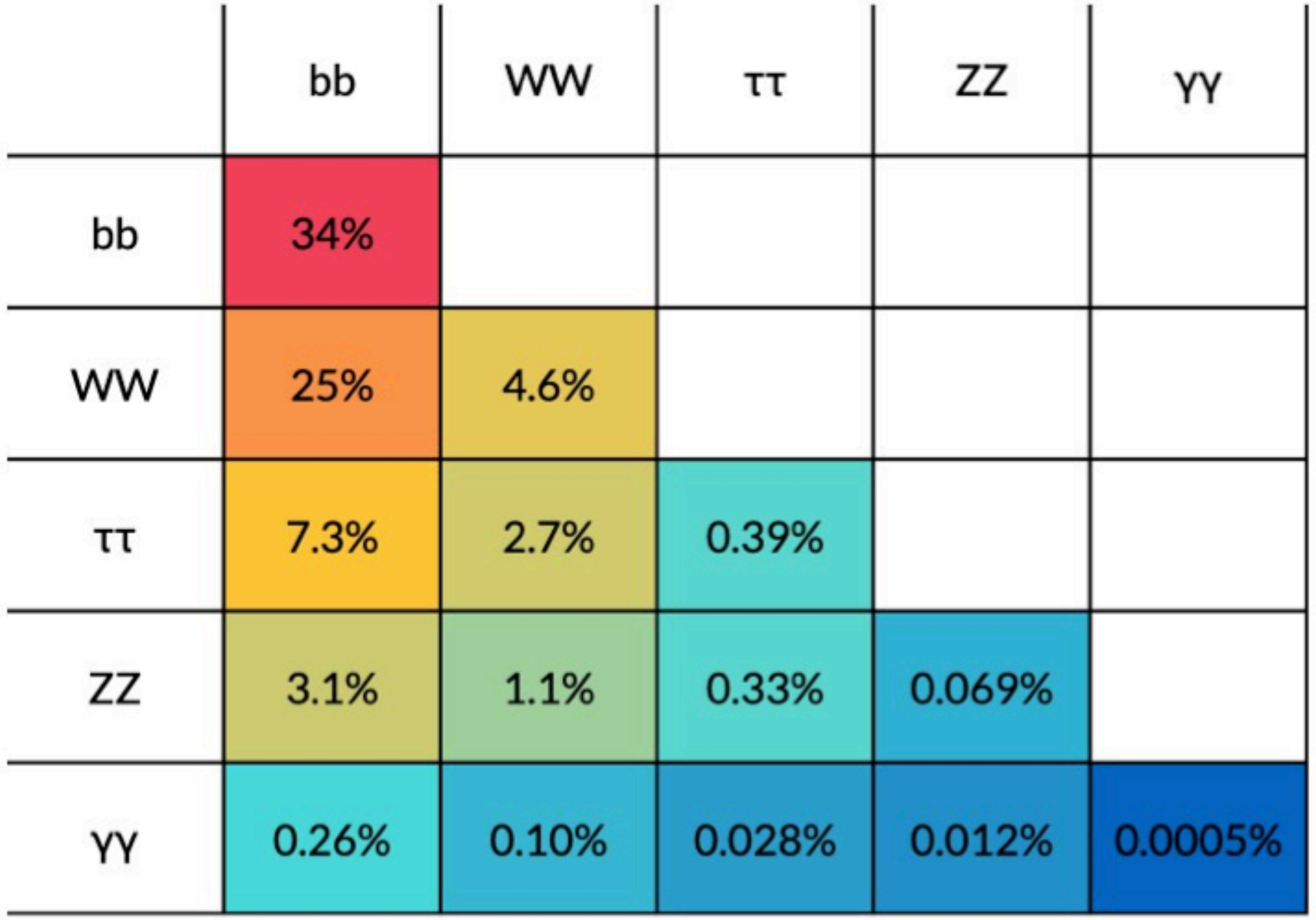

	bb	WW	ττ	ZZ	γγ
bb	34%				
WW	25%	4.6%			
ττ	7.3%	2.7%	0.39%		
ZZ	3.1%	1.1%	0.33%	0.069%	
γγ	0.26%	0.10%	0.028%	0.012%	0.0005%

Probing Higgs boson self-coupling using boosted Higgs

- Phys. Rev. Lett. 131 (2023) 041803

Probing Higgs boson self-coupling using boosted Higgs

- **HH→4b decay** channel has the **largest branching ratio (34%),**
- **~1.5k** HH→4b events produced in Run 2
- **~15%** HH→4b events with two boosted Higgs (p_T > 250 GeV)

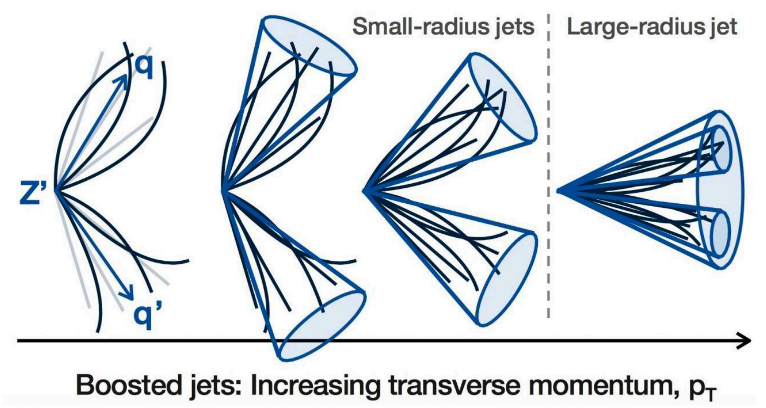

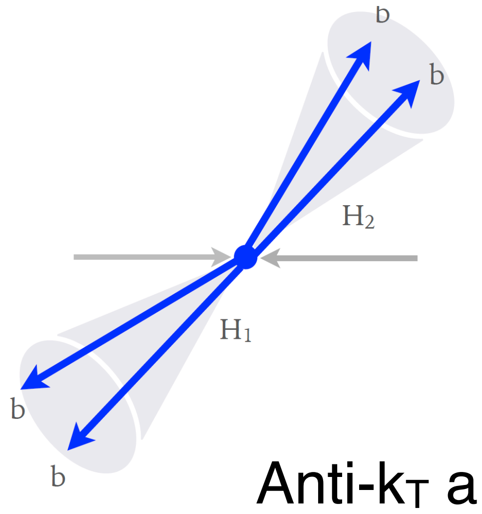

Anti-k_T algorithm with R=0.8 (AK8) jets

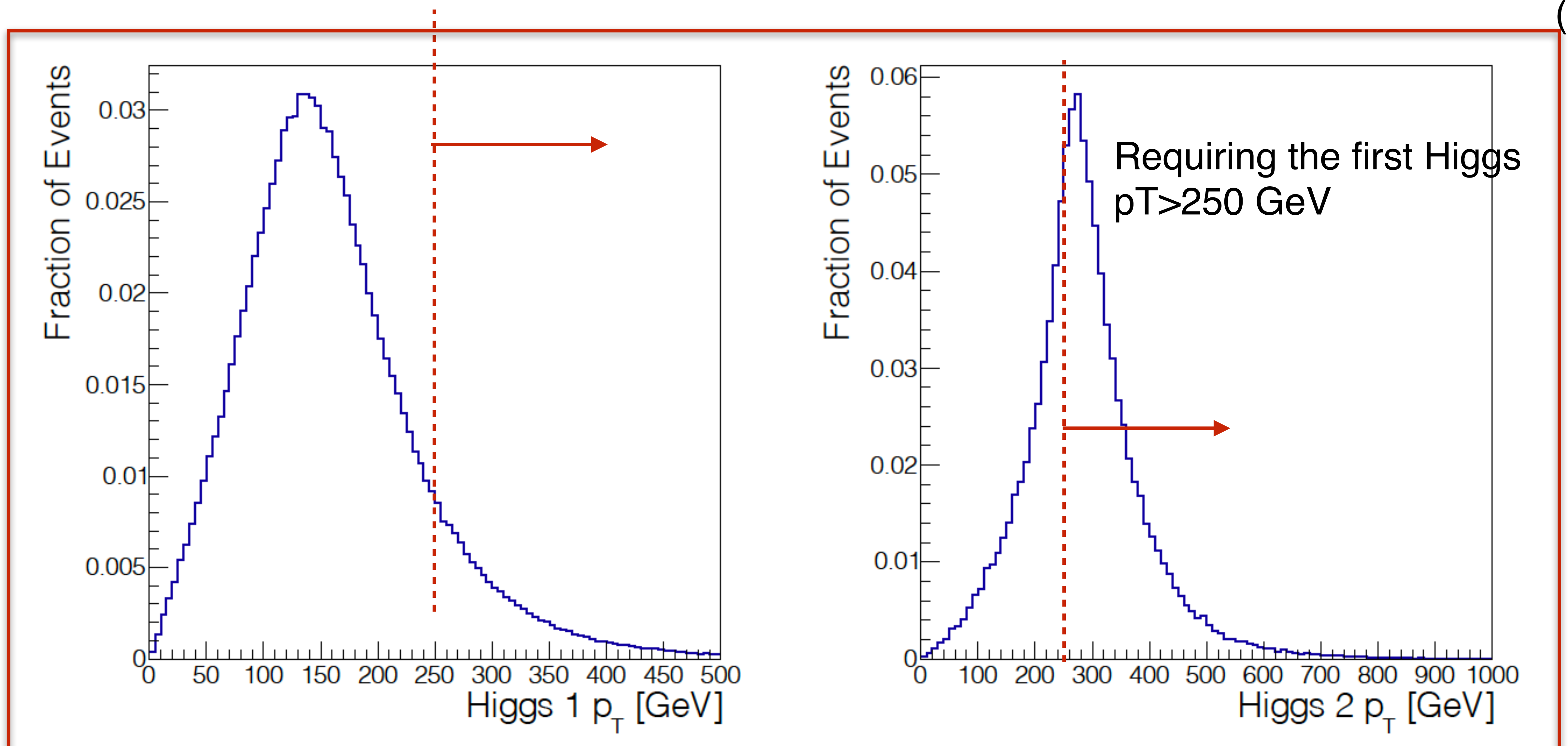

Requiring the first Higgs pT>250 GeV

~20% acceptance for the first Higgs to have high pT > 250 GeV

Requiring first Higgs pT>250 GeV, large acceptance (75%) for having a second boosted Higgs

ParticleNet Jet tagger for AK8 jets

ParticleNet: A multi-class jet classifier for top,

Higgs, W or Z tagging for large radius jets

- "New Approaches for Jet Tagging With Machine Learning" TDLI/SJTU HEP Seminar - June 30, 2021 by Huilin Qu
- PRD 101, 056019 (Huilin Qu, Loukas Gouskos)
- ParticleNet CMS note (CMS-DP-2020-002)

Mass decorrelated ParticleNet-MD:

background efficiency of ~0.1% for signal efficiency of 50%

- Compare to DeepAK8-MD, background

rejection improved by a factor of ~2 per jet

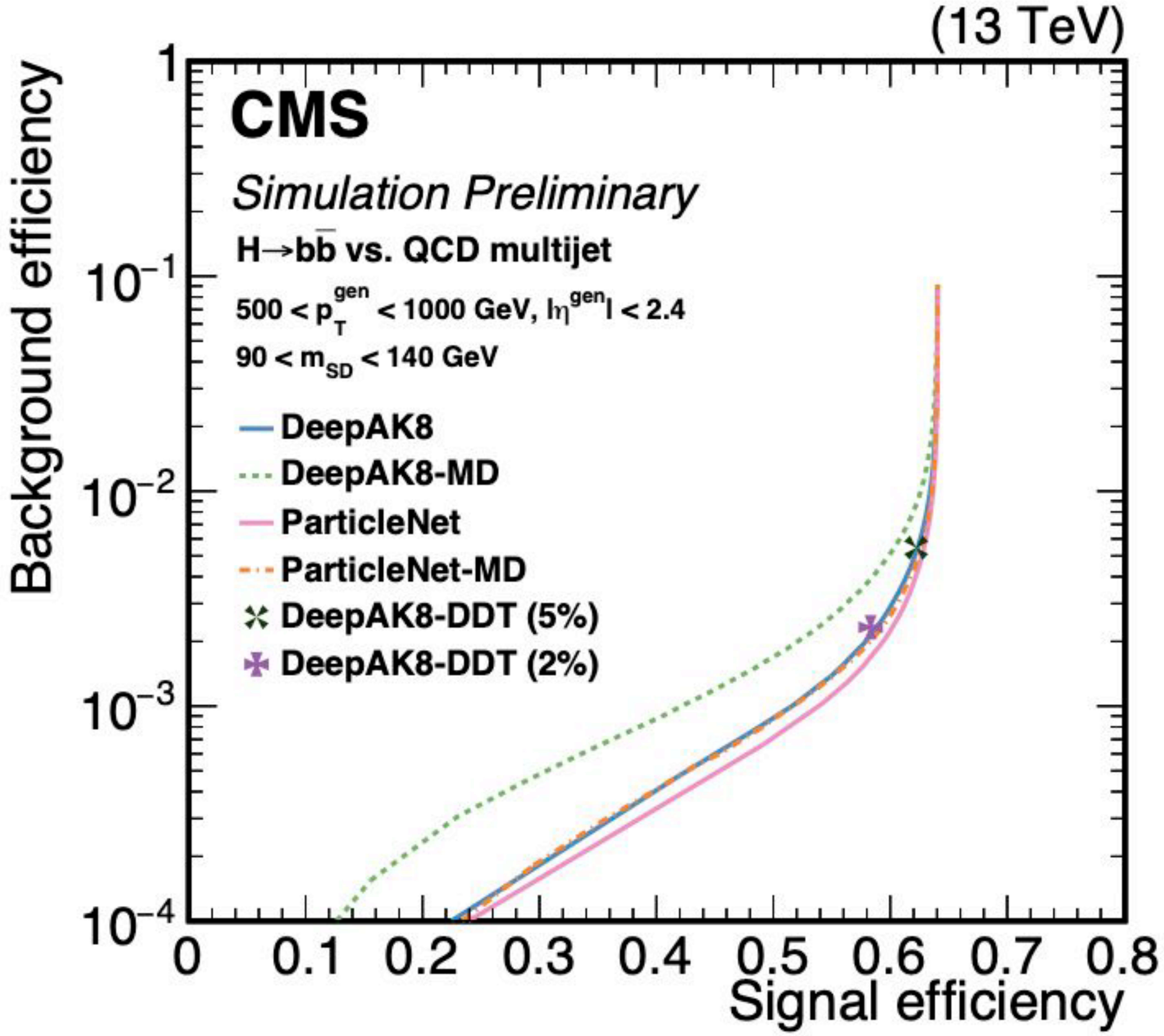

ParticleNet Jet tagger for AK8 jets

ParticleNet output scores: X→bb, X→cc, X→light quarks, QCD jets

- search for boosted HH → bbbb, discriminate X→bb vs QCD jets:

$$T_{Xbb} = \frac{P_{Xbb}}{P_{Xbb} + P_{QCD}}$$

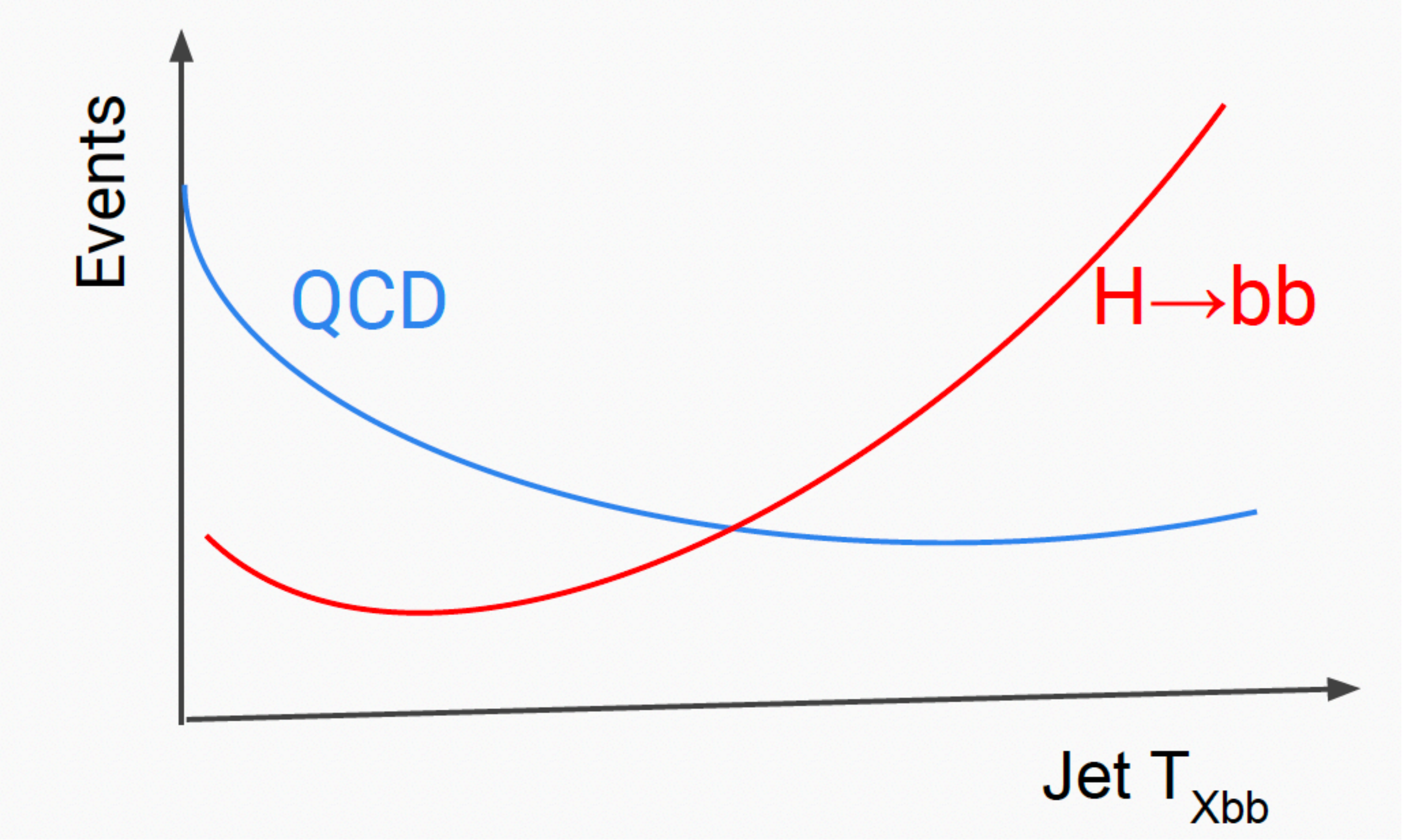

Trigger

- A combination of several trigger algorithms: requiring large total hadronic transverse energy in the event (H_T) or AK8 jet with large p_T. a minimum triggering threshold on the jet mass is imposed in order to reduce the H_T or p_T thresholds.

- Trigger efficiency:10 ~ 95% for jets with $300 < p_T < 450$ GeV, fully efficient for jets with $p_T > 500$ GeV

- Trigger is a crucial factor for this analysis.

Event selection

- Two complementary ggF and VBF analyses:
  - VBF selection: two AK4 jets: m_{jj}>400 GeV, $\Delta\eta_{jj} > 4.0$
  - ggF analysis veto VBF selection
- Identify boosted high-p_T Higgs candidate jets：
  - ParticleNet $H \rightarrow bb$ tagger T_{Xbb}
  - ParticleNet regressed jet mass $m_{regressed}$
- ggF analysis preselection:
  - at least two AK8 Jets with $p_T > 300$ GeV
  - rank Jets based on T_{Xbb}
  - Jet 1 soft drop mass $m_{SD} > 50$ GeV
  - Jet 2 ParticleNet regressed mass $m_{regressed} > 50$ GeV
  - Jet 1 $T_{Xbb} > 0.8$

BDT discriminant for background rejection

After preselection, train BDT to separate gluon fusion HH signal and main backgrounds (QCD multijet and $t\bar{t}$)

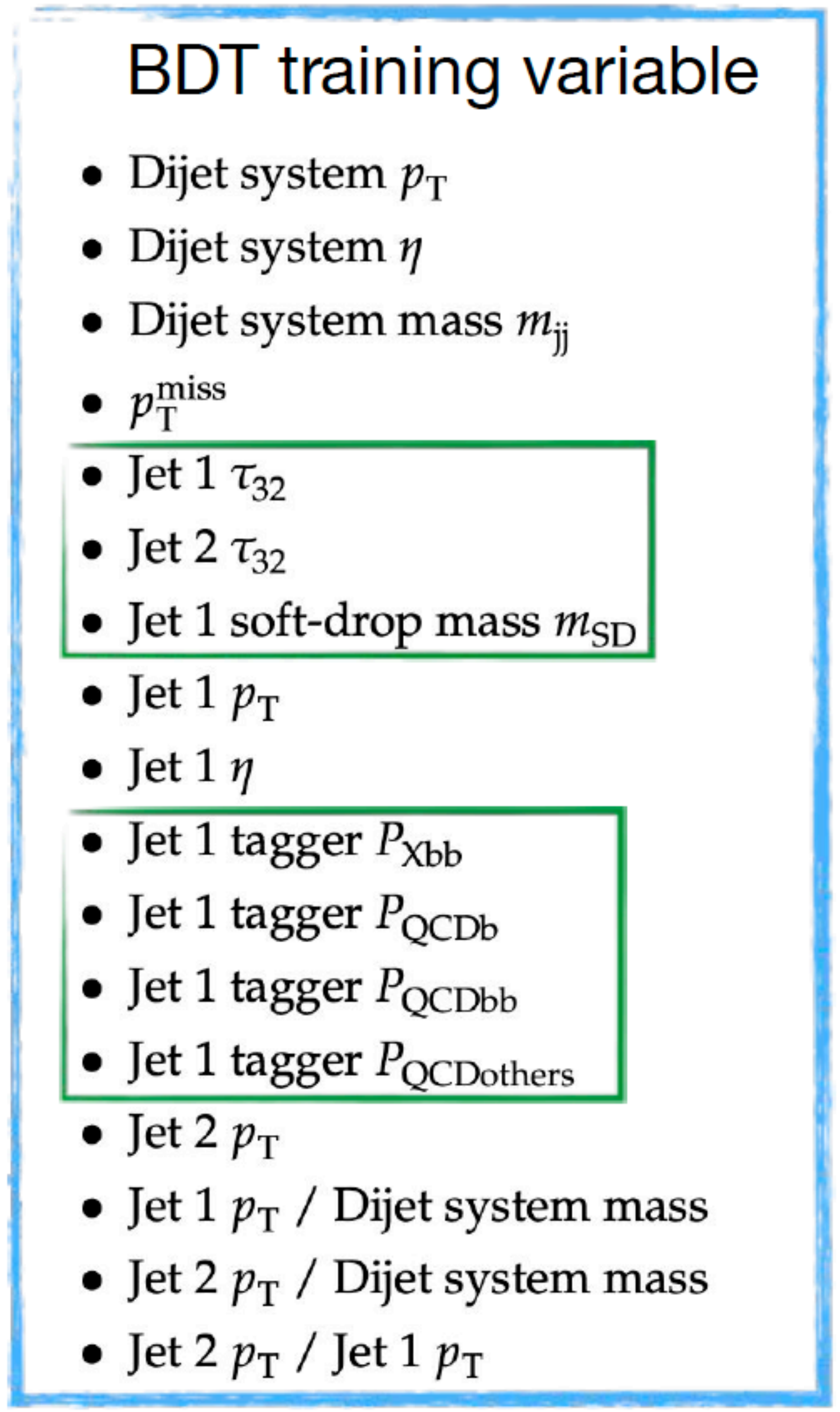

BDT training variable

- Dijet system p_{T}
- Dijet system η
- Dijet system mass m_{jj}
- $p_{\mathrm{T}}^{\mathrm{miss}}$
- Jet 1 τ_{32}
- Jet 2 τ_{32}
- Jet 1 soft-drop mass m_{SD}
- Jet 1 p_{T}
- Jet 1 η
- Jet 1 tagger P_{Xbb}
- Jet 1 tagger P_{QCDb}
- Jet 1 tagger P_{QCDbb}
- Jet 1 tagger $P_{\mathrm{QCDothers}}$
- Jet 2 p_{T}
- Jet 1 p_{T} / Dijet system mass
- Jet 2 p_{T} / Dijet system mass
- Jet 2 p_{T} / Jet 1 p_{T}

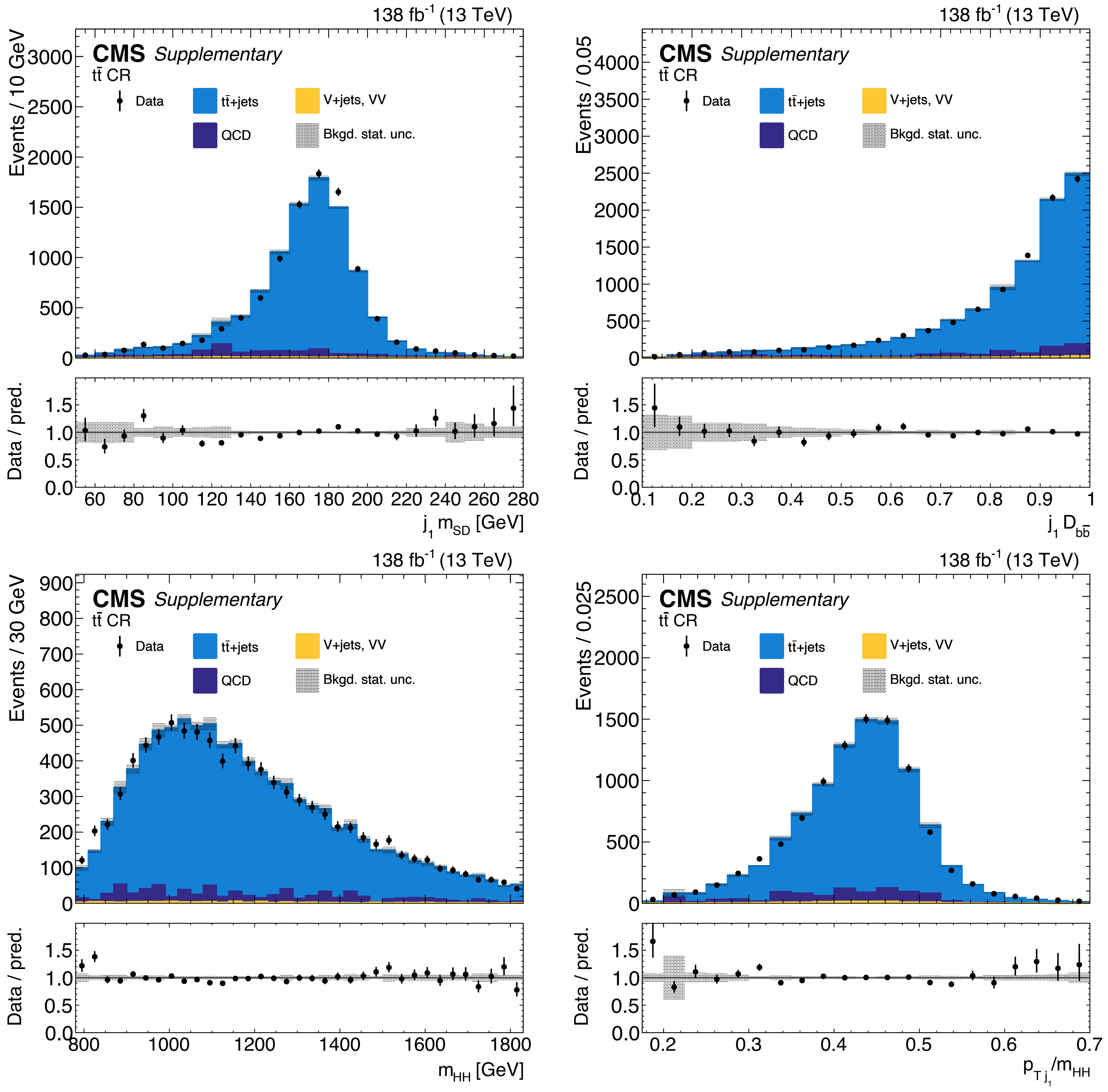

Event Categories

- Three event categories (Bin 1, 2 and 3) optimized based on BDT score and Jet 2 T_{xbb} tagger score
- QCD control region used to estimate QCD multijet background

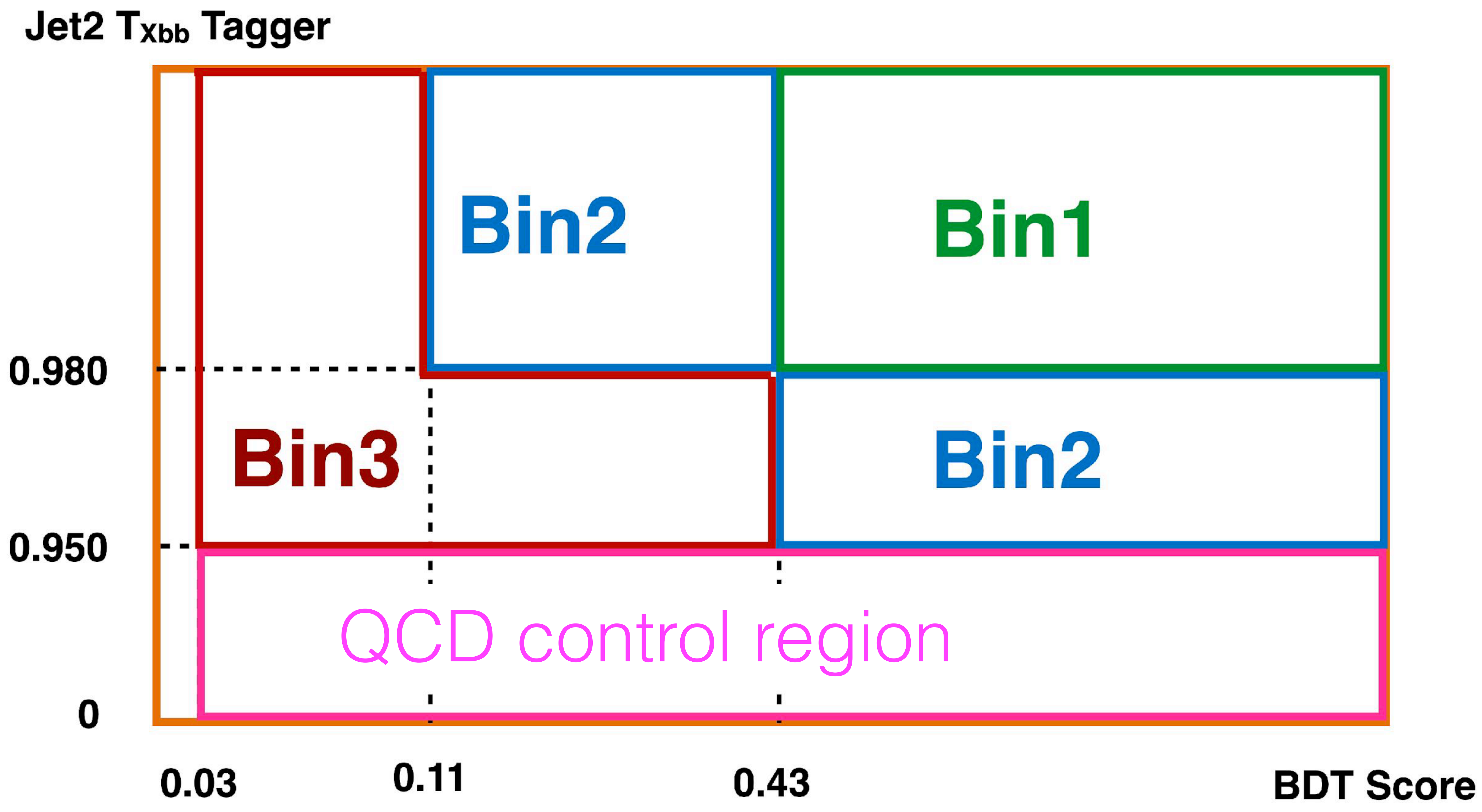

Background estimation

QCD multijet

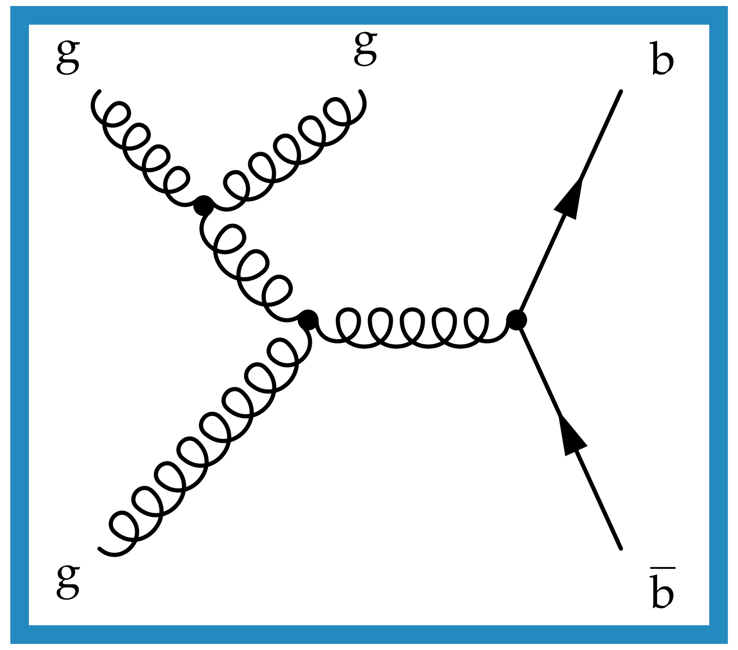

$t\bar{t}$+jets

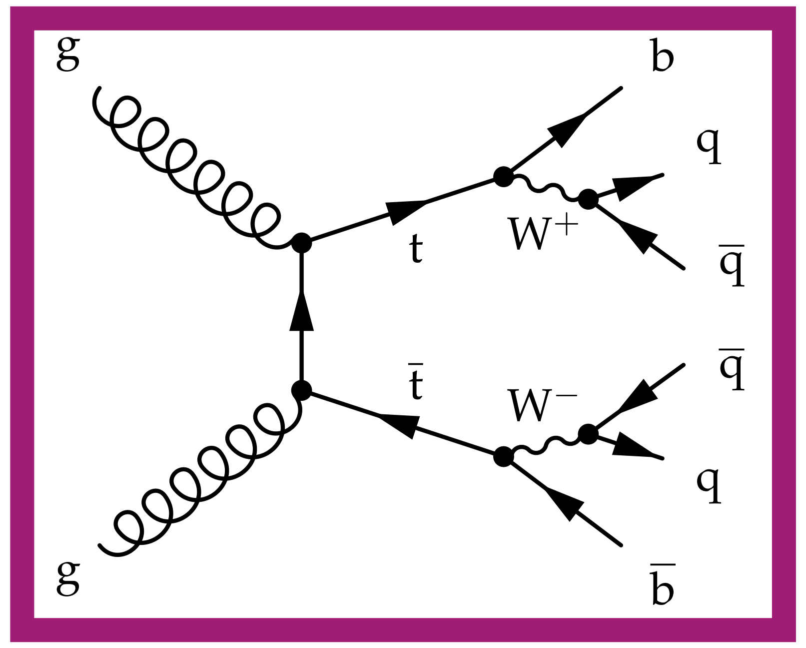

- Main backgrounds:
  - $t\bar{t}$+jets: simulation with corrections derived in data
  - QCD multijet production: parametric fit to data in control region

QCD control region × transfer factor = signal region: BDT Bin

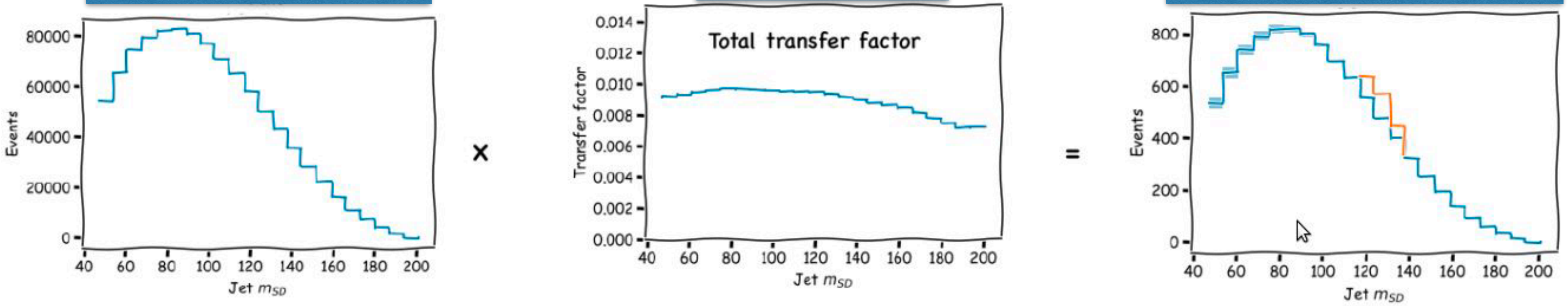

- Other backgrounds estimated by simulation:
  - VH, ttH
  - V+jets, VV

Results

- Observed (expected) upper limit at 95% CL on HH cross section: 9.9 (5.1) × SM
  - driven by ggF analysis

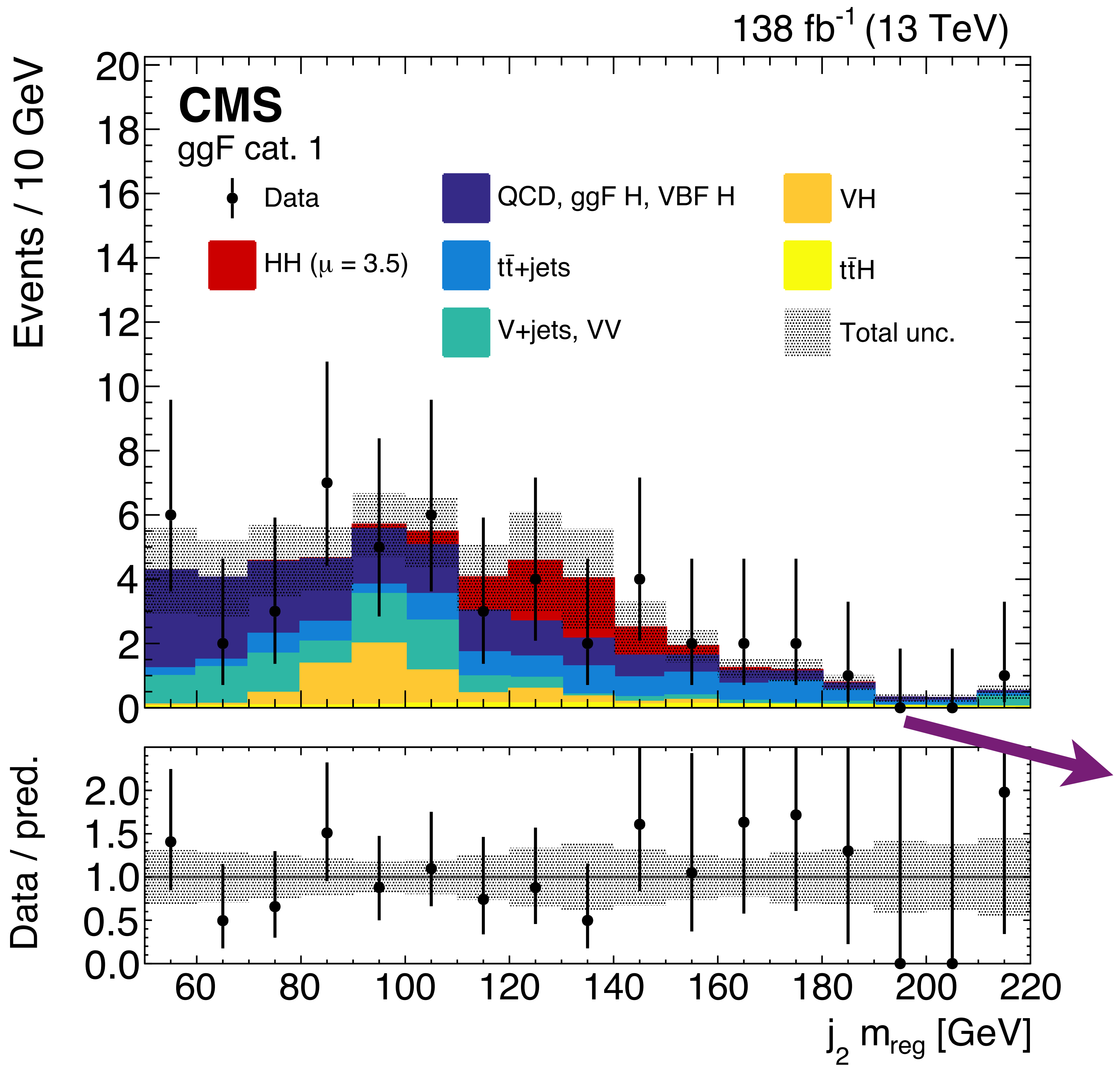

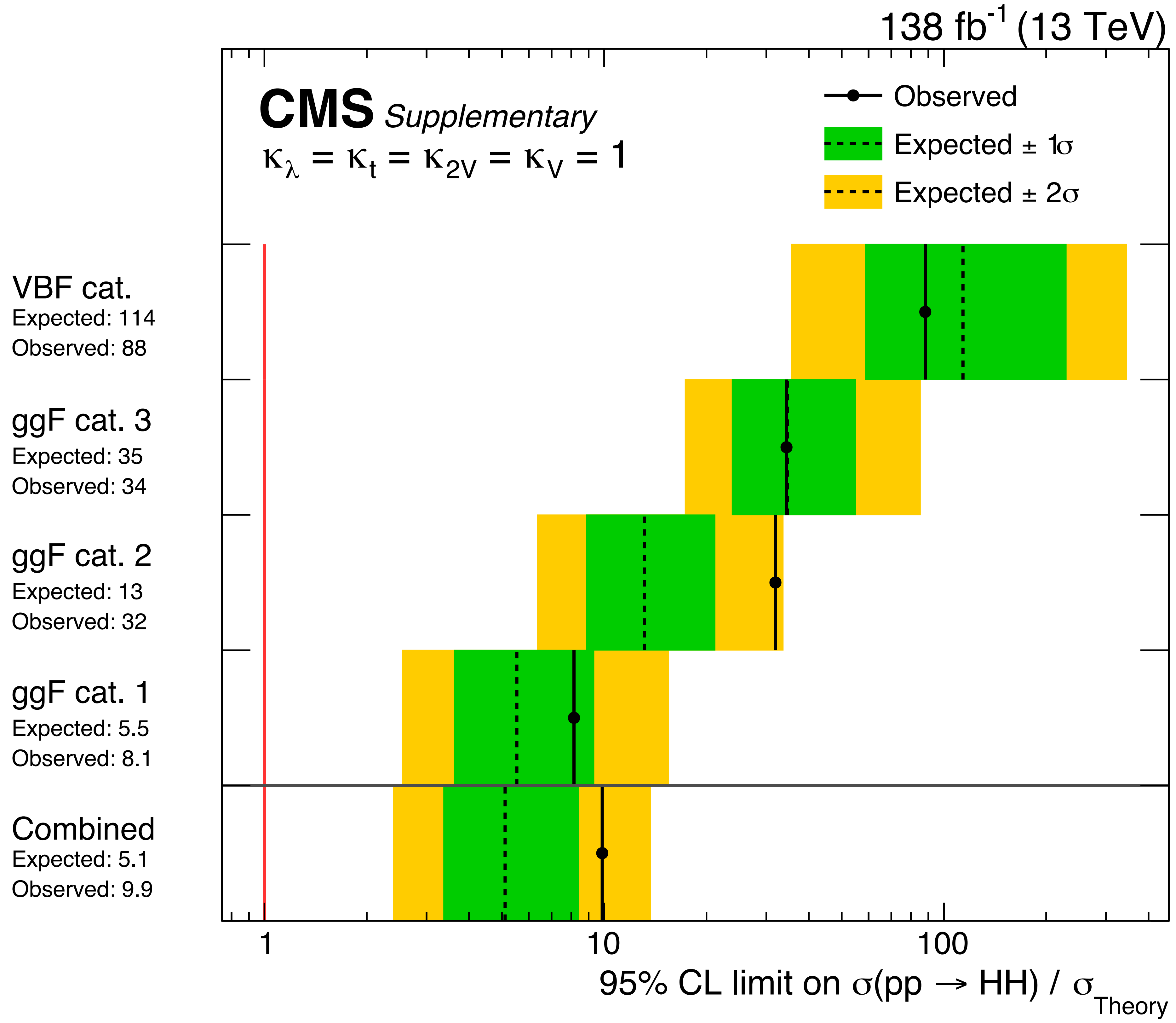

Results

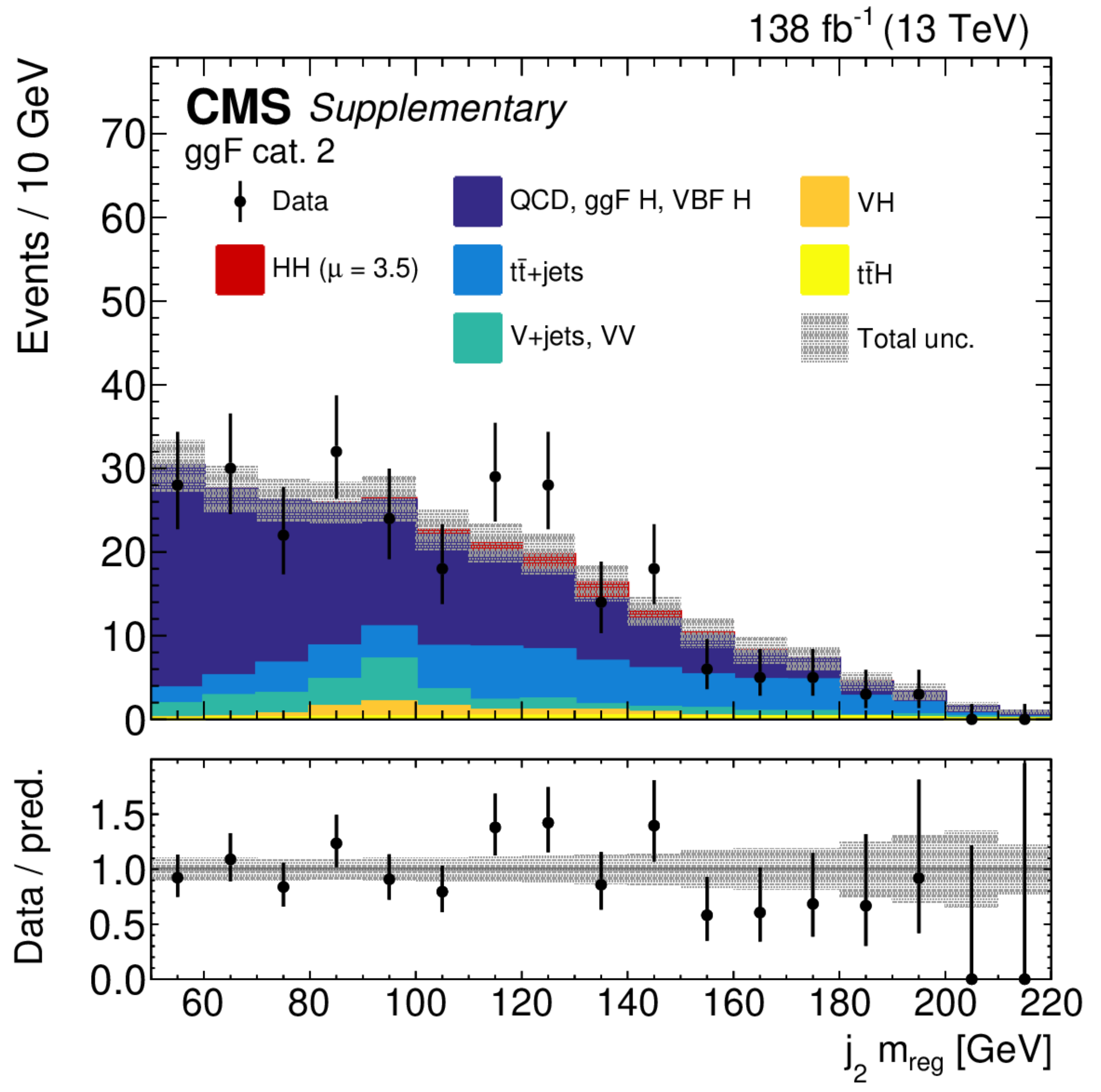
138 fb^{-1} (13 TeV)
CMS Supplementary
ggF cat. 2
Data
QCD, ggF H, VBF H
VH
HH (μ = 3.5)
tt̄+jets
tt̄H
V+jets, VV
Total unc.
Events / 10 GeV
0
10
20
30
40
50
60
70
Data / pred.
0.0
0.5
1.0
1.5
60
80
100
120
140
160
180
200
220
j$_2$ m$_{reg}$ [GeV]

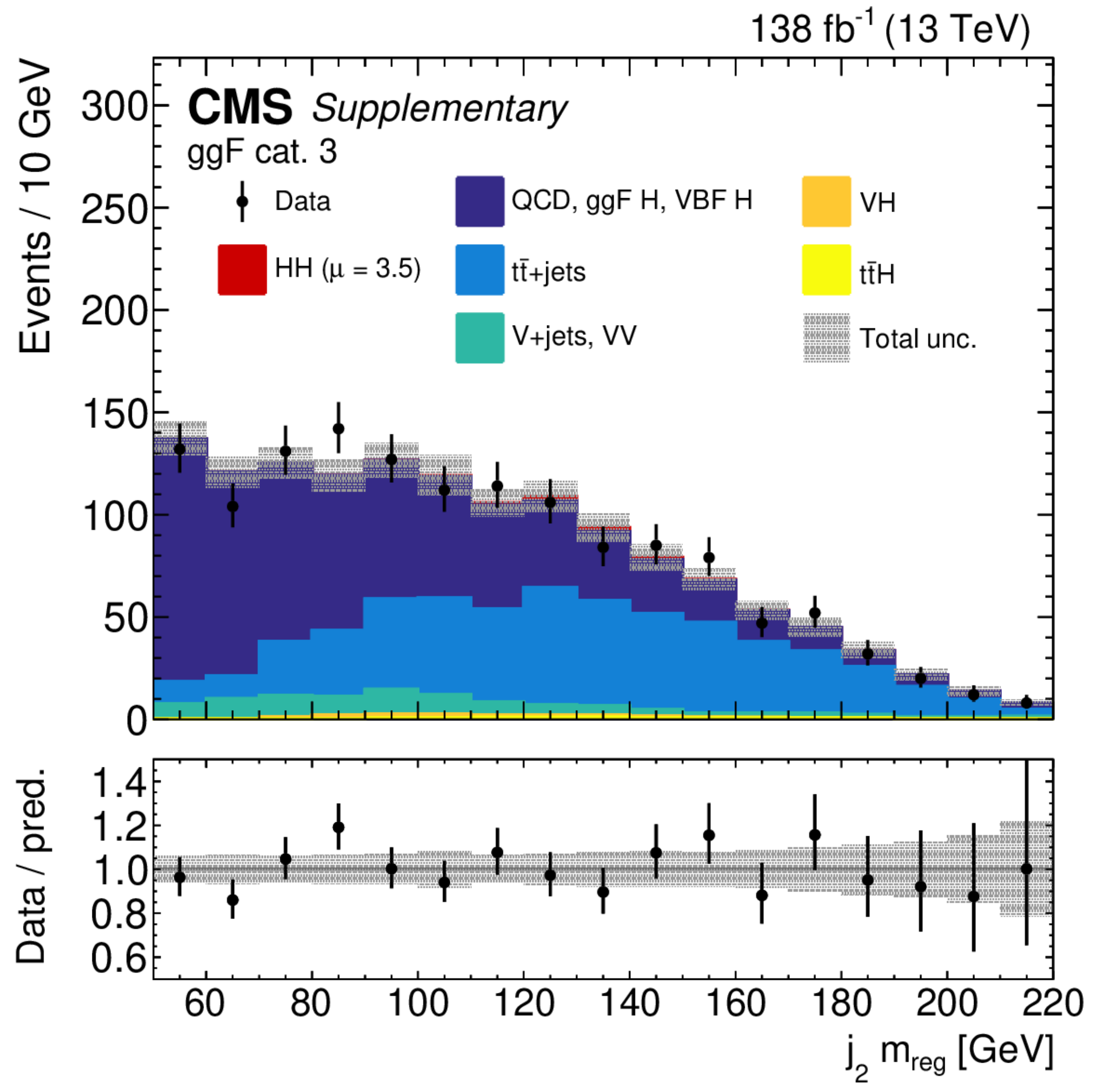
138 fb^{-1} (13 TeV)
CMS Supplementary
ggF cat. 3
Data
QCD, ggF H, VBF H
VH
HH (μ = 3.5)
tt̄+jets
tt̄H
V+jets, VV
Total unc.
Events / 10 GeV
0
50
100
150
200
250
300
Data / pred.
0.6
0.8
1.0
1.2
1.4
60
80
100
120
140
160
180
200
220
j$_2$ m$_{reg}$ [GeV]

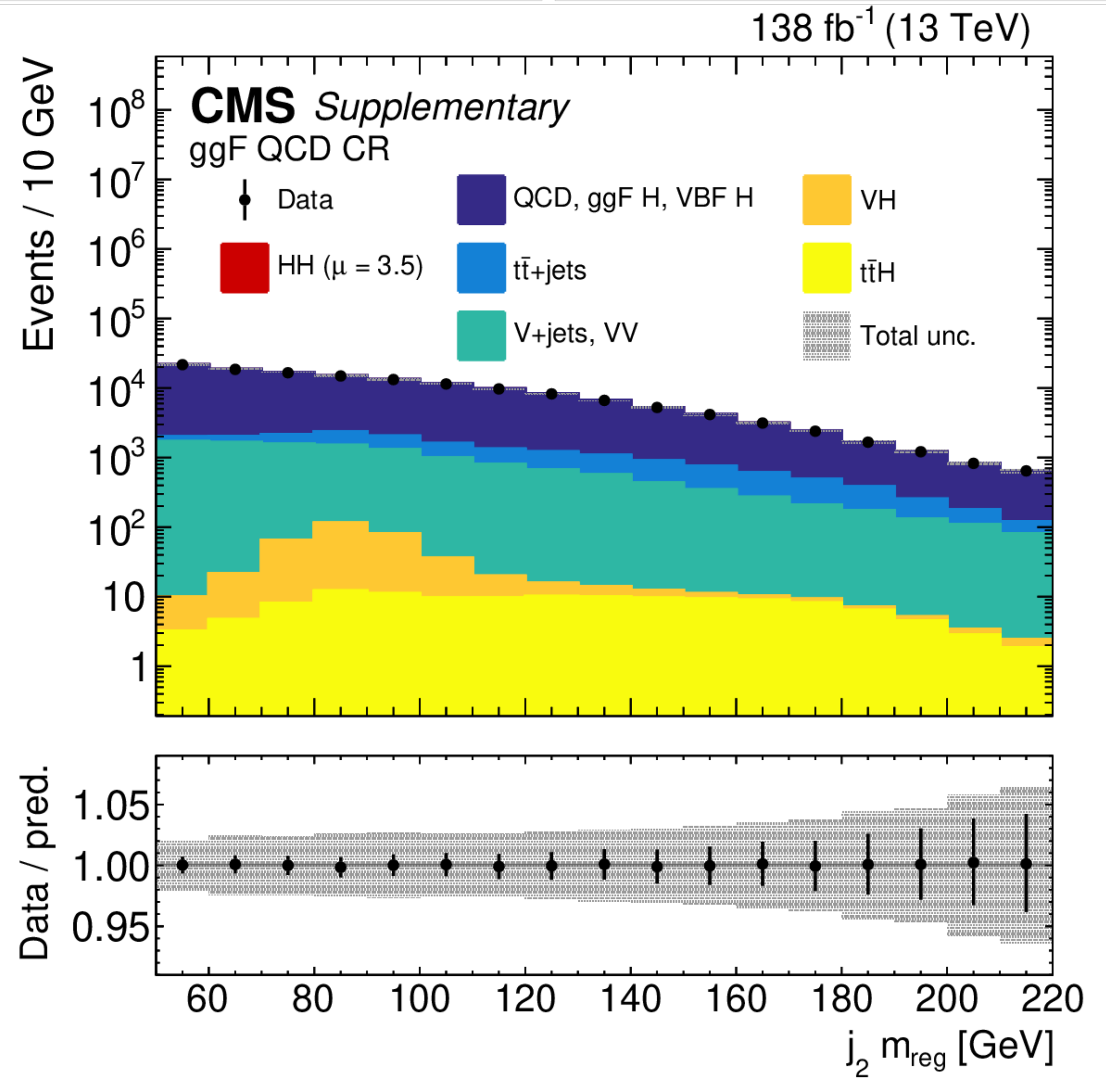
138 fb^{-1} (13 TeV)
CMS Supplementary
ggF QCD CR
Data
QCD, ggF H, VBF H
VH
HH (μ = 3.5)
tt̄+jets
tt̄H
V+jets, VV
Total unc.
Events / 10 GeV
1
10
10^2
10^3
10^4
10^5
10^6
10^7
10^8
Data / pred.
0.95
1.00
1.05
60
80
100
120
140
160
180
200
220
j$_2$ m$_{reg}$ [GeV]

boosted HH→4b results

- κ_λ constrained to be in [-9.9, 16.9] at 95% CL, sensitivity dominated by ggF analysis
- $\kappa_{2V}=0$ excluded at 6.3σ, assuming other H couplings to be SM values, sensitivity dominated by VBF analysis
- 2D likelihood scan (κ_λ , κ_{2V}) shows complementarity between two analyses

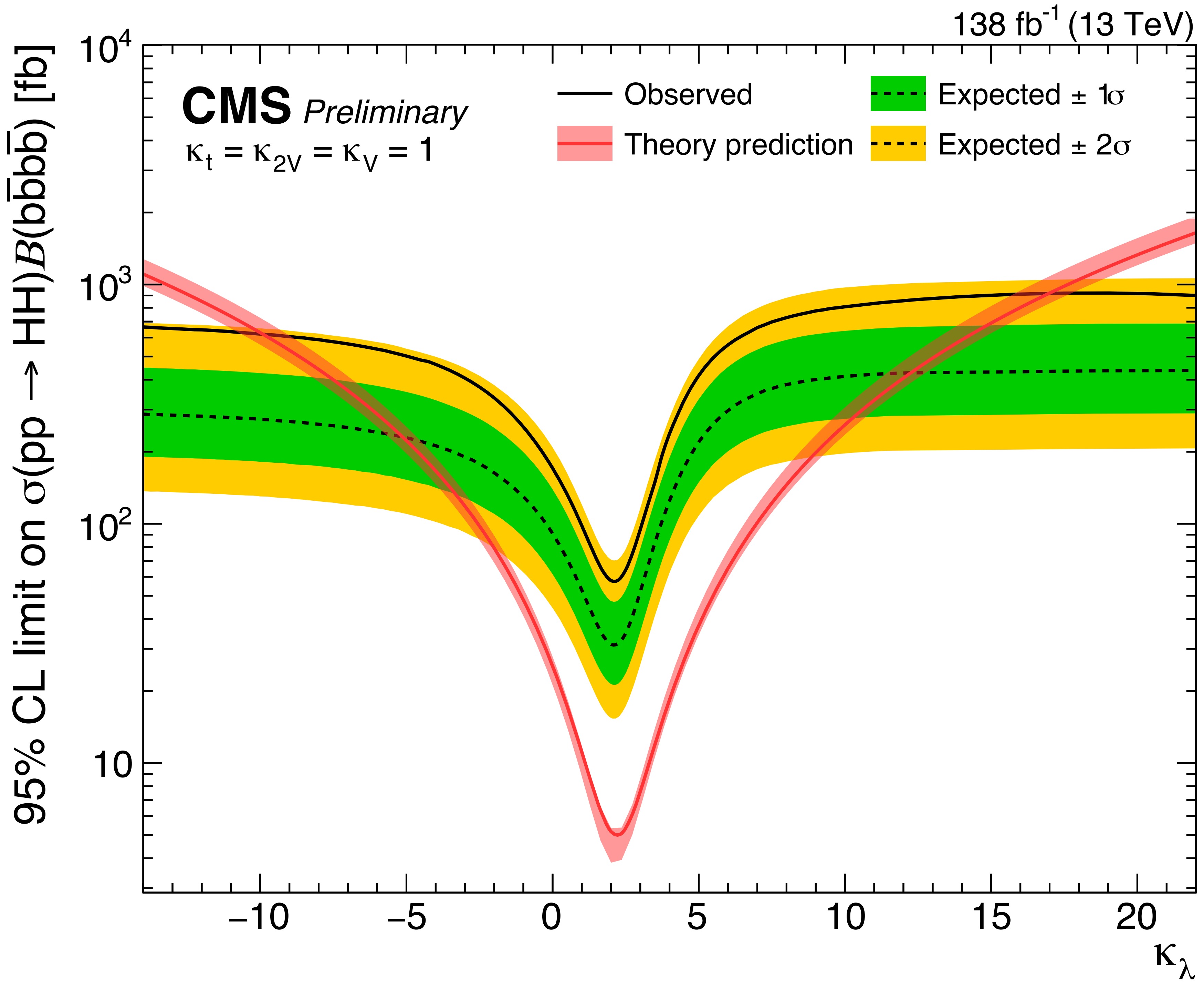

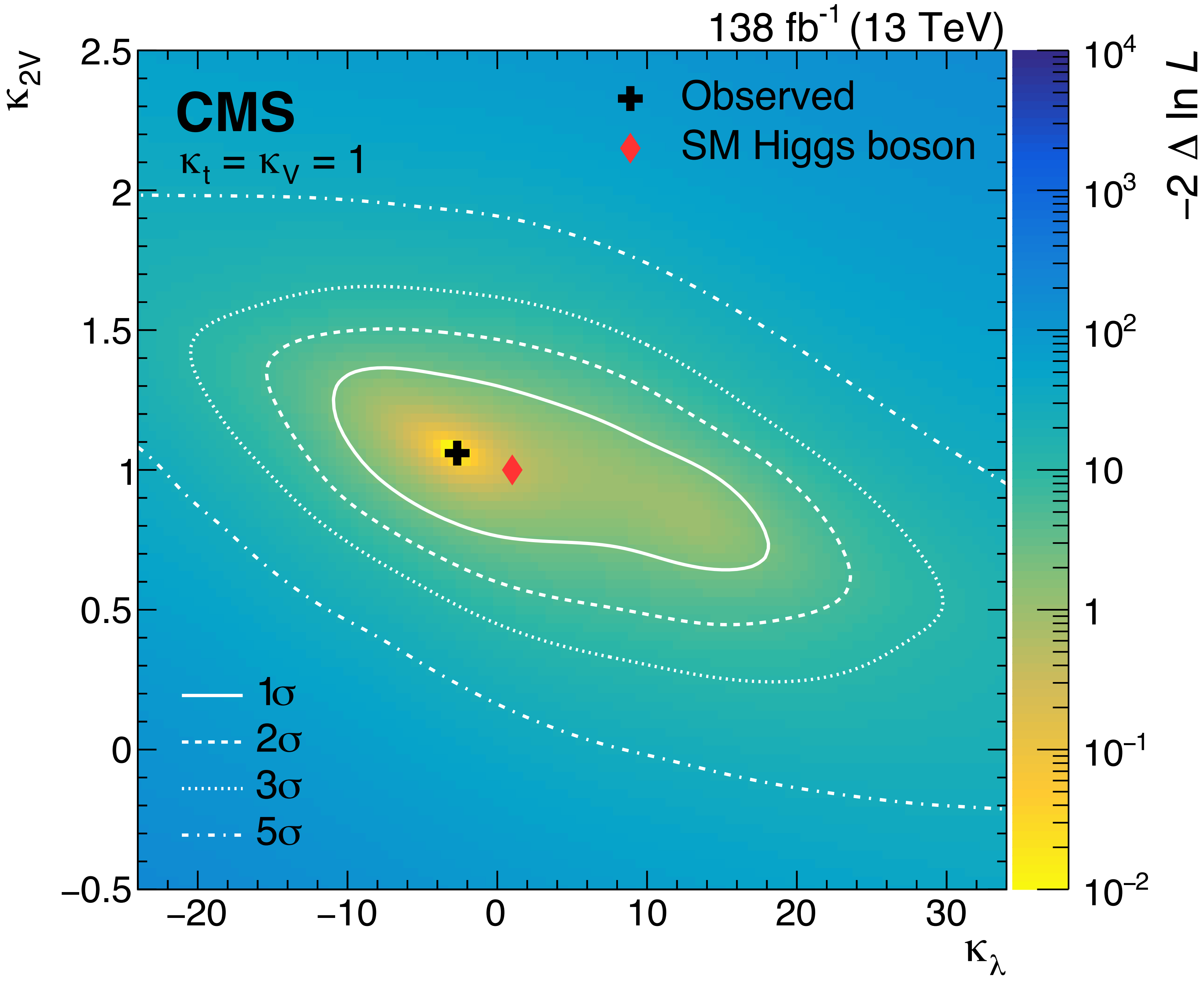

Candidate events

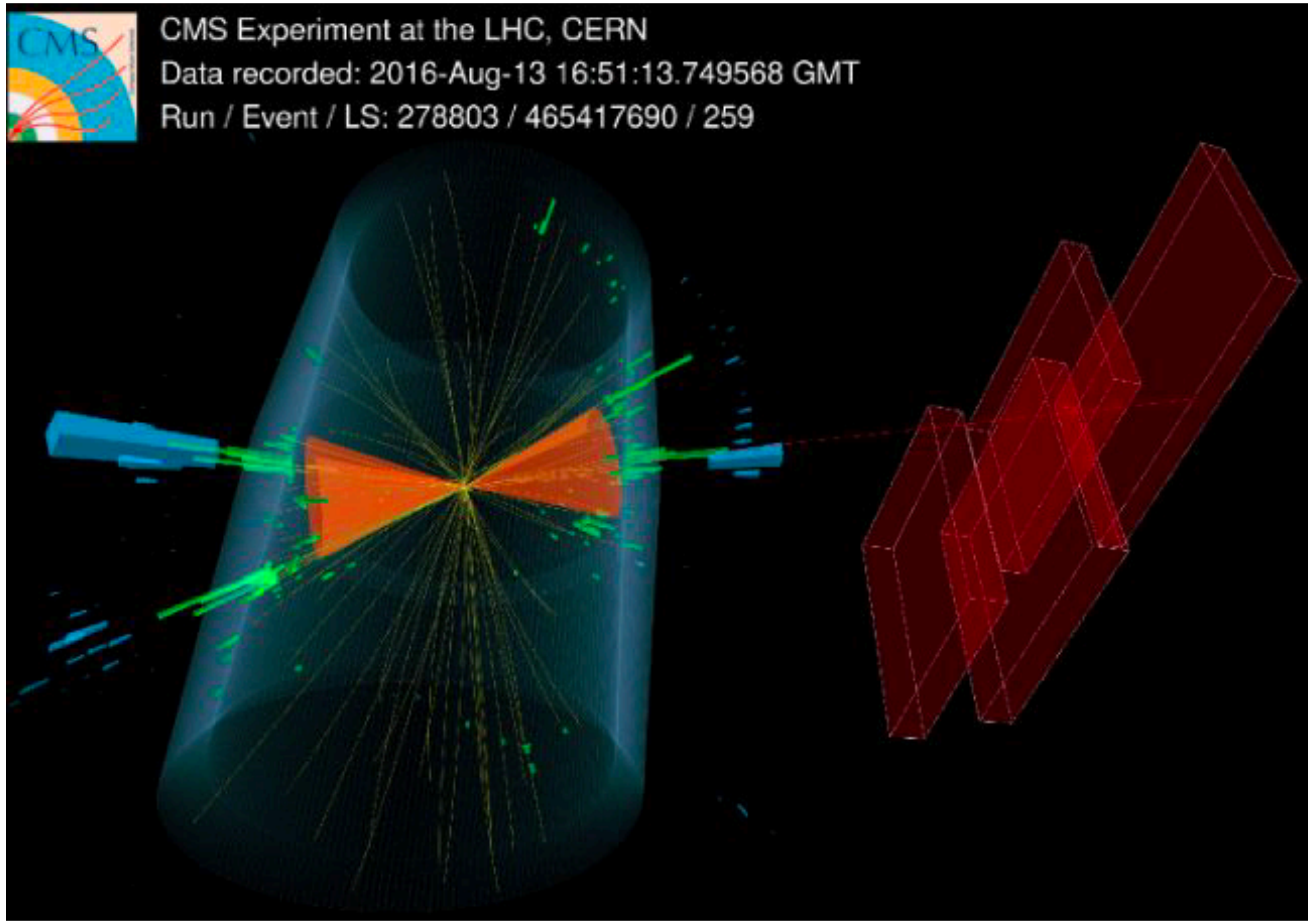

A ggF like event

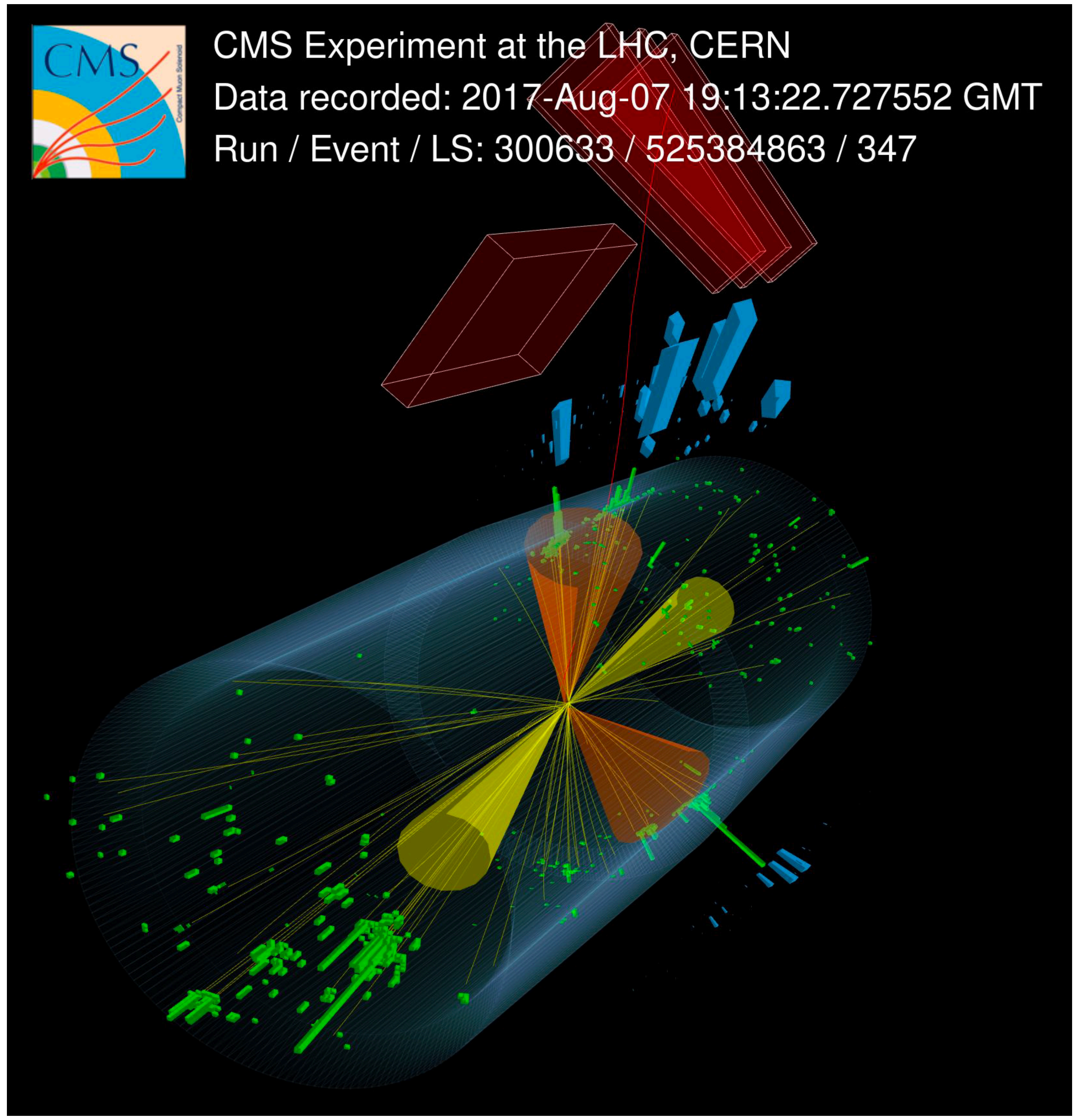

A VBF like event

Recent Higgs results: probing the Higgs Self-coupling

- *Upper limit for $\sigma(HH)/\sigma_{SM(HH)}$ λ: ATLAS obs. 6.9 (exp. 10) CMS obs. 22.2 (exp. 12.8)*
- *Limit from Higgs self-coupling:*
  - *CMS: $-11.8 < k_\lambda < 18.8$ from HH, from single Higgs $-3.5 < \kappa_\lambda < 14.5$*
  - *ATLAS: $-5.0 < \kappa_\lambda < 12.0$ from HH, $-2.3 < \kappa_\lambda < 10.3$ from HH+H*

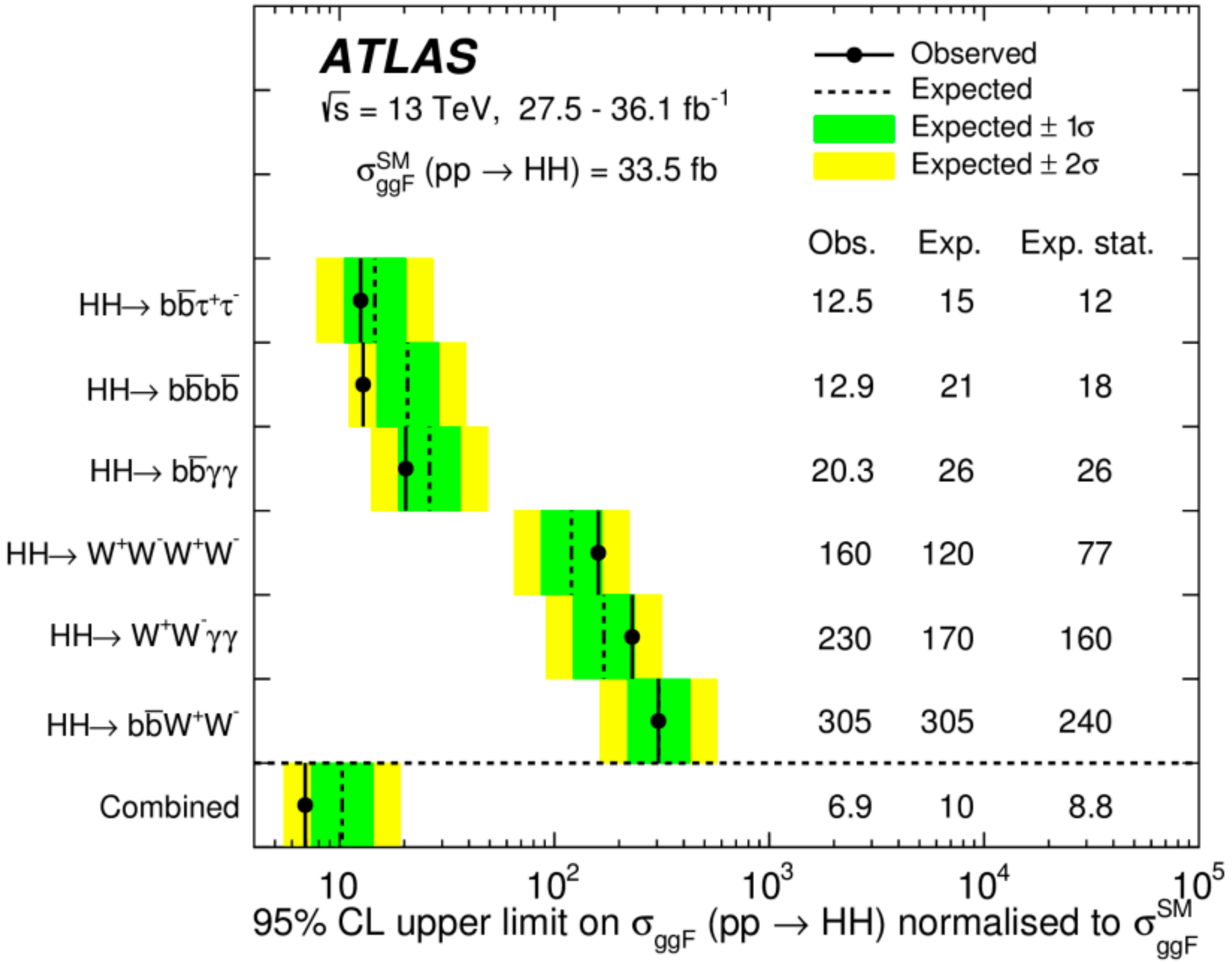

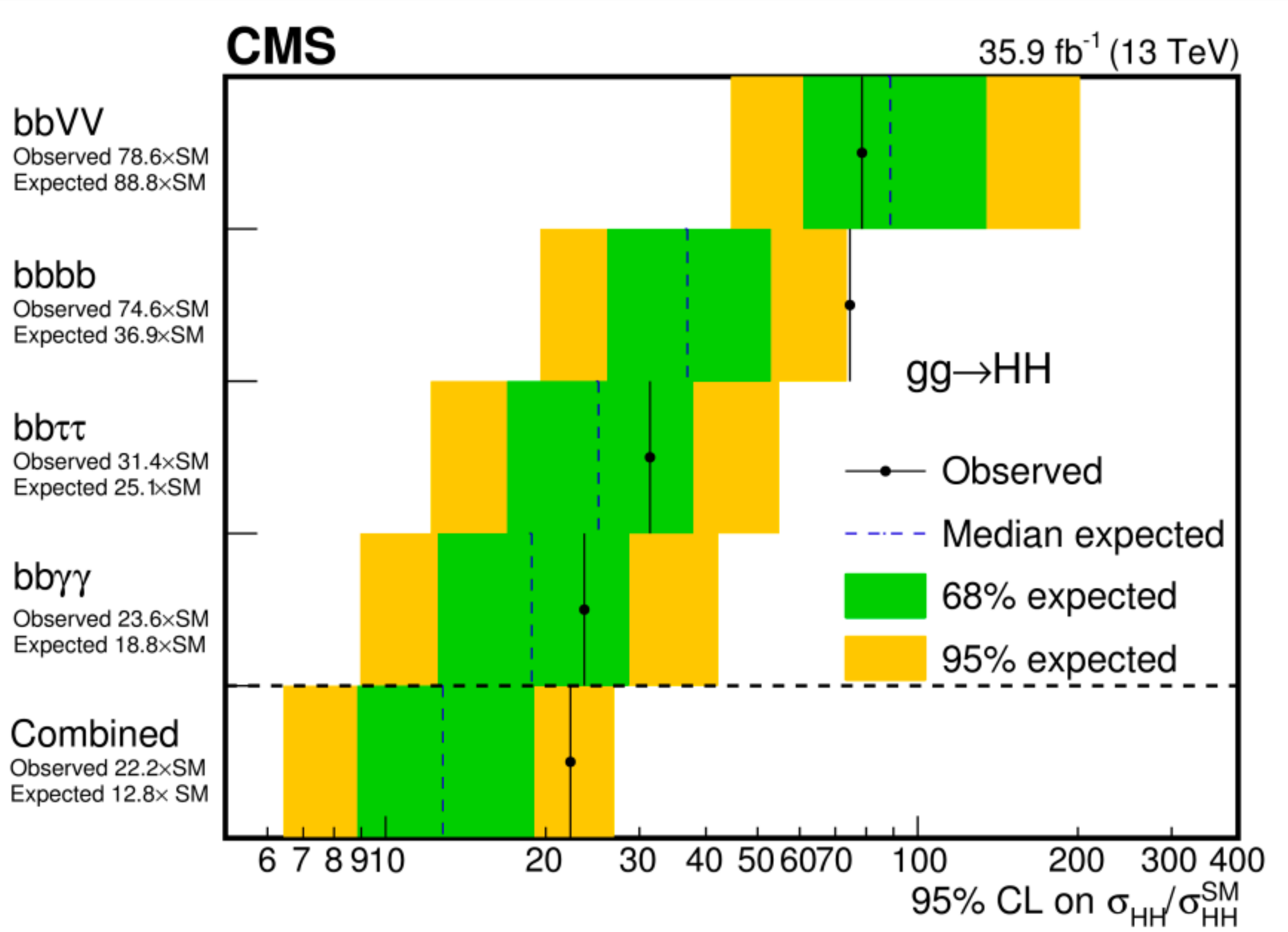

Phys. Lett. B 800 (2020) 135103, Phys. Rev. Lett. 122 (2019) 121803
CMS PAS HIG-19-005, ATLAS-CONF-2019-049

- https://videos.cern.ch/record/3021024